Post-translational Preprotein Targeting to Plant Organelles

Dissertation

der Fakultät für Biologie

der Ludwig-Maximilians-Universität München

vorgelegt von

Regina Schweiger

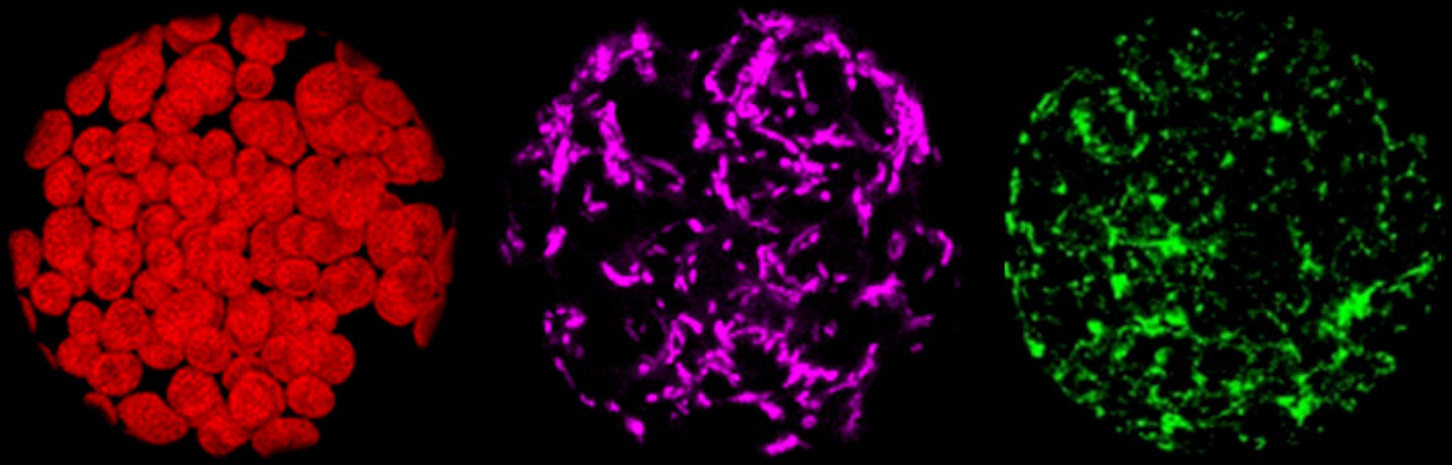

München

24. September 2013

1. Gutachter: Prof. Dr. Jürgen Soll
2. Gutachter: Prof. Dr. Marc Bramkamp

Tag der mündlichen Prüfung: 8. November 2013

Eidesstattliche Versicherung und Erklärung

Ich versichere hiermit an Eides statt, dass die vorgelegte Dissertation von mir selbstständig und ohne unerlaubte Hilfe angefertigt wurde. Ich habe weder anderweitig versucht, eine Dissertation einzureichen oder eine Doktorprüfung durchzuführen, noch habe ich diese Dissertation oder Teile derselben einer anderen Prüfungskommission vorgelegt**.**

München, den_____ _____

Table of contents

Abbreviations

Aha1	activator of heat shock protein 90 ATPase
At	*Arabidopsis thaliana*
ATP	adenosine triphosphate
BiFC	bimolecular fluorescence complementation
C-terminus	carboxy-terminus
E. coli	*Escherichia coli*
ER	endoplasmic reticulum
FKBP	FK506 binding protein
GTP	guanosine triphosphate
HOP	HSP70/HSP90 organizing protein
HSP	heat shock protein
K_D	binding affinity
kDa	kilodalton
MST	microscale thermophoresis
N-terminus	amino-terminus
OM	outer membrane
PPIase	peptidyl-prolyl isomerase
SPR	surface plasmon resonance
SRP	signal recognition particle
TOC	translocon at the outer envelope of chloroplasts
TOM	translocon at the outer membrane of mitochondria
TPR	tetratricopeptide repeat

List of Publications

1. **Fellerer C., Schweiger R., Schöngruber K., Soll J. and Schwenkert S.** (2011). Cytosolic HSP90 Co-chaperones HOP and FKBP interact with freshly synthesized chloroplast preproteins of *Arabidopsis*. Mol. Plant **2**, 1051-1058.
   R. S. performed size exclusion chromatography and *in vitro* transcription and translation.

2. **Schweiger R., Müller N.C., Schmitt M.J., Soll J. and Schwenkert S.** (2012). AtTPR7 is a chaperone-docking protein of the Sec translocon in *Arabidopsis.* J Cell Sci. **125**, 5196-5207.
   R. S. performed all experiments except the complementation experiment in yeast and was involved in writing the manuscript.

3. **Schweiger R. and Schwenkert S.** (2013). AtTPR7 as part of the *Arabidopsis* Sec post-translocon. Plant Signaling & Behavior; 8:e25286; PMID: 23759546; http://dx.doi.org/10.4161/psb.25286.
   R. S. performed all experiments. The manuscript was written by R. S. and revised by S. S.

4. **Schweiger R. and Schwenkert S.** (2013). Protein-Protein Interactions Visualized by Bimolecular Fluorescence Complementation in Tobacco Protoplasts and Leaves. JoVE (accepted).
   R. S. performed all experiments. R. S. was involved in writing the manuscript.

5. **Schweiger R., Soll J., Jung K., Heermann R. and Schwenkert S.** (2013). Quantification of interaction strengths between chaperones and tetratricopeptide repeat domain containing membrane proteins. JBC; doi:10.1074/jbc.M113.493015jbc.M113.493015.
   R. S. performed all experiments, the evaluation of the SRP data was done by R. H.. R. S. was involved in writing the manuscript.

I hereby confirm the above statements

Regina Schweiger

Prof. Dr. Jürgen Soll

Zusammenfassung

In der eukaryotischen Zelle werden die meisten Proteine als Vorstufenproteine im Zytosol translatiert und müssen daraufhin in einem importkompetenten Zustand zu den jeweiligen Organellen gelangen. Im Zytosol kann es jedoch leicht zu Aggregation oder Fehlfaltung der Vorstufenproteine kommen, was den Import verhindert. Die vorliegende Arbeit analysierte die molekulare und regulatorische Bedeutung zytosolischer Chaperone und deren Rezeptoren an den Organellenoberflächen bei der Sortierung plastidärer und mitochondrieller als auch sekretorischer Vorstufenproteine während des post-translationalen Transports zu den jeweiligen Funktionsorten. Insbesondere wurde die Funktion der Hitzeschockproteine HSP70 und HSP90 und deren Rezeptoren untersucht. HSP90 und HSP70 assoziieren nicht nur unmittelbar nach der Translation im Zytosol mit den Vorstufenproteinen, sondern sie spielen auch eine Rolle beim Andocken der Vorstufenproteine an der Organellenoberfläche. Es entsteht hierbei eine Interaktion mit Rezeptoren, die über zytosolische Domänen mit TPR (*tetratricopeptide repeat*) Motiven verfügen. Toc64 (in der äußeren Chloroplasten Membran) und OM64 (in der äußeren Mitochondrien Membran) fungieren als TPR-Rezeptoren der jeweiligen Translokons. Im Rahmen dieser Arbeit wurde AtTPR7 als TPR-Rezeptor im endoplasmatischen Retikulum lokalisiert. Biochemische Analysen zeigten, dass AtTPR7 nicht nur mit dem Sec-Translokon in der Membran sondern auch mit HSP70 und HSP90 im Zytosol interagiert. Weiterhin konnte AtTPR7 eine Hefemutante komplementieren, die einen Defekt im post-translationalen Import zeigt. Diese Daten lassen stark vermuten, dass AtTPR7 eine Rolle im post-translationalen Import von Proteinen in das endoplasmatische Retikulum in *Arabidopsis* spielt. Um eine Beteiligung der Chaperone bei der Sortierung der Vorstufenproteine im Zytosol zu untersuchen wurde eine Kombination aus biochemischen und biophysikalischen Methoden angewendet. Die Bindeaffinitäten zwischen den vier zytosolischen HSP90 Isoformen bzw. HSP70.1 und den TPR-Rezeptoren Toc64, OM64 und AtTPR7 wurden bestimmt. Erstaunlicherweise zeigte OM64 eine stärkere Bindung an HSP70.1 im Gegensatz zu Toc64, welches alle getesteten Chaperone ähnlich stark band. AtTPR7 als auch OM64 zeigten nur eine schwache Bindung an die Hitzeschock induzierte Isoform HSP90.1. Dies impliziert eine führende Rolle der konstitutiv exprimierten Chaperone während des Sortierungs-Prozesses der Vorstufenproteine zu den jeweiligen Organellen.

Summary

Most proteins localized to cellular organelles are translated in the cytosol and have to be targeted to their destined compartments. Chloroplast and mitochondrial preproteins are imported post-translationally whereas import into the endoplasmic reticulum can either occur co- or post-translationally. During post-translational import preproteins have to be kept in an import competent state and aggregation due to molecular crowding has to be prevented. Molecular chaperones not only prevent misfolding and aggregation but also facilitate interaction of the preproteins with the translocon complexes at the organellar surfaces. Recognition of the preproteins is mediated either via the preprotein itself or via chaperones of the heat shock protein (HSP) 70 and 90 family which are recognized by so called tetratricopeptide (TPR) repeat domain containing docking proteins as part of the translocon complexes. In this thesis not only the chaperone preprotein interactions within the cytosol but also the interactions between chaperones and the TPR domain containing docking proteins at the organellar surfaces were analyzed. Moreover a new TPR domain containing docking protein, AtTPR7, at the endoplasmic reticulum membrane was identified. Biochemical experiments revealed that AtTPR7 is part of the Sec post-translocon and interacts with cytosolic HSP70 and HSP90 proteins. Furthermore, AtTPR7 can complement a mutant, deficient in post-translational import into the endoplasmic reticulum in yeast. These data strongly suggest AtTPR7 to be involved in post-translational import into the endoplasmic reticulum in *Arabidopsis.* To investigate the involvement of cytosolic chaperones in early sorting steps of preproteins in the cytosol a combination of biochemical and biophysical approaches was used to measure binding affinities between the four different HSP90 isoforms as well as HSP70.1 to the TPR domain containing docking proteins AtTPR7 at the endoplasmic reticulum membrane, Toc64 at the outer envelope of chloroplasts and OM64 at the outer membrane of mitochondria. Surprisingly, OM64 binds mainly to HSP70.1 in contrast to Toc64 which binds to all HSPs with the same affinity, although both having highly homologous TPR domains. The binding affinity of AtTPR7 as well as OM64 to the mainly heat shock induced isoform HSP90.1 was approximately 10 times weaker compared to the other isoforms, indicating a predominant role of the constitutively expressed chaperone isoforms during preprotein targeting to the organelles.

1 Introduction

1.1 Protein sorting in the plant cytosol

In the eukaryotic cell nuclear encoded proteins are synthesized on cytosolic ribosomes and need to be targeted to their place of function. Due to gene transfer from the endosymbiotic organelles 99 % of mitochondrial and more than 95 % of chloroplastic proteins are today encoded in the nucleus and need to be translocated back to the correct organelles (Martin and Herrmann, 1998). The plant cell must be able to distinguish proteins destined for the chloroplasts from proteins intended for other compartments like mitochondria or the endoplasmic reticulum (ER). Several different cytosolic mechanisms facilitate proper targeting of preproteins. On the one hand preproteins are synthesized containing so called signal sequences, specific for the target organelle, which are cleaved off after translocation (Dalbey and Von Heijne, 1992). On the other hand molecular chaperones have been described to play an important role during preprotein transport to the correct compartment (Schlegel et al., 2007). Thereby post-translational modifications like phosphorylation can indicate binding sites for specific chaperones, such as 14-3-3 proteins, whereas other chaperones bind to hydrophobic stretches within the preprotein sequences.

Import into the endosymbiotic organelles chloroplasts and mitochondria occurs post-translationally whereas targeting to the ER can either occur post- or co-translationally (Schleiff and Becker, 2011; Wickner and Schekman, 2005). During co-translational import precursor peptides are transported to the ER with the help of the signal recognition particle (SRP) and its receptor at the ER membrane. Thereby, the nascent polypeptide chain is recognized at a signal sequence at the N-terminus emerging from the ribosomal exit tunnel by the SRP resulting in an arrest of elongation. This allows the complex of ribosome, nascent polypeptide chain and SRP to reach the ER membrane. Translation into the ER through the protein conducting channel continues when the SRP binds to the SRP receptor at the ER membrane (Saraogi and Shan, 2011). During post-translational import the proteins are fully synthesized and released from the ribosomes and are transported through the cytosol to the respective organelles with the help of molecular chaperones.

1.2 Targeting signals of organellar preproteins

One aspect to prevent missorting of proteins within the cytosol is the synthesis of preproteins carrying a targeting sequence specific for the respective organelles. In the case of chloroplasts the majority of preproteins have an N-terminal signal sequence, designated as transit peptide. These sequences contain a high amount of hydroxylated residues especially serine residues and are generally reduced in acidic residues creating a net positive charge. The size can vary considerably from 20 to 100 residues (Bruce, 2000; von Heijne and Nishikawa, 1991). Similar to chloroplast preproteins the majority of nuclear-encoded mitochondrial preproteins also have an N-terminal presequence that serves as a targeting sequence with no primary amino acid sequence conservation. Mitochondrial presequences contain a high amount of positively charged residues and have the ability to form an amphiphilic alpha helix (Huang et al., 2009). In addition, for both, chloroplasts and mitochondria, preproteins with internal, non-cleavable signals have been described, often carrying their targeting information within hydrophobic stretches like for example a transmembrane domain (Schleiff and Becker, 2011). The signal peptides for ER targeting are 15 to 30 amino acids long and have a tripartite organization consisting of a hydrophobic core flanked by a positively charged N-terminal and a polar, but uncharged C-terminal region (von Heijne, 1985). Each of these targeting signals facilitates several interactions with components of the translocon machinery at the organellar surfaces and cytosolic molecular chaperones.

1.3 Chaperones involved in post-translational import into organelles

During post-translational import soluble factors within the cytosol are indispensable. Molecular chaperones bind to exposed hydrophobic stretches and prevent aggregation as well as misfolding of the preproteins which can easily happen due to molecular crowding within the cytosol. Moreover, chaperones keep preproteins in an import competent state and mediate interaction with the translocon complexes at the organellar surfaces.

Members of the heat shock protein (HSP) 70 and HSP40 chaperone family have been described to assist the translocation of ER preproteins but also participate in the targeting of preproteins to chloroplasts and mitochondria (Ngosuwan et al., 2003) (**Figure 1**). In the case of chloroplasts, preproteins are recognized directly after translation by HSP70 which can either function alone

or in concert with other cytosolic factors like 14-3-3 or together with HSP90 (Fellerer et al., 2011). The guidance complex containing HSP70 as well as a 14-3-3 protein is formed when pre-

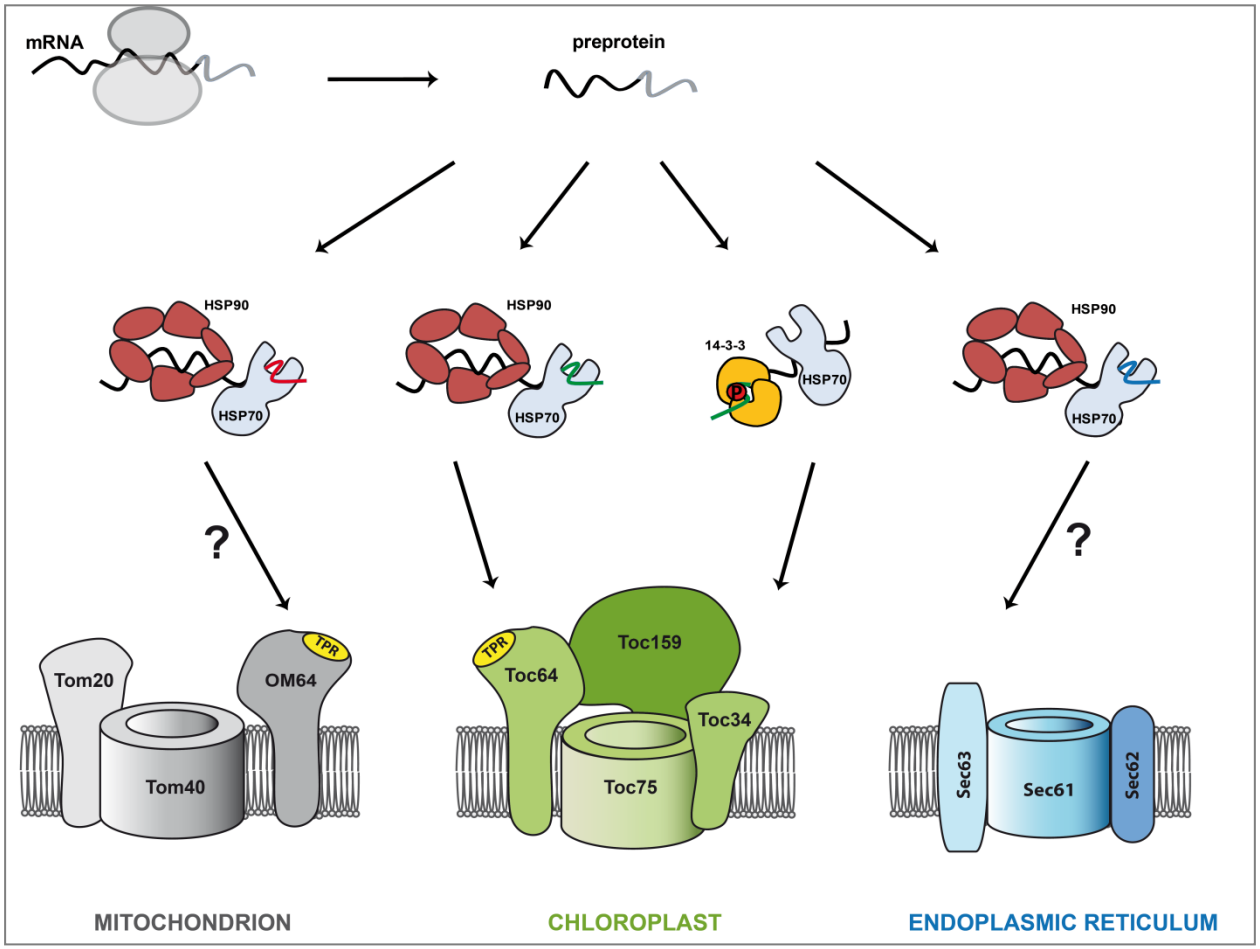

Figure 1: Interaction of preproteins with chaperones in the plant cytosol.

Chloroplast preproteins either sequentially associate with components of the HSP90 chaperone machinery or with 14-3-3. Preproteins bound by the HSP90/70 guidance complex are indirectly recognized via the TPR domain containing docking protein Toc64. Phosphorylated preproteins are bound by the 14-3-3/HSP70 guidance complex and are directly bound by the receptor protein Toc34. The mitochondrial TPR domain containing docking protein OM64 might functionally replace Tom70 in plants and therefore might interact with HSP70 and/or HSP90 bound mitochondrial preproteins. No TPR domain containing docking protein as part of the ER Sec post-translocon was identified to date.

proteins are phosphorylated within their transit peptide (Waegemann and Soll, 1996). Additionally, HSP70 was described to target preproteins to mitochondria in yeast while in mammals HSP70 functions in cooperation with HSP90 during mitochondrial preprotein delivery (Young et al., 2003). Moreover, several ER preproteins are post-translationally imported via the HSP70 and HSP40 system in yeast (Ast et al., 2013). However, chaperone involvement in post-translational targeting of mitochondrial and ER preproteins in plants has not been investigated in much detail to date.

Preproteins bound to HSP90 and HSP70 are recognized by so called tetratricopeptide repeat (TPR) domain containing docking proteins distributed across almost all organellar membranes and organisms as parts of the translocon complexes (Kriechbaumer et al., 2012; Schlegel et al., 2007). TPR domains contain a triple repeat of 34 amino acids forming a dicarboxylate clamp which coordinates the aspartate residue within the conserved EEVD motif at the very C-terminus of HSP70 and HSP90 (Scheufler et al., 2000) (**Figure 2**). HSP70 as well as HSP90 are believed to be key players in post-translational preprotein guidance through the cytosol to the TPR domain containing docking proteins at the organellar surfaces.

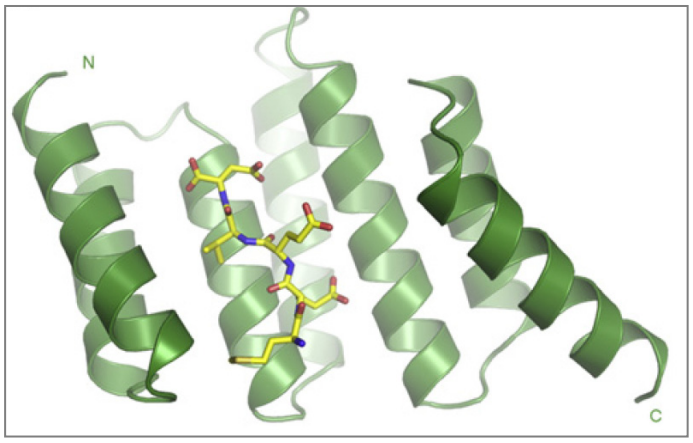

Figure 2: Structure of a typical clamp-type TPR domain with its bound peptide (Zeytuni and Zarivach, 2012).

TPR2A Domain of the HSP70/90 organizing protein (HOP) in complex with a HSP90 derived peptide.

1.4 HSP90 and its co-chaperones

In the cytosol of eukaryotic cells HSP90 is selectively recognizing partially folded clients of different protein families, in contrast to HSP70, which interacts with newly synthesized unfolded polypeptide chains in a rather unspecific manner. Thereby HSP90 prevents cellular stress by binding proteins in unstable conformations (Dittmar et al., 1997). HSP90 functions as a dimer consisting of three specific domains, the N-terminal ATP-binding domain, a middle domain and a C-terminal dimerization domain (Bracher and Hartl, 2006). Without any nucleotide bound, HSP90 stays in an open conformation where the dimer is only linked at the C-terminal dimerization domain. Upon nucleotide binding the N-terminal ATP-binding domains associate and induce the closed conformation of HSP90. ATP hydrolysis leads to the release of the nucleotide and to a switch back to the open conformation (Huai et al., 2005; Shiau et al., 2006) (**Figure 3**).

HSP90 does not function alone but with the help of several co-chaperones (**Figure 4**). As a client recruiter HSP70/90 organizing protein (HOP) has been demonstrated to deliver substrates from HSP70 to HSP90 by binding both chaperones via its TPR domains, thereby stabilizing the open conformation of HSP90 (Lee et al., 2012; Scheufler et al., 2000). As a next step a peptidyl-prolyl isomerase (PPIase) binds to the HSP90 complex, interacting directly with the client protein (Bose et al., 1996). Subsequently the binding of activator of heat shock protein 90 ATPase (Aha1) promotes the conformational change to the closed state and activates the ATPase activity of the HSP90 dimer (Meyer et al., 2004; Retzlaff et al., 2010). Thereby the binding of HOP to HSP90 is weakened leading to the release of HOP as well as HSP70. As a last step p23 is displacing Aha1 thereby stabilizing the closed conformation. After ATP hydrolysis p23 as well as the client protein are released and the HSP90 dimer undergoes conformational changes back to the open conformation (McLaughlin et al., 2006).

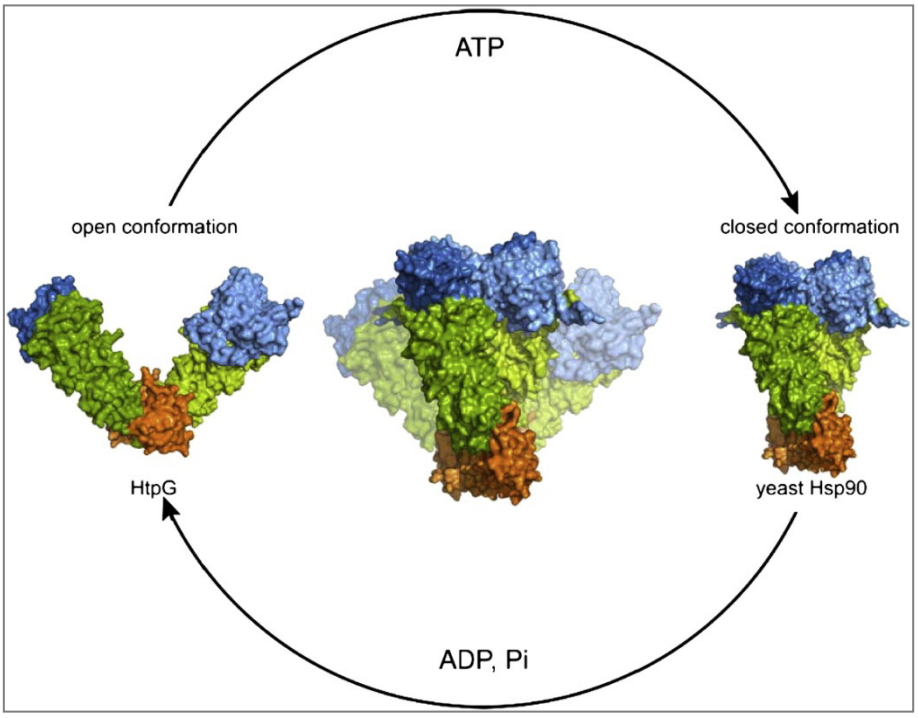

Figure 3: Crystal structures of HSP90 (Li et al., 2012).

E. coli HSP90 dimer (HtpG) in open conformation (left). Nucleotide bound yeast HSP90 dimer in closed conformation (right). The N-domain is depicted in blue, the M-domain in green and the C-domain in orange.

This mechanism of HSP90 is conserved among different HSP90 homologs. In the *Arabidopsis* cytosol four isoforms of HSP90 are described (HSP90.1, HSP90.2, HSP90.3 and HSP90.4) with HSP90.1 being the most heat shock induced isoform while HSP90.2, HSP90.3 and HSP90.4 are constitutively expressed (Cha et al., 2013; Krishna and Gloor, 2001). The three constitutively

expressed isoforms share at least 96 % identical amino acids among each other and show approximately 87 % identity to HSP90.1. All isoforms contain a highly conserved MEEVD motif at the very C-terminus, which is recognized by the TPR domain containing docking proteins at the organellar surfaces.

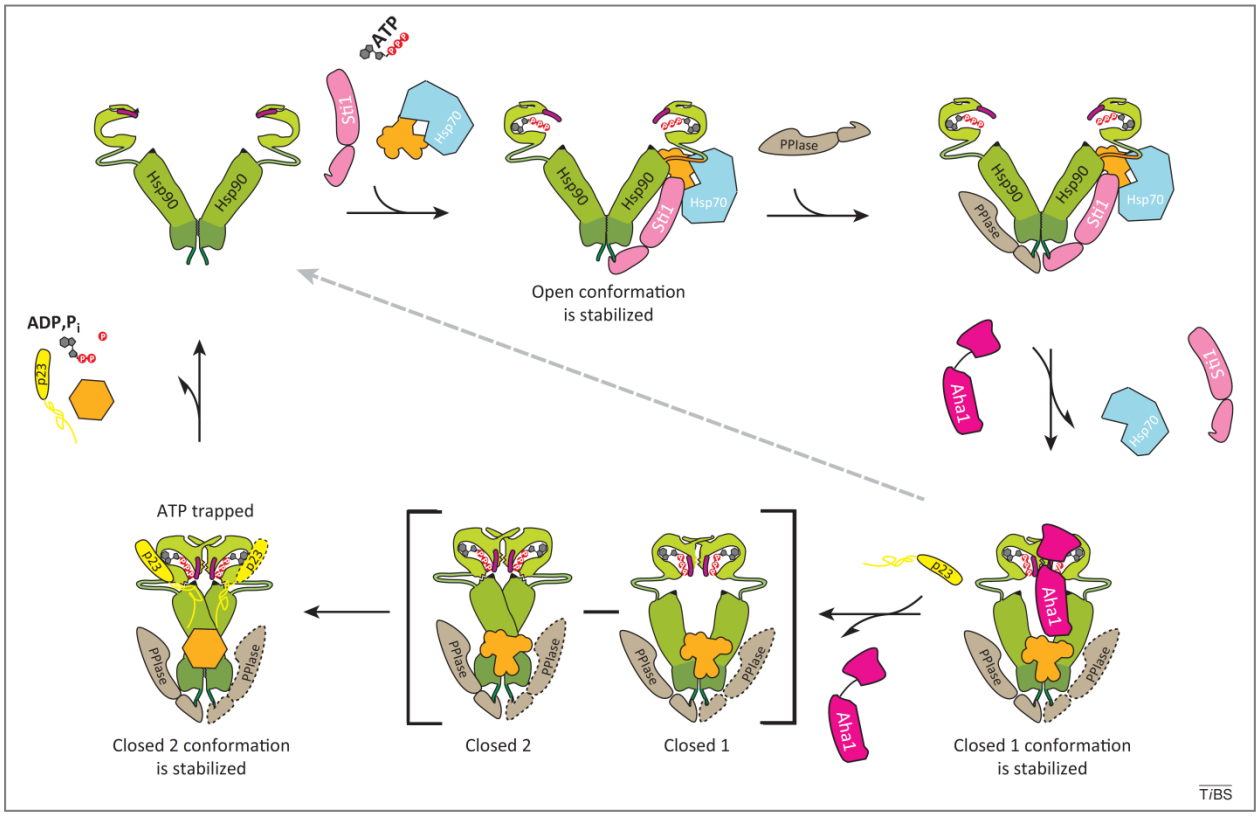

Figure 4: HSP90 co-chaperone cycle (Rohl et al., 2013).

The client protein is transferred to the open HSP90 dimer with the help of the adaptor protein HOP. Subsequently ATP is binding at the N-domain of HSP90. The intrinsic ATPase activity of HSP90 is inhibited at that stage. A PPIase is binding to the second TPR-acceptor site leading to an asymmetric complex. Upon binding of Aha1 HSP70 as well as the HOP protein are released. Aha1 accelerates the formation of the N-terminal closed state (Closed 1) as well as ATP hydrolysis. Binding of p23 displaces Aha1 and leads to the completely closed state (Closed 2). ATP hydrolysis leads to the release of p23, PPIase as well as the client protein.

1.5 The translocon at the outer envelope of chloroplasts

The translocon at the outer envelope of chloroplasts (TOC) catalyzes the transfer of preproteins across the outer membrane of chloroplasts (**Figure 1**). The TOC core complex consists of the channel protein Toc75 and two auxiliary receptor proteins Toc159 and Toc34 (Hirsch et al., 1994; Kessler et al., 1994; Seedorf et al., 1995). Both receptors are integral GTPases at the outer membrane. Toc34 recognizes chloroplast preproteins whereas Toc159 is required for the import process by providing the driving force for the translocation event (Becker et al., 2004;

Schleiff et al., 2003). Preproteins can either be directly recognized by the receptor protein Toc34 (May and Soll, 2000) or indirectly via bound chaperones by another component of the TOC complex, Toc64. Toc64 is a TPR domain containing docking protein which is dynamically associated with the TOC core complex (Sohrt and Soll, 2000).

1.6 The translocon at the outer membrane of mitochondria

Like the TOC complex, the translocon at the outer membrane of mitochondria (TOM) facilitates the transfer of mitochondrial preproteins across the outer membrane of mitochondria (**Figure 1**). The central component of the TOM complex is Tom40, a ß-barrel membrane protein forming the pore. In yeast, the Tom40 channel has two associated TPR domain containing surface receptors, Tom20 and Tom70 and a secondary receptor protein Tom22 (Chacinska et al., 2009). Tom22 is important for transferring mitochondrial preproteins from the primary TPR domain containing receptors to the import pore (van Wilpe et al., 1999). Furthermore, small TOMs, Tom5, Tom6 and Tom7 regulate the formation and function of the TOM complex. In yeast, Tom20 has a large exposed TPR motif directly interacting with mitochondrial preproteins via their N-terminal presequence (Abe et al., 2000). In contrast, Tom70 recognizes internal targeting sequences of mitochondrial preproteins such as carrier proteins of the inner mitochondrial membrane (Brix et al., 1997). In mammals, Tom34 is an additional TPR domain containing protein interacting with mitochondrial preproteins in the cytosol (Faou and Hoogenraad, 2012).

In plants, Tom22 as well as Tom70 are absent while Tom9 was identified as a truncated form of the yeast Tom22 lacking the large cytoplasmic region (Macasev et al., 2000). Tom70 might be functionally replaced by OM64 in plants, a close homolog of the chloroplast Toc64 receptor with 51 % overall identity to each other (Chew et al., 2004). Like Toc64, OM64 might be associated with the translocon complex and contains a cytosolic exposed TPR domain, therefore having a proposed receptor function (Lister et al., 2007).

1.7 The Sec translocon at the membrane of the endoplasmic reticulum

The Sec translocon in yeast and mammalian cells is known to translocate proteins not only co-translationally but also post-translationally into the ER. In yeast both pathways are equally important whereas in mammals the co-translational pathway is the predominant one

(Zimmermann et al., 2011). Post-translational import into the yeast ER is mainly used by preproteins with more hydrophobic signal sequences (Ng et al., 1996). In mammals preproteins with a chain length shorter than 160 amino acids are imported post-translationally (Lakkaraju et al., 2012). In yeast, translocation involves the heterotrimeric protein conducting channel Sec61 (Sec61p, Sbh1p and Sss1p) as well as additional factors such as the ER luminal HSP70 protein BiP (Kar2p) and the J-domain protein Sec63p (Zimmermann et al., 2011). Post-translational import occurs via a heptameric post-translocon composed of the protein conducting channel and a heterotetrameric Sec62/Sec63 complex, comprising Sec63p and three proteins serving as signal peptide receptor, Sec62p, Sec71p and Sec72p (Dunnwald et al., 1999; Feldheim and Schekman, 1994; Harada et al., 2011; Plath et al., 1998) (**Figure 5**).

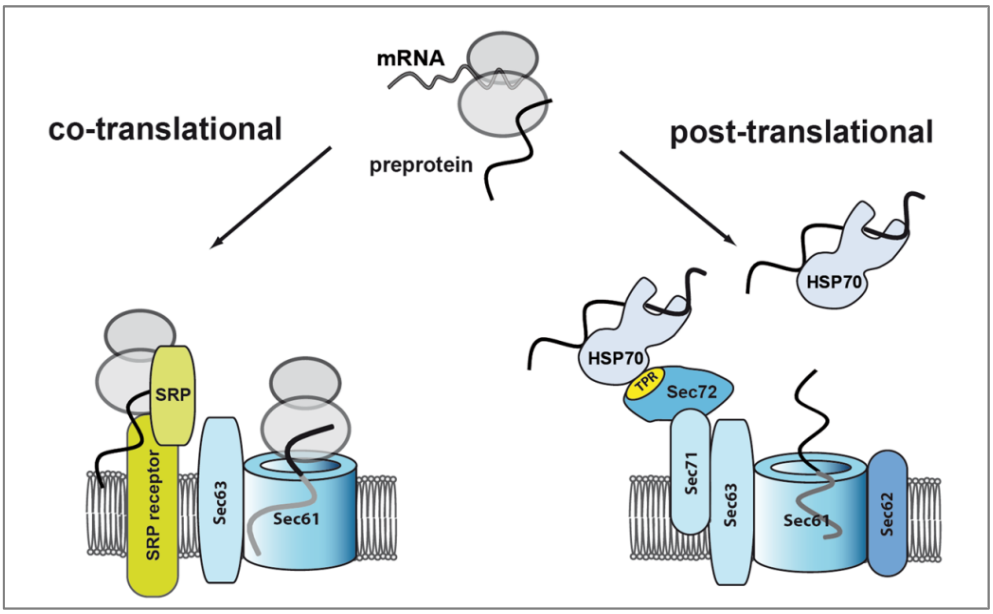

Figure 5: Co- and post-translational import into the yeast ER.

During co-translational import the nascent polypeptide chain is recognized by the SRP and elongation is arrested. Translation continues when the SRP is bound to its SRP receptor at the ER membrane and translocation through the Sec61 conducting channel occurs (left). Fully synthesized proteins are bound by HSP70 in the cytosol. The TPR domain containing docking protein Sec72 binds to HSP70 and therefore the preprotein is indirectly recognized and transferred to the Sec61 channel (right).

Like in yeast, co-translational import into the mammalian ER is facilitated by the heterotrimeric Sec61 complex (Sec61α, Sec61β and Sec61γ) together with Sec63 and the ER-luminal HSP70 partner BiP (Zimmermann et al., 2011). Sec62 is associated with the trimeric Sec61 channel and forms a stable complex with Sec63 (Meyer et al., 2000; Tyedmers et al., 2000). Additionally, mammalian Sec62 has a ribosomal binding site suggesting a different function than its yeast homolog (Muller et al., 2010). However, mammalian Sec62 has been shown to be required for

post-translational protein import of secretory proteins smaller than 160 amino acids (Lakkaraju et al., 2012). To date homologs of yeast Sec71p and Sec72p have not been identified in mammalian cells.

Not much is known about the mechanisms of protein translocation into the ER in plants so far. Homologs for the major components of the Sec translocon can also be identified in plant genomes, Sec61α is present as three isoforms, Sec62 as a single gene and two isoforms of Sec63, AtERdj2A and AtERdj2B, were identified (**Figure 1**) (Yamamoto et al., 2008). Like in mammalian cells no homologs for yeast Sec71p and Sec72p have been identified in plants.

1.8 TPR domain containing docking proteins in post-translational import

TPR domain containing docking proteins are part of all organellar membrane translocons and thereby involved in post-translational import (Kriechbaumer et al., 2012) (**Figure 6**). Preproteins bound to HSP70 and HSP90 are recognized indirectly by interaction of the TPR domain with the conserved C-terminus of the chaperones thereby increasing the efficiency of protein targeting (Feldheim and Schekman, 1994; Qbadou et al., 2006; Young et al., 2003). In mammals and yeast the best characterized TPR domain containing docking protein is Tom70 in the outer membrane of mitochondria containing a conserved domain structure with 11 TPR motifs organized in three distinct domains (Chan et al., 2006). The three N-terminal TPR motifs form a clamp-type TPR domain and have been shown to bind cytosolic HSP70 as well as HSP90 in mammals, whereas in yeast only HSP70 binding has been demonstrated (Young et al., 2003). Next to Tom70, Tom34 was identified as a potential co-chaperone of HSP70 and HSP90 in the mammalian cytosol containing two TPR domains (Faou and Hoogenraad, 2012). Furthermore, Sec72p in the Sec post-translocon is thought to bind to HSP70 via its clamp-type TPR domain during post-translational import into the ER in yeast.

In plants, Toc64 indirectly recognizes HSP90 bound preproteins by interacting specifically via its cytosolic exposed TPR domain with the conserved C-terminus of HSP90 before dissociation of the preprotein from the chaperone initiates its subsequent recognition and import by Toc34 (Qbadou et al., 2007; Qbadou et al., 2006). No homolog of the yeast and mammalian Tom70 can be identified in plants, but OM64 appears to functionally replace Tom70 (Chew et al., 2004; Lister et al., 2007), although chaperone binding has not been investigated to date.

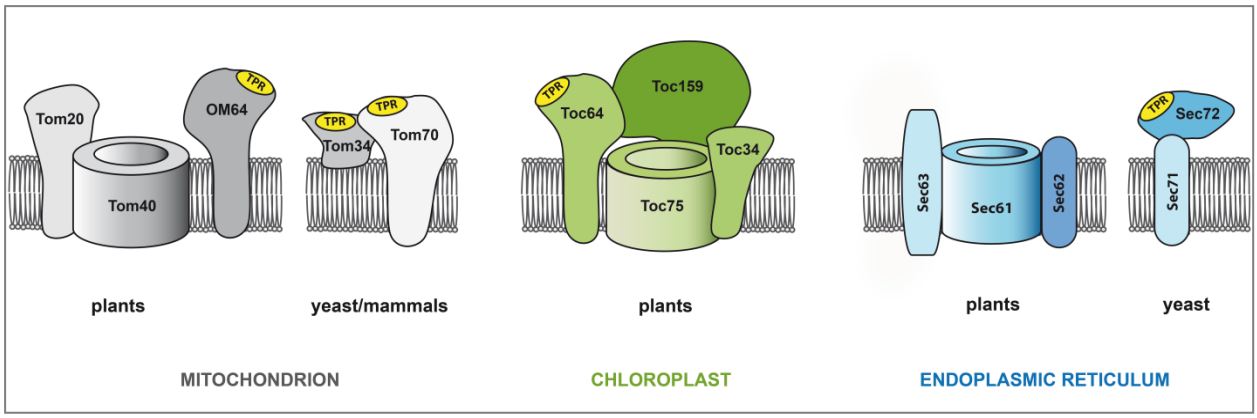

Figure 6: TPR domain containing docking proteins of the translocon complexes in mammals, yeast and plants.

The TOM complex is depicted in grey. Tom40, the main channel of the TOM complex at the outer membrane of mitochondria, as well as Tom20 are present in all organisms. Tom70 is present in yeast and mammals whereas Tom34 is present in mammals. OM64 might functionally complement Tom70 in plants. The TOC complex is depicted in green. The TOC core complex at the outer envelope of chloroplasts consists of the channel protein Toc75 and the two receptor proteins Toc34 and Toc159. Toc64 is dynamically associated to the TOC core complex. The Sec post-translocon at the ER membrane is depicted in blue. Sec61 is the main channel in all organisms. Sec62 as well as Sec63 are present in mammals, yeast and plants. In yeast Sec71 and Sec72 form a protein receptor not found in plants and mammals.

Furthermore, plants do not contain a Sec72p homolog. Interestingly, none of these clamp-type TPR domain containing docking proteins is essential for cell survival (Aronsson et al., 2007; Fang and Green, 1994; Lister et al., 2007; Young et al., 2003). In contrast to that, the genes for Tom20, Toc34 as well as Sec62 are essential (Constan et al., 2004; Deshaies and Schekman, 1989; Moczko et al., 1994). Therefore HSP90/HSP70 guided preproteins must be able to directly interact with other translocon receptors like Tom20, Toc34 or Sec62, although efficiency may be lower. Nevertheless it remains a challenge to investigate the role of TPR domain containing docking proteins as well as the role of HSP70 and HSP90 in the sorting process of preproteins during post-translational import into various organelles.

2 Aims of the Thesis

In this study post-translational transport of preproteins to various organelles should be highlighted in more detail concerning chaperone involvement within the cytosol as well as the role of TPR domain containing docking proteins as part of the translocon complexes at the organellar membranes.

2.1 TPR domain containing docking proteins

Although the translocons at the outer envelope of chloroplasts and the outer membrane of mitochondria are quite extensively studied nothing is known about the Sec translocon at the endoplasmic reticulum in plants. Both, the translocon at the chloroplast and the mitochondrion, respectively, include TPR domain containing docking proteins which are supposed to play a role in post-translational import by recognizing chaperone bound preproteins. One major aim of this work was to identify and to characterize further TPR domain containing docking proteins in plants. With the help of *in silico* approaches a novel TPR domain containing protein, AtTPR7, in addition to Toc64 at the outer envelope of chloroplasts and OM64 at the outer membrane of mitochondria, was identified. To gain better insight into the function of AtTPR7, the protein should be studied using *in vivo* analyses in *Arabidopsis* and tobacco as well as *in vitro* approaches to investigate not only the localization and topology of AtTPR7 but also interaction partners and its overall function within the cell.

2.2 Chaperone involvement in the sorting process of preproteins in the cytosol

During post-translational translocation the newly synthesized preproteins in the cytosol require the assistance of molecular chaperones to be kept in an import competent state and to prevent aggregation and misfolding in the cytosol. HSP70 and HSP90 facilitate the interaction at the organellar surfaces by binding to the TPR domain containing docking proteins which are part of the translocon complexes. Therefore the aim was to investigate the binding affinities of HSP70 as well as the four cytosolic HSP90 isoforms of *Arabidopsis* to the TPR domain containing docking proteins Toc64, OM64 and AtTPR7, to examine a potential role of HSP70 and HSP90 in the sorting process of preproteins in the cytosol. To investigate this, the proteins should be overexpressed in *E.coli* and *in vitro* studies should be performed using a combination of

biochemical and biophysical approaches like pull down analysis, surface plasmon resonance and microscale thermophoresis measurements.

3 Publication I

Fellerer C., Schweiger R., Schöngruber K., Soll J. and Schwenkert S., (2011). *Cytosolic HSP90 Co-chaperones HOP and FKBP interact with freshly synthesized chloroplast preproteins of Arabidopsis*. Mol. Plant **2**, 1051-1058.

Molecular Plant • Volume 4 • Number 6 • Pages 1133–1145 • November 2011 RESEARCH ARTICLE

Cytosolic HSP90 Cochaperones HOP and FKBP Interact with Freshly Synthesized Chloroplast Preproteins of *Arabidopsis*

Christine Fellerer[a,b], Regina Schweiger[a,b], Katharina Schöngruber[a,b], Jürgen Soll[a,b] and Serena Schwenkert[a,b,1]

a Department of Biology I, Botany, Ludwig-Maximilians-Universität München, Groβhaderner Strasse 2–4, D-82152 Planegg-Martinsried, Germany
b Munich Center for Integrated Protein Science CiPSM, Ludwig-Maximilians-Universität München, Feodor-Lynen-Strasse 25, D-81377 Munich, Germany

ABSTRACT Most chloroplast and mitochondrial proteins are synthesized in the cytosol of the plant cell and have to be imported into the organelles post-translationally. Molecular chaperones play an important role in preventing protein aggregation of freshly translated preproteins and assist in maintaining the preproteins in an import competent state. Preproteins can associate with HSP70, HSP90, and 14–3–3 proteins in the cytosol. In this study, we analyzed a large set of wheat germ-translated chloroplast preproteins with respect to their chaperone binding. Our results demonstrate that the formation of distinct 14–3–3 or HSP90 containing preprotein complexes is a common feature in post-translational protein transport in addition to preproteins that seem to interact solely with HSP70. We were able to identify a diverse and extensive class of preproteins as HSP90 substrates, thus providing a tool for the investigation of HSP90 client protein association. The analyses of chimeric HSP90 and 14–3–3 binding preproteins with exchanged transit peptides indicate an involvement of both the transit peptide and the mature part of the proteins, in HSP90 binding. We identified two partner components of the HSP90 cycle, which were present in the preprotein containing high-molecular-weight complexes, the HSP70/HSP90 organizing protein HOP, as well as the immunophilin FKBP73. The results establish chloroplast preproteins as a general class of HSP90 client proteins in plants using HOP and FKBP as novel cochaperones.

Key words: Wheat germ; *in vitro* translation; chloroplast import; chaperone.

INTRODUCTION

Plant organelles, such as plastids and mitochondria, are integrated into the regulative network of the cell, since most (>95%) of the organellar proteins are encoded for in the nucleus (Martin et al., 1998). Inevitably, these proteins, which are synthesized in the cytosol, must be imported into the chloroplast or mitochondria to exert their functions. Plastid and mitochondrial preproteins are mostly equipped with an N-terminal targeting sequence, serving as an entry ticket for the intended organelle, which is cleaved off after their translocation across the organellar membranes. The Toc (**t**ranslocon at the **o**uter membrane of **c**hloroplasts) and the Tic (**t**ranslocon at the **i**nner membrane of **c**hloroplasts) translocons are multiprotein complexes facilitating transport of preproteins across both chloroplast membranes (Jarvis, 2008; Balsera et al., 2009). The Toc core complex consists of Toc159, Toc34, and Toc75, where Toc34 and Toc159 are GTPases acting as receptors for preproteins and Toc75 forms the channel protein. Another component, Toc64, is loosely associated with the core complex and has a cytosolic exposed tetratricopeptide repeat (TPR) domain.

Chaperone association of preproteins in the cytosol assists in keeping them in an import competent state and prevents their premature interaction with other proteins. This is essential, since the cytosol is a hostile environment for non-native polypeptides, which are prone to aggregation in a high-density cytosol. A non-specific chaperone, which recognizes exposed hydrophobic polypeptide stretches, HSP70, associates with most preproteins in an unfolded state soon after translation (Zhang and Glaser, 2002; Ruprecht et al., 2010). Additionally,

[1] To whom correspondence should be addressed at address [a]. E-mail serena.schwenkert@lrz.uni-muenchen.de, tel. +49 +89 2180 74760, fax +49 +89 2180 74752.

doi: 10.1093/mp/ssr037, Advance Access publication 18 May 2011
Received 22 February 2011; accepted 4 April 2011

some chloroplast preproteins are phosphorylated in their presequences, subsequently leading to the binding of a 14–3–3 dimer (Waegemann and Soll, 1996; May and Soll, 2000; Martin et al., 2006), which improves their import kinetics. Other preproteins were shown to use still a further pathway across the cytosol. These preproteins, namely pNTT, pPC1, and pOE33, were shown to associate with HSP90 (Qbadou et al., 2006). Preprotein HSP90 complexes are bound to the chloroplast surface by an interaction between the TPR domain of Toc64 and HSP90 (Qbadou et al., 2006, 2007). However, Toc64 can most likely be bypassed during protein import, since Toc64 is not essential in *Arabidopsis* and *Physcomitrella* as shown by mutant studies (Hofmann and Theg, 2005; Aronsson et al., 2007). Some mitochondrial preproteins likewise have been shown to bind HSP90 in mammals and are recognized by the mitochondrial import receptor Tom70 (Young et al., 2003; Fan et al., 2006). In plant mitochondria, which lack Tom70, a homolog of Toc64 is localized in the outer mitochondrial membrane, the function of which has not been assigned so far (Chew et al., 2004), but which could also act as a docking protein. The involvement of HSP90 in the targeting of plant mitochondrial preproteins, however, is still elusive.

The mechanistic functioning of HSP90 in other organisms, such as mammals or yeast, is well documented. Several *in vitro* experiments and crystal structures have elucidated its binding to client proteins in an ATP-dependant manner and its interactions with various assisting cochaperones (for recent reviews, see Bracher and Hartl, 2006; Pearl and Prodromou, 2006; Wandinger et al., 2008). Among these are immunophilins and HOP (HSP70 and HSP90 organizing proteins) proteins, the latter mediating an interaction between client proteins and the chaperones HSP70 and HSP90, thus transferring the HSP70 bound client proteins subsequentially to the HSP90 chaperone machinery. Immunophilins and HOP are both able to associate with HSP90 through repetitive TPR domains (Smith, 2004). Structurally, HSP90 functions as a flexible dimer and is composed of three major domains. The N-terminal domain binds to ATP and is regulated by the middle domain, whereas the C-terminal residues are responsible for dimerization. The latter are also important for binding to the TPR regions of cochaperones and Toc64. Although HSP70 and HSP90 do not share any sequence similarities, they both terminate with the amino acids EEVD, which have been shown to facilitate binding to TPR domains (Smith, 2004). In contrast to HSP70, the set of identified HSP90 client proteins is more limited. So far, transcription factors and kinases are among known clients, glucocorticoid receptors being the best characterized. Although even four cytosolic isoforms of HSP90 exist in *Arabidopsis* (Krishna and Gloor, 2001), HSP90 clients have not been analyzed in great detail in plants, with the exception of NLR (nucleotide binding and leucine-rich repeat) proteins, which function in plant immunity (Shirasu, 2009).

In order to investigate preprotein binding to chaperones, we have chosen wheat germ lysate as a model plant cytosol. Since preproteins are only present transiently in the plant cytosol, it is not feasible to work in a system involving whole plant cells. The wheat germ lysate is therefore uniquely suited to study the preprotein chaperone interactions, as it allows *in vitro* translation of preproteins, resulting in sufficient amounts of preproteins for further analysis of complex formation. Since only few examples of preproteins binding to cytosolic chaperones have been identified up to date, our aim in this study was to investigate whether HSP90 and 14–3–3 binding to preproteins is a guiding mechanism restricted to only a minor group of chloroplast proteins or whether it is a common principle in post-translational protein transport. Therefore, we have analyzed a large set of preproteins with respect to their binding to chaperones. Indeed, many of the tested preproteins were found to be associated with either HSP90 or 14–3–3. The mode of HSP90 and preprotein interaction was investigated further by the analysis of chimeric preproteins, demonstrating that neither the transit peptide nor the mature part of HSP90 clients is sufficient to mediate HSP90 binding. Furthermore, we present preproteins as the first client proteins of the HSP90 cochaperones FKBP73 (FK506 binding protein) and HOP (HSP70/HSP90 organizing protein) in plants and propose an extended model for chaperone and cochaperone binding of preproteins in the cytosol.

RESULTS

Classification of Preproteins Binding to HSP90 or 14–3–3

Qbadou et al. (2006) have identified three distinct proteins with the ability to bind HSP90 in a wheat germ lysate: pOE33, pNTT1, and pPC1. Furthermore, 14–3–3 proteins have been described to associate with the phosphorylated presequence of pSSU and pOE23 (May and Soll, 2000). In order to determine, whether binding to cytosolic chaperones is indeed a general phenomenon during the guiding of preproteins to the chloroplast, we have analyzed a larger number (41 preproteins) of *in vitro* translated proteins with respect to their ability to bind chaperones. The preproteins were selected from chloroplast localized proteins in order to cover a representative mixture of proteins in respect of their localization in the chloroplast, length of the transit peptide, and function of the mature protein. An overview of the preproteins, their associated chaperones, their functions, and their localization in the chloroplast is given in Table 1. The full-length cDNAs were transcribed *in vitro* and subsequently translated in a wheat germ lysate under conditions that favor the retention of the complex according to our experience (25°C, 40 min). The radioactively labeled proteins were co-immunoprecipitated immediately after the translation reaction with antibodies specifically recognizing HSP90, 14–3–3, or HSP70. All precipitated preproteins were separated by SDS–PAGE and preproteins associated with any of the three chaperones could then be detected by autoradiography (Figure 1A–1C). The quantified mean values of at least two independent experiments are represented in Figure 1A–1C. Values corresponding to the amount of precipitated preprotein with preimmunserum (PS)

Table 1. Summary and Description of All Analyzed Preproteins.

Protein/ abbreviation	Associated chaperone	Accession	Localization	Function	Reference
pAPE1	HSP90	At5g38660	Thylakoid	Acclimation of photosynthesis to environment	Sun et al., 2009
pAtpD	HSP90	At4g09650	Thylakoid	CF1–ATP synthase subunit	Friso et al., 2004
pClpP	HSP90	At1g11750	Stroma	Proteolytic subunit of Clp-type serine protease	Shanklin et al., 1995
pDHAR3	HSP90	At5g16710	Stroma	Dehydroascorbate reductase	Sun et al., 2009
pEMB1241	HSP90	At5g17710	Stroma	GrpE-like cochaperone	Sun et al., 2009
pGAPB	HSP90	At1g42970	Stroma	Glyceraldehyde 3-phosphate dehydrogenase	Sun et al., 2009
pHO1	HSP90	At2g26670	Stroma	Heme oxygenase	Muramoto et al., 1999
pNFU2	HSP90	At5g49940	Stroma	Iron sulfur cluster assembly	Leon et al., 2003
pPAC	HSP90	At2g48120	Stroma	Chloroplast development	Meurer et al., 1998
pPC1	HSP90	At1g76100	Lumen	Plastocyanin (photosyntetic electron transport)	Peltier et al., 2002
pPsaE1	HSP90	At4g28750	Thylakoid	Photosystem I subunit	Friso et al., 2004
pPsb29	HSP90	At2g20890	Stroma	Thylakoid formation	Wang et al., 2004
pATPR	14–3–3	At4g21210	Stroma	Phosphoprotein phosphatase/protein kinase	Sun et al., 2009
pCAO	14–3–3	At1g44446	Thylakoid	Chlorophyllid a oxygenase	Reinbothe et al., 2006
pDPE1	14–3–3	At5g64860	Stroma	4-alpha-glucanotransferase	Stettler et al., 2009
pGPS1	14–3–3	At4g36810	Stroma	Geranyl diphosphate synthase	Sun et al., 2009
pGS2	14–3–3	At5g35630	Stroma	Glutamin synthetase	Bartsch et al., 2008
pIM	14–3–3	At4g22260	Thylakoid	Terminal oxidase	Carol et al., 1999
pNdhM	14–3–3	At4g37925	Thylakoid	NDH complex subunit	Sun et al., 2009
pPetC	14–3–3	At4g03280	Thylakoid	cytb_6f complex subunit	Friso et al., 2004
pPGRL1.2	14–3–3	At4g11960	Thylakoid	Required for cyclic electron flow in photosystem I	DalCorso et al., 2008
pPORA	14–3–3	At4g27440	Stroma	NADPH-protochlorophyllide oxidoreductase	Sun et al., 2009
pSSU	14–3–3	AAA34116	Stroma	Ribulose 1,5 bisphosphate carboxylase subunit	Klein and Salvucci, 1992
p6PGDH	HSP70	At1g17650	Stroma	Glyoxylate reductase	Simpson et al., 2008
pAPO1	HSP70	At1g64810	Stroma	Accumulation of photosystem I	Watkins et al., 2011
pCAB1	HSP70	At1g29930	Thylakoid	Light-harvesting complex of photosystem II	Sun et al., 2009
pClp2	HSP70	At1g12410	Stroma	Clp protease subunit	Sun et al., 2009
pDSP4	HSP70	At3g52180	Stroma	Tyrosine protein phosphatase	Kerk et al., 2006
pEGY1	HSP70	At5g35220	Thylakoid	Membrane-associated metalloprotease	Chen et al., 2005
pFd2	HSP70	At1g60950	Stroma	Ferredoxin	Hanke et al., 2004
pFer1	HSP70	At5g01600	Stroma	Putative ferritin 1	Sun et al., 2009
pFNRL1	HSP70	At5g66190	Stroma	Ferredoxin-NADP$^{(+)}$-oxidoreductase	Lintala et al., 2007
pFtsZ	HSP70	At5g55280	Stroma	Chloroplast division	El Kafafi et al., 2008
pHCF101	HSP70	At3g24430	Stroma	Iron sulfur cluster assembly	Lezhneva et al., 2004
pLHCA5	HSP70	At1g45474	Thylakoid	Light-harvesting complex protein of photosystem I	Sun et al., 2009
pPsaK	HSP70	At1g30380	Thylakoid	Photosystem I subunit	Sun et al., 2009
pPsbS	HSP70	At1g44575	Thylakoid	Photosystem II subunit	Sun et al., 2009
pPsbT	HSP70	At3g21055	Thylakoid	Photosystem II subunit	Sun et al., 2009
pPsbX	HSP70	At2g06520	Thylakoid	Photosystem II subunit	Sun et al., 2009
pRPL28	HSP70	At2g33450	Stroma	L28-type protein of S50 ribosomal subunit	Sun et al., 2009
pSMTR	HSP70	At2g30200	Stroma	Malonyl-CoA:ACP transacylase	Sun et al., 2009

were subtracted as background from the values of HSP90, HSP70, and 14–3–3 pull-downs, which were set to 100%. To exclude the possibility of unspecific reactions of the PS with chaperones, we have tested the specificity of the antibodies and PS in wheat germ lysate (Supplemental Figure 1A). Since the wheat germ lysate might contain chaperones from proplastides, we confirmed the specific reactivity of our antibodies against the cytosolic isoforms. An immunoblot analysis of isolated wheat chloroplasts as well as wheat germ lysate demonstrated specific reactivity only against wheat germ lysate chaperones and not against the chloroplast isoforms (Supplemental Figure 1B).

Previous results have demonstrated an association of HSP70 along with HSP90 or 14–3–3 (May and Soll, 2000; Qbadou et al., 2006). We therefore only randomly tested the additional

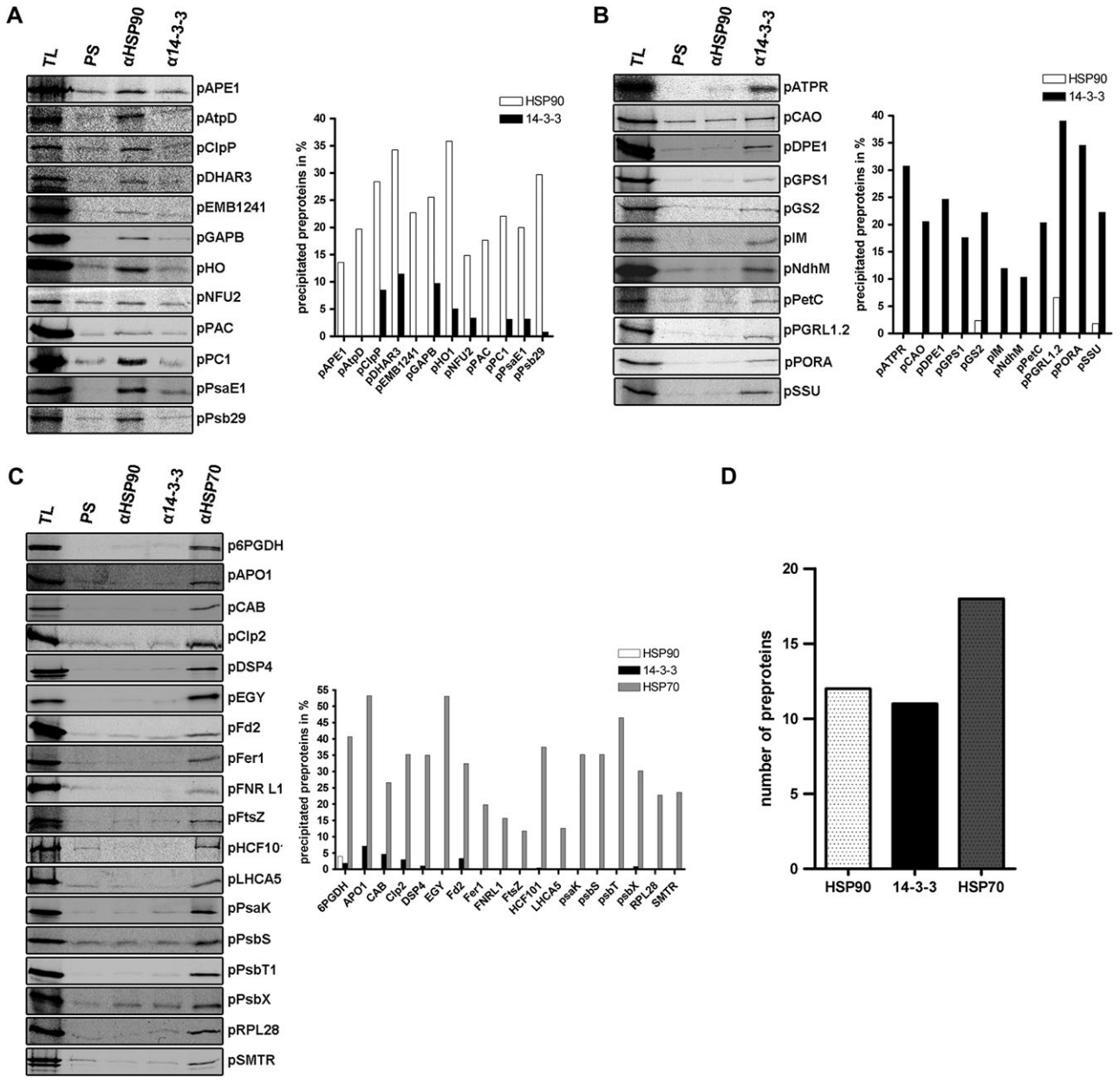

Figure 1. Identification of Chloroplast Preproteins Associating either with HSP70, HSP90, or 14–3–3.

(A–C) Radiolabeled preproteins were translated in wheat germ lysate and co-immunoprecipitated with antisera against HSP70, HSP90, 14–3–3, and PS as a control. A representative autoradiograph is shown in the left panels (A–C). 5% input of the translation product (TL) were loaded in lane 1. The amount of precipitated proteins was quantified from autoradiographs (A–C, right panels). The amount of precipitated HSP90, 14–3–3, and HSP70 was set to 100% in (A), (B), and (C), respectively, and the background (PS) was subtracted from all values. Mean values for at least two independent experiments are given. The preproteins can be divided into three classes: 12 proteins were found to bind HSP90 (A), 11 associated with 14–3–3 (B), and 18 interacted only with HSP70 (C).

(D) Distribution of the preproteins in the different classes.

association of HSP90/14–3–3 binding proteins with HSP70 (Supplemental Figure 1C). All preproteins that were found to be associated with neither HSP90 nor 14–3–3 were then tested for their ability to bind HSP70 (Figure 1C and 1D). The results revealed that complexes involving HSP70, HSP90, or 14–3–3 were almost evenly distributed among the analyzed proteins. Eighteen out of 41 proteins tested were found to be associated only with HSP70, 12 with HSP90, and 11 with 14–3–3 (Figure 1). Simultaneous binding of both HSP90 and 14–3–3 on the same preprotein was only detected in a few proteins to a neglectable extent. Our data suggest that HSP90 and 14–3–3 binding is a common feature in the post-translational

pathway of chloroplast preproteins. The results further establish preproteins as a distinguished class of HSP90 client proteins that have a common origin in the cytosol, but are highly diverse in function.

Neither the Transit Peptide nor the Mature Part of the Preprotein Is Sufficient to Mediate HSP90 Binding

In order to test whether HSP90 binds to the transit peptide, we generated a number of chimeric fusion proteins combining the N-terminal transit peptides of four HSP90 binding proteins—tpPC1, tpDHAR3, tpAPE1, and tpPsb29—with the mature part of SSU (mSSU), which only binds to HSP70 (May and Soll, 2000). The chimeric preproteins were translated in wheat germ lysate and co-immunoprecipitated with antibodies against HSP70, 14–3–3, and HSP90 as before. Interestingly, none of the chimeric proteins was able to bind HSP90, indicating that association of HSP90 does not solely occur within the transit peptides (Figure 2A). We therefore wondered whether HSP90 preferentially associates with the mature part of the proteins, possibly mediated by a partial folding of these parts of the proteins. Consequently, we generated chimeric proteins containing the mature parts of the HSP90 binding preproteins and the transit peptide of SSU (tpSSU), which binds 14–3–3. However, these proteins also did not associate with HSP90 but they maintained their ability to bind 14–3–3 (Figure 2B). These results indicate that HSP90 binding requires structural information from both the transit peptide and the mature part of the preprotein, to facilitate client protein association. This is unlike HSP70, which associated with all authentic and chimeric proteins in agreement with its client protein specificity, which recognizes exposed hydrophobic elements (Figure 2 and Supplemental Figure 1D).

HSP90 Containing Preprotein Complexes Are of High Molecular Weight

To investigate the oligomeric state of the heterocomplexes, we separated freshly translated preprotein complexes by size exclusion chromatography (Figure 3). Postribosomal supernatants of the translation products were subjected to a size exclusion matrix; the eluted fractions were precipitated by TCA, separated by SDS–PAGE, and visualized by autoradiography. The HSP90 binding preproteins pNFU2, pClpP, pEMB1241, and pPC1 displayed a similar elution pattern and were found in several fractions ranging from approximately 500–100 kDa (fractions 3–8), suggesting their association with the same cofactors. Fractions containing low-molecular-weight proteins most likely contain dissociated preproteins (fractions 10–11). The HSP70 and HSP90 machines are known to interact dynamically. HSP70 bound client proteins are very likely transferred to the HSP90 machine followed by the formation of several intermediate and transitory complexes until the client protein is released (Bracher and Hartl, 2006). Therefore, the wide molecular-weight range in which the HSP90 binding preproteins are found is consistent with the idea that HSP70, HSP90, and several other cochaperones are associated with the preprotein dynamically and sequentially, thus leading to the accumulation of different

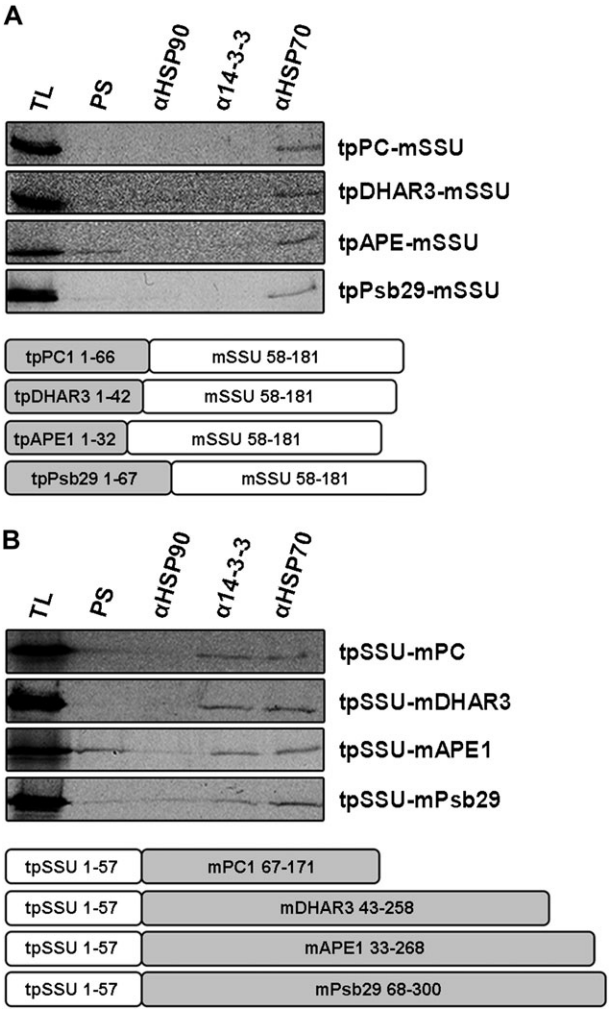

Figure 2. HSP90 Binding Requires Both the Transit Peptide and the Mature Part of the Preprotein.

(A) Chimeric proteins were generated using the indicated transit peptides of the HSP90 binding preproteins tpPC1, tpDHAR3, tpAPE1, and tpPsb29, fusing them with the mature mSSU (constructs are shown in the lower panel). All proteins were subjected to co-immunoprecipitation and were found to associate solely with HSP70 (upper panel).

(B) The mature parts of the same HSP90 binding preproteins were fused with tpSSU transit peptide. Co-immunoprecipitation revealed that binding of 14–3–3 in tpSSU was not abolished in the chimeric constructs, but no HSP90 binding occurred. Binding of HSP70 was not affected.

levels of intermediate complexes of preproteins with HSP70, HSP90, and cochaperones. All these intermediate complexes are present simultaneously in the wheat germ lysate during and after the translation process. In comparison, 14–3–3 binding preproteins are found in smaller complexes of approximately 120 kDa and only HSP70 binding proteins show no distinct elution pattern (Supplemental Figure 2).

FKBP73 Is an Interaction Partner of the HSP90 Preprotein Complex

Since the apparent size of the HSP90 preprotein complexes strongly suggested the involvement of additional cofactors,

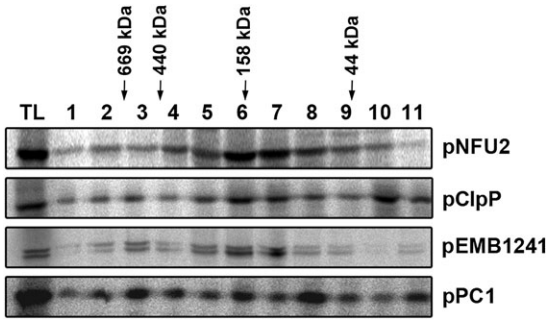

Figure 3. Chaperone-Bound Preproteins Accumulate in Higher Molecular Weight Complexes.

Postribosomal supernatants of translated pNFU2, pClpP, pEMB1241, and pPC1 were fractionated by size exclusion chromatography. The obtained fractions (1–11) were precipitated with TCA and separated on SDS–PAGE. All preproteins accumulated in higher-molecular-weight complexes of 500–100 kDa.

we attempted to identify further associated proteins by co-immunoprecipitation. pNFU2, which was shown to bind HSP90 (Figure 1A), as well as 14–3–3 binding pSSU were translated at a large scale (100 μl) and immunoprecipitation was performed using antibodies against either HSP90 or 14–3–3 and PS as a control (Figure 4A). Co-precipitated proteins were separated by SDS–PAGE and visualized by silver staining. Precipitated HSP90 (1) and 14–3–3 proteins (2) were visible in the respective samples and are marked with an asterisk at 90 and 29 kDa, respectively in Figure 4A. Note that preproteins and chaperones are not present in stochiometric amounts, since several isoforms of the chaperones are present in the wheat germ lysate and not all precipitated chaperone proteins are associated with preproteins. The HSP90 translation product ratio has been described to range from 300:1 to 1500:1 in reticulocyte lysate, which contains comparable amounts of HSP90 to wheat germ lysate (Supplemental Figure 1E and Dalman et al., 1989). Nevertheless, an additional band at ~65 kDa (indicated by an arrow in Figure 4A) was detected in the HSP90 as well as in the 14–3–3 precipitated sample and was therefore analyzed by mass spectrometry.

Peptides matching two interesting proteins were identified exclusively in the HSP90 precipitated sample. One of the proteins was found to be the immunophilin FKBP73 (62 kDa), recently identified in wheat (Blecher et al., 1996). Matching peptides for FKBP73 are given in Supplemental Figure 3 (coverage 59%). FKBP73 belongs to the superfamily of peptidyl prolyl *cis/trans* isomerases, which are known to act as cochaperones for HSP90. They interact with HSP90 via a TPR domain and thus promote stable association of the client proteins during their maturation.

As a further confirmation that the immunophilin specifically interacts with the preprotein chaperone complex, both FKBP73 and HSP90 could be directly co-immunoprecipitated together using an antiserum against the translated preprotein pPC1 (Figure 4B, lane 4). Efficient pull-down of pPC1 is demonstrated by detection of the radiolabeled preprotein (lower panel). Both FKBP73 and HSP90 (upper and middle panels) could be detected associated with the preprotein by immunoblotting with the respective antibodies. Neither pPC1 nor the chaperones were detected in the control (lane 5), where a mock precipitation was performed with PS and pPC1 translation product. In addition, the following further co-immunoprecipitation with HSP90 antibodies was performed as controls and confirmation. pNFU2 (lane 1), which was used in the initial experiment (Figure 4A), was also found to associate with FKBP73 (upper panel). In another mock pull down with HSP90 antibodies of 14–3–3 binding pSSU translation product (lane 2), small amounts of FKBP73 were co-precipitated (upper panel), although no pSSU was precipitated (controls for efficient translation are presented in Figure 4C), showing that FKBP73 and HSP90 are associated also in the absence of preproteins in wheat germ lysate. However, further unidentified client proteins of HSP90 might exist in this heterogeneous protein mixture. As expected, an increasing amount of precipitated FKBP73 can be observed in the presence of preproteins (pPC1 and pNFU2).

To additionally confirm the interaction of FKBP73 with preproteins, we used FKBP73 antisera, which successfully co-precipitated wheat germ translated pPC1 along with FKBP73 (Figure 4D). Both proteins are not precipitated with PS from translated pPC1.

Identification of a Novel Wheat cDNA Encoding for a Protein with High Similarity to HOP

Mass spectrometric results of the HSP90 co-precipitated analyzed band in Figure 4A (also containing HSP70 and FKBP73) retrieved a third protein with a rather high coverage (23%) of 65 kDa. The identified peptides aligned with an unknown maize protein (NP001151932). Sequence analysis of this maize protein revealed a close homology to the HOP protein from other organisms (Supplemental Figure 4 and Figure 5B), since it contained the three typical TPR regions. Therefore, the corresponding wheat cDNA was amplified and sequenced. The retrieved wheat (*Triticum aestivum*) HOP (TaHOP) protein sequence was aligned with the maize sequence and found to be 86.5% identical. The peptides obtained from the mass spectrometric analysis fitted perfectly on the deduced protein sequence (Figure 5A). We therefore conclude that we identified a HOP cochaperone from wheat. HOP is known from other organisms to interact with both HSP70 and HSP90, thus allowing the transfer of client proteins from HSP70 to HSP90 (Smith, 2004). Proteins similar to HOP in plants are described only in soybean, where three HOP isoforms have been isolated (Zhang et al., 2003). TaHOP contains three tandem repeats of the conserved 34-amino acid consensus sequence [WLF]-X(2)-[LIM]-[GAS]-X(2)-[YLF]-X(8)-[ASE]-X(3)-[FYL]-X(2)-[ASL]-X(4)-[PKE] in each TPR motif (Figure 5B), which is also the case for all other HOP proteins. A protein alignment of the newly identified wheat HOP (Supplemental Figure 4) and the described soybean HOP revealed a sequence identity of 62.2%. For the non-plant homologs in *Homo sapiens* (HsHOP) and

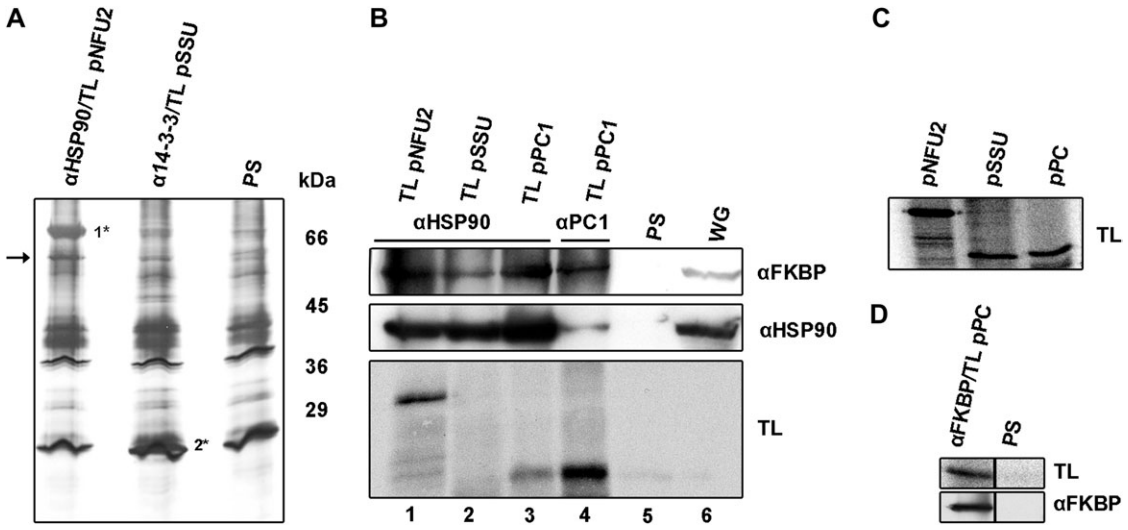

Figure 4. The HSP90 Preprotein Complex Contains FKBP73.

(A) Translated pSSU and pNFU2 were co-immunoprecipitated with 14–3–3 and HSP90 antisera, respectively. PS was used as a control. The precipitated proteins were separated by SDS–PAGE and silver stained. HSP90 and 14–3–3 proteins are clearly visible in the stained gel, indicated as 1* and 2*, respectively. An additional band appeared at ~65 kDa, in both the 14–3–3 and the HSP90 precipitated sample, but not the PS control. The band was therefore analyzed by mass spectrometry and found to contain HSP70 in both cases. The HSP90 precipitated sample contained two further proteins in the same band: FKBP73 and HOP (matching peptides are shown in Supplemental Figure 2 and Figure 5A, respectively). The analyzed band is indicated by an arrow.

(B) The interaction between FKBP73 and the HSP90 preprotein complex was further confirmed by pull-down experiments with HSP90 and pPC1 antisera. Translated pNFU2 and pPC1 were pulled down with HSP90 antisera, in contrast to pSSU (lanes 1–3, lower panel). Efficient translation of pSSU is shown in (C). Note that radioactively labeled pSSU is absent from this probe. In all three sample, co-immunoprecipitated FKBP73 could be detected by immunoblotting (upper panel) along with HSP90 (middle panel). The amount of precipitated FKBP73 in the sample containing translated pSSU (lane 2) is significantly lower compared with the samples containing pNFU2 and pPC1, resulting from the association of HSP90 and FKBP73 without substrate protein. Precipitation of FKBP73 and HSP90 and pPC1 with pPC1 antisera (lane 4) proves the interaction of the three proteins. No proteins were detected in a mock precipitation of pPC1 with PS (lane 5). 20 μg of wheat germ lysate were loaded in lane 6 (wheat germ) as a control.

(C) Translation input used for the co-immunoprecipitation in *B* of pNFU2, pSSU, and pPC1 is shown.

(D) Translated and radioactively labeled pPC1 could be successfully precipitated with specific FKBP73 antisera, but not with PS. Samples were run on the same gel.

Saccharomyces cerevisiae (ScHOP), the consensus reached 43.7% and 38.4%, respectively. A blast search against the *Arabidopsis* database led to the identification of three closely related isoforms to the TaHOP protein, recently assigned as AtHOP1–3 (Prasad et al., 2010). The three proteins are 62.8% identical in their amino acid composition and share 51.5% identity with TaHOP. Up to date, no client proteins have been identified for plant HOP homologs nor is it known which cellular processes theses cochaperones are involved in.

HOP Is Associated with the Preprotein Complex

Since HOP is known to associate with HSP90 via its TPR domains, it was necessary to test its direct participation in the formation of the preprotein complex. We precipitated pPC1 translation product using PC1 antisera and sequenced a band corresponding to the molecular weight of HOP. Indeed, four peptides matching the TaHOP protein were identified (coverage: 9.9%), indicated with zigzag lines in Figure 5A. As a control reaction, 14–3–3 binding pSSU was used for a mock co-immunoprecipitation with pPC1 antisera. The corresponding band yielded no peptides matching TaHOP.

DISCUSSION

The data obtained demonstrate that major components of the HSP90 machinery are involved in chaperoning preproteins in the plant cytosol. Taking information on the HSP70/HSP90 cycle into account as it is known from mammalian systems (Bracher and Hartl, 2006), we have developed a working hypothesis (Figure 6). Most likely, all preproteins interact with HSP70 directly after translation, providing an immediate protection against protein aggregation and misfolding. This subsequently leads to the association of HSP90 in a subclass of preproteins—a process assisted by HOP, which binds to HSP90 and HSP70 simultaneously through separate TPR domains. Therefore, FKBP73 probably replaces HOP associating with HSP90 with its TPR domain (Owens-Grillo et al., 1996). This might have a stabilizing effect on the complex until the preprotein complex reaches the chloroplast. HSP90 can then mediate docking at the translocon component Toc64, from where the preprotein is transferred to the transit peptide receptor Toc34 and finally imported into the chloroplast. Possibly, the HSP90 pathway is restricted to preproteins that tend

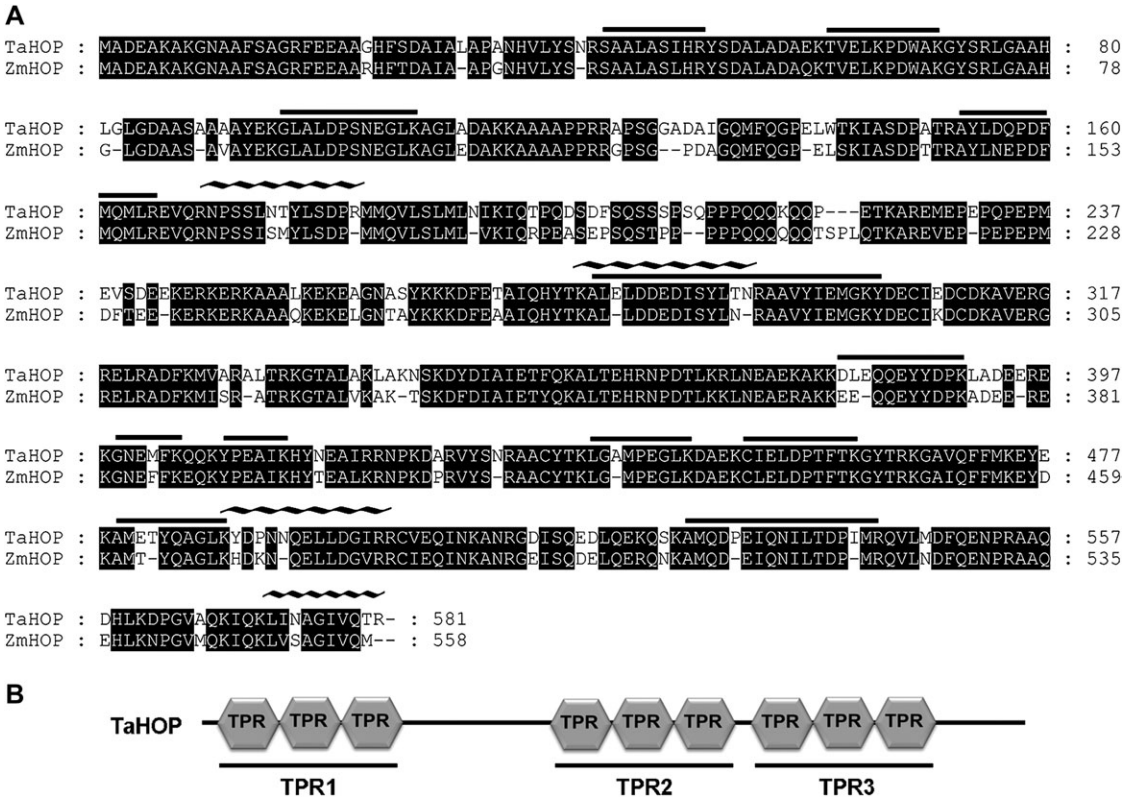

Figure 5. HOP Specifically Interacts with the HSP90 Preprotein Chaperone Complex.

(A) Sequence alignment of HOP in *Z. mays* (ZmHOP) and *T. aestivum* (TaHOP). The protein sequences show 80% identity. Sequenced peptides from the sample described in Figure 4A are indicated with bold lines; zigzag lines indicate peptides obtained from a pull-down with PC1 antisera.

(B) TaHOP domain structure.

to adapt a higher-order secondary structure during their passage through the cytosol in comparison to proteins only binding to HSP70. However, since Toc64 is dispensable for viability in *Arabidopsis* and *Physcomitrella* (Hofmann and Theg, 2005; Aronsson et al., 2007), the pathway can be bypassed and preproteins associated with either only HSP70 or HSP90 and HSP70 can still be recognized by the TOC translocon in the absence of Toc64. In this case, HSP90 might dissociate from the preprotein before the chloroplast surface is reached and the preprotein enters the channel via Toc34. Phosphorylated preproteins, in association with HSP70 and 14–3–3 proteins, represent another form of chaperoned preproteins, which show greatly improved import kinetics in comparison to non-phosphorylated proteins.

The association of chloroplast preproteins with either HSP90 or 14–3–3 has been shown in the past using only very few client proteins (May and Soll, 2000; Qbadou et al., 2006). It remains unclear whether formation of these chaperone complexes is a common feature in escorting preproteins across the cytosol and thus represents a general phenomenon. We therefore analyzed an extensive subset of preproteins in respect to their associated chaperones after translation. The preproteins were selected randomly in order to avoid any biased results. Eighteen of the analyzed preproteins only bound to HSP70, although an association with yet unidentified chaperones cannot be excluded and remains to be investigated. Nevertheless, our co-immunoprecipitation experiments indicate that binding to HSP90 and 14–3–3 is not a rare exception, but that more than half of the preproteins are using this more complex route. Moreover, 12 of these preproteins tested specifically bound to HSP90. This is intriguing, since the number of known HSP90 client protein classes is quite limited in other organisms in contrast to HSP70 client proteins. HSP90 is mainly known to assist kinases and hormone receptors in yeast and mammals, and although the list of client proteins has grown in the past years, a binding motif in these client proteins is not known up to date (Wandinger et al., 2008; Taipale et al., 2010). In an attempt to find a consensus in our newly identified clients, we have analyzed them in respect to their amino acid distribution, localization within the chloroplast, and expression levels (Table 1 and data not shown). However, no consistency could be detected in primary sequence elements or functional properties of the proteins, unlike HSP70, which is known to recognize short hydrophobic motifs (Rudiger et al., 1997). Apparently, choosing of a cytosolic routing pathway depends neither on preprotein function and localization in the chloroplast nor on obvious

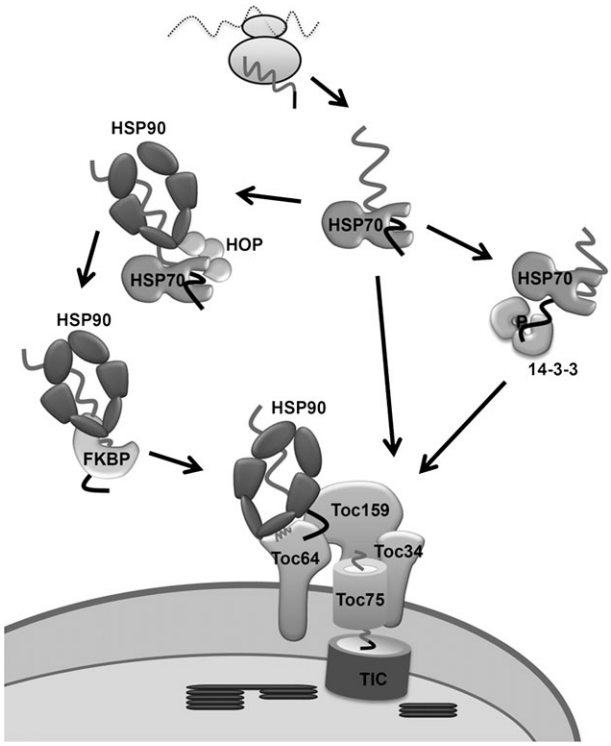

Figure 6. Working Model for the Interaction of Preproteins with Chaperones in the Plant Cytosol.

Preproteins either sequentially associate with components of the HSP90 chaperone machinery or with 14–3–3 proteins. Alternatively, preproteins only interact with HSP70. HOP interacts with HSP70 and HSP90 chaperones and thus could transfer the substrate protein. Furthermore, the immunophilin FKBP73 interacts with the chaperon complex, possibly acting as a stabilizing factor.

features of the proteins. Moreover, our results indicate an involvement of the entire preprotein in HSP90 recognition and/or association, since chimeric proteins with exchanged transit peptides and exchanged mature parts maintained their ability to bind HSP70 and 14–3–3, but could no longer associate with HSP90. The exact natures of the required amino acids for HSP90 recognition most likely differ for each protein and remain to be elucidated.

HSP90 mediated guiding of the chloroplast preproteins and the TPR mediated docking at Toc64 is not essential for plant viability, since plants lacking Toc64 do not show any effects on protein import under standard conditions (Hofmann and Theg, 2005; Aronsson et al., 2007). The role of HSP90 mediated recognition at the chloroplast membrane could therefore be a regulative pathway during chloroplast development or under stress conditions.

Although four homologs of HSP90 are located in the plant cytosol, our knowledge of their functions and interactions with client proteins in plants is limited. Several studies making use of HSP90 knockdown lines and plants treated with HSP90 inhibitors suggest a general involvement in buffering of genetic variation (Queitsch et al., 2002; Sangster et al., 2007, 2008). Moreover, an involvement in disease resistance has been implied, since plant NLR proteins (nucleotide binding and leucine-rich repeat protein), which confer resistance to pathogens, are HSP90 client proteins (Hubert et al., 2003). They associate with two other components—RAR1 and SGT1—and are thereby kept in a signal competent conformation and possibly stabilized against degradation. SGT1, which has a TPR domain, interacts with HSP90 and HSP70 (Noel et al., 2007; Stuttmann et al., 2008), thus fulfilling a similar function to HOP. Both SGT1 and RAR1 are also predicted to have structural homology to the HSP90 cochaperone p23 (Hubert et al., 2003, 2009). It therefore seems that the plant resistance machinery makes use of a very specialized set of HSP90 cochaperones to meet its needs, in a similar manner as Cdc37 in mammalian systems, which acts as a specific cochaperone for HSP90 associated kinases (Taipale et al., 2010).

Direct evidence for a functional HSP90 machinery in plants involving 'classical' cochaperones, such as HOP or immunophilins, has experimentally only been partly analyzed *in vitro* using human client proteins (Reddy et al., 1998; Zhang et al., 2003). Therefore, the second aim of our study was to identify further components involved in the HSP90 complex. Mass spectrometric analysis of proteins co-immunoprecipitated with HSP90 revealed the presence of two such cochaperones. A HOP-like protein was identified, as well as an immunophilin, FKBP73. Since HSP70 is possibly always a component of the preprotein chaperone complexes (May and Soll, 2000; Rial et al., 2000; Qbadou et al., 2006), it is feasible to assume that preproteins associate with HSP70 immediately after translation and are then passed on to HSP90 mediated by HOP. Sequence analyses of several plant genomes indicated the presence of HOP in several plant species, often as multi-gene families. Nevertheless, no client proteins have been identified *in vivo* so far (Zhang et al., 2003).

Wheat FKBP73 has been described as a protein with chaperone function *in vitro*, using citrate synthase as a client protein and FKBP73 also has been found associated with HSP90 in wheat germ lysate (Kurek et al., 2002). However, true clients of plant FKBPs have not been identified in contrast to its mammalian homologs FKBP51 and FKBP52, which have a well assigned function as HSP90 cochaperones participating in maturation of steroid hormone receptors (Schiene-Fischer and Yu, 2001). FKBP73 is constitutively expressed in young tissues and does not show a striking phenotype upon overexpression, differing from its stress-induced isoform FKBP77, where overexpressors suffered from morphological abnormalities (Kurek et al., 1999, 2002). Two homologous isoforms are found in *Arabidopsis*—ROF1 (FKBP67) and ROF2 (FKBP65)—which have recently been shown to be involved in thermotolerance (Kurek et al., 1999; Aviezer-Hagai et al., 2007; Meiri and Breiman, 2009; Meiri et al., 2010). All these interactions have so far been found to occur with AtHSP90.1; the function or redundancy of other *Arabidopsis* isoforms remains to be established. In this study, we present FKBP73 as a cochaperone of chloroplast preproteins.

Since, so far, no binding motif or structural property of a protein could definitely be assigned to induce HSP90 binding,

cofactors have been suggested to be involved in mediating HSP90 and client protein complex formation (Taipale et al., 2010). Considering that it was previously shown that no HSP90 preprotein complexes are formed with chloroplast preproteins in reticulocyte lysate (Qbadou et al., 2006), it is tempting to assume that either HOP or FKBP73 act as a plant-specific factor, conferring interaction with HSP90. Interestingly, a study of the cochaperones in mammalian HSP90 preprotein complexes could not identify immunophilins within the complexes (Bhangoo et al., 2007), again supporting the idea that immunophilins act as specific components conferring recognition of plastid preproteins.

In summary, our data could establish a large number of preproteins, which associate with HSP90 or 14–3–3 proteins in wheat germ lysate. Additionally, two partner proteins were identified, which are involved in the HSP90 preprotein complex, namely HOP and FKBP73.

METHODS

Sequence Analysis and Cloning of Wheat HOP

Blast searches and analysis of conserved protein domains were performed using NCBI Blast (Altschul et al., 1990) and Prosite (Hulo et al., 2006). Protein alignments were performed with AlignX/ClustalW (Invitrogen). Wheat (*Triticum aestivum* (Ta)) RNA was isolated (RNeasy, Qiagen) from 7-day-old wheat, grown under greenhouse conditions. cDNA was generated using M-MLV reverse transcriptase (Invitrogen). Subsequently, the full-length cDNA of wheat HOP (TaHOP) was amplified using the following oligonucleotides: TaHOP-for: 5′-CGATGCTAGCGCCGACGAGGCGAAGGC-3′, TaHOP-rev: 5′-CGATCTCGAGTCTCGTTTGGACTATTCCAG-3′, introducing a *Nhe*I and a *Xho*I restriction site for further subcloning. The PCR fragment was cloned blunt end into PCRII blunt (Invitrogen) and sequenced.

Cloning of cDNAs Encoding for Preproteins and Generation of Chimeric Preproteins

Randomly selected full-length cDNAs of preproteins were either amplified from *A. thaliana* Col-0 cDNA or templates were obtained from other sources and cloned into a pSP65 or pF3A (Promega) vector, both allowing translation under the SP6 promoter. With the exception of pSSU (*Nicotiana tabacum*), all genes were from *Arabidopsis* (see Table 1 for accessions). ChloroP was used for the determination of transit peptide sequences (Emanuelsson et al., 1999). Chimeric constructs were generated by overlap PCR, using appropriate oligonucleotides fusing the desired gene fragments. All used oligonucleotides are available on request.

In Vitro Transcription and Translation

In vitro transcription was performed from linearized template plasmids with SP6 RNA polymerase (Fermentas). Translation active wheat germ lysate was prepared as follows. Fresh wheat germs were floated in a mixture of carbontetrachloride with n-Hexan (ratio 4:1). The floating germs were dried, ground in liquid nitrogen, and suspended in homogenization buffer (20 mM HEPES/KOH pH 7.6, 50 mM KAc, 2.5 mM MgAc, 1 mM $CaCl_2$, 2 mM DTT, 0.1 mM Benzamidine (BAM), 2.5 mM Aminocaproic acid (ACA), 0.2 U ml^{-1} Rnasin). The suspension was centrifuged twice (64 000 *g*, 30 min, 4°C) and the supernatant subjected to a sephadex G-25 (GE Healthcare) matrix. Eluted fractions were tested for their translational activity, frozen in liquid nitrogen, and stored at –80°C. Protein synthesis occurred in a mixture containing 50% wheat germ lysate, 14 mM HEPES/KOH pH 7.6, 1.25 mM MgAc, 2 mM DTT, 1.25 mM ATP, 1.25 mM GTP, 0.4 mM Spermidine, 0.05 mM wheat tRNA, 16 mM creatine phosphate, 0.45mg creatine phosphate kinase, and 1 mM of each amino acid. In the case of radioactive labeling of the translation product, 11 μCi ^{35}S-labeled Methionine and Cysteine (Perkin Elmer, Massachusetts, USA) was added per 10-μl sample. One to 10% *in vitro* transcribed RNA of the translation volume was added to the translation reaction. The ideal amount of KAc was determined for each transcript and added in an appropriate amount (0–100 mM). The translation reaction was performed for 40 min at 25°C. 10 mM ADP was added directly after the translation for stabilization of the HSP90 complex and the postribosomal supernatant (centrifugation for 10 min, 40 000 *g*, 4°C) was used for all further experiments.

Antisera Production and Immunoprecipitation

Coding sequences for wheat HSP70, HSP90, and pea 14–3–3 (May and Soll, 2000) were cloned into pET21d$^+$ (Novagen), overexpressed in *E. coli*, and purified via Ni-NTA-affinity chromatography. Polyclonal antisera against the purified proteins were generated by Biogenes (Berlin, Germany). PC1 and FKBP73 Antisera were kindly provided by Jörg Meurer and Adina Breiman, respectively. The HSP90 antiserum 4F3.E8 (HSP90 total) from StressMarq Biosciences (Victoria, Canada) was used for detection of HSP90 in wheat germ and reticulocyte lysate.

For immunoprecipitation experiments, antisera were coupled to protein A Sepharose CL-4B (GE Healthcare) and binding of wheat germ proteins was performed for 30 min at 4°C. Since preproteins reside in the cytosol *in vivo* for only a short time, the interaction was also tested after 15 min to exclude the possibility of unspecific interactions (Supplemental Figure 1G). PBS buffer was used as a binding and washing buffer. Proteins were eluted in SDS–PAGE loading buffer (0.25 M Tris-HCl, pH 6.8, 8% SDS, 40% glycerol, 20% β-mercaptoethanol, and 0.016% Bromophenol Blue). Autoradiographs were quantified using the AIDA image analyzer software. For subsequent mass spectrometry, the antisera were cross-linked with 0.02 M dimethyl pimelimidate to protein A Sepharose.

SDS–PAGE, Immunoblotting, and Mass Spectrometry

Proteins were separated on 12% or 15% polyacrylamide gels and radiolabeled proteins were detected by autoradiography. Gels were stained with either coomassie or silver for mass

spectrometry (Helmut Blum, 1987). For immunodetection, proteins were transferred onto PVDF (polyvinylidenfluorid) membrane, incubated with specific antibodies, and visualized by chemiluminescence with a solution containing 1% luminol, 0.18% H_2O_2, and 0.44% coomaric acid.

Mass spectrometric analyses were performed either at the Protein Analysis Unit of the Adolf-Butenandt-Institute (Ludwig-Maximilians-Universität, Munich, Germany) or at the mass spectrometry service of the Department Biologie I (Ludwig-Maximilians-Universität, Munich, Germany).

Size Exclusion Chromatography

Wheat germ translated proteins were centrifuged (2 × 10 min, 390 000 *g*, 4°C) and loaded onto a size exclusion column (G3000SWXL; Tosoh Bioscience). 50 mM sodium phosphate pH 7.0 and 300 mM NaCl was used as a running buffer. Samples of 0.25ml fractions were collected, precipitated by 15% TCA, separated by SDS–PAGE, and signals were visualized by autoradiography. Molecular weights were calculated according to the calibration of the column with standard proteins from the gel filtration HMW calibration kit (GE Healthcare).

Wheat Chloroplast Isolation

Chloroplasts were isolated from 7-day-old wheat leaves according the same procedure as applied earlier for the isolation of pea chloroplasts (Waegemann and Soll, 1996).

Accession Numbers

Sequence data from this article can be found in the NCBI data libraries under accession numbers: NP001151932 (Maize HOP), HM998695 (HOP *T. aestivum*), At1g12270 (AtHOP-1), At1g62740 (AtHOP-2), At4g12400 (AtHOP-3), GmHOP (X79770), HsHOP (M86752), and ScHOP (M28486), 3023751 (FKBP73 *T. aestivum*).

SUPPLEMENTARY DATA

Supplementary Data are available at *Molecular Plant Online.*

FUNDING

This work was supported by the DFG.

ACKNOWLEDGMENTS

We would like to thank the Protein Analysis Unit at the Adolf-Butenandt-Institute (Ludwig-Maximilians-Universität, Munich, Germany) as well as the mass spectrometry service of the Department Biologie I (Ludwig-Maximilians-Universität, Munich, Germany) for mass spectrometry analyses and Ulrike Oster (Ludwig-Maximilians-Universität, Munich, Germany) for the analysis of protein sequencing results. We greatly appreciate the generous gift of antisera from Adina Breiman (Tel Aviv University, Tel Aviv, Israel), Brian Freeman (University of Illinois, Urbana, USA), and Jörg Meurer (Ludwig-Maximilians-Universität, Munich, Germany). Dario Leister and Jörg Meurer are further acknowledged for providing cDNA clones (Ludwig-Maximilians-Universität, Munich, Germany). We would like to express our gratitude to Roland Beckmann and Shashi Bhushan (Ludwig-Maximilians-Universität, Munich, Germany) for their support in wheat germ preparation. No conflict of interest declared.

REFERENCES

Altschul, S.F., Gish, W., Miller, W., Myers, E.W., and Lipman, D.J. (1990). Basic local alignment search tool. J. Mol. Biol. **215,** 403–410.

Aronsson, H., Boij, P., Patel, R., Wardle, A., Topel, M., and Jarvis, P. (2007). Toc64/OEP64 is not essential for the efficient import of proteins into chloroplasts in *Arabidopsis thaliana*. Plant J. **52,** 53–68.

Aviezer-Hagai, K., et al. (2007). *Arabidopsis* immunophilins ROF1 (AtFKBP62) and ROF2 (AtFKBP65) exhibit tissue specificity, are heat-stress induced, and bind HSP90. Plant Mol. Biol. **63,** 237–255.

Balsera, M., Soll, J., and Bolter, B. (2009). Protein import machineries in endosymbiotic organelles. Cell Mol. Life Sci. **66,** 1903–1923.

Bartsch, S., et al. (2008). Three thioredoxin targets in the inner envelope membrane of chloroplasts function in protein import and chlorophyll metabolism. Proc. Natl Acad. Sci. U S A. **105,** 4933–4938.

Bhangoo, M.K., Tzankov, S., Fan, A.C., Dejgaard, K., Thomas, D.Y., and Young, J.C. (2007). Multiple 40-kDa heat-shock protein chaperones function in Tom70-dependent mitochondrial import. Mol. Biol. Cell. **18,** 3414–3428.

Blecher, O., Erel, N., Callebaut, I., Aviezer, K., and Breiman, A. (1996). A novel plant peptidyl-prolyl-*cis-trans*-isomerase (PPIase): cDNA cloning, structural analysis, enzymatic activity and expression. Plant Mol. Biol. **32,** 493–504.

Bracher, A., and Hartl, F.U. (2006). Hsp90 structure: when two ends meet. Nat. Struct. Mol. Biol. **13,** 478–480.

Carol, P., et al. (1999). Mutations in the *Arabidopsis* gene IMMUTANS cause a variegated phenotype by inactivating a chloroplast terminal oxidase associated with phytoene desaturation. Plant Cell. **11,** 57–68.

Chen, G., Bi, Y.R., and Li, N. (2005). EGY1 encodes a membrane-associated and ATP-independent metalloprotease that is required for chloroplast development. Plant J. **41,** 364–375.

Chew, O., et al. (2004). A plant outer mitochondrial membrane protein with high amino acid sequence identity to a chloroplast protein import receptor. FEBS Lett. **557,** 109–114.

DalCorso, G., et al. (2008). A complex containing PGRL1 and PGR5 is involved in the switch between linear and cyclic electron flow in *Arabidopsis*. Cell. **132,** 273–285.

Dalman, F.C., Bresnick, E.H., Patel, P.D., Perdew, G.H., Watson, S.J., Jr. and Pratt, W.B. (1989). Direct evidence that the glucocorticoid receptor binds to hsp90 at or near the termination of receptor translation *in vitro*. J. Biol. Chem. **264,** 19815–19821.

El Kafafi, E., et al. (2008). Developmentally regulated association of plastid division protein FtsZ1 with thylakoid membranes in *Arabidopsis thaliana*. Biochem. J. **409,** 87–94.

Emanuelsson, O., Nielsen, H., and von Heijne, G. (1999). ChloroP, a neural network-based method for predicting chloroplast transit peptides and their cleavage sites. Protein Sci. **8,** 978–984.

Fan, A.C., Bhangoo, M.K., and Young, J.C. (2006). Hsp90 functions in the targeting and outer membrane translocation steps of Tom70-mediated mitochondrial import. J. Biol. Chem. **281,** 33313–33324.

Friso, G., et al. (2004). In-depth analysis of the thylakoid membrane proteome of *Arabidopsis thaliana* chloroplasts: new proteins, new functions, and a plastid proteome database. Plant Cell. **16,** 478–499.

Hanke, G.T., Kimata-Ariga, Y., Taniguchi, I., and Hase, T. (2004). A post genomic characterization of *Arabidopsis* ferredoxins. Plant Physiol. **134,** 255–264.

Helmut Blum, D.H.B.H.J.G. (1987). Improved silver staining of plant proteins, RNA and DNA in polyacrylamide gels. Electrophoresis. **8,** 93–99.

Hofmann, N.R., and Theg, S.M. (2005). Toc64 is not required for import of proteins into chloroplasts in the moss *Physcomitrella patens*. Plant J. **43,** 675–687.

Hubert, D.A., et al. (2003). Cytosolic HSP90 associates with and modulates the *Arabidopsis* RPM1 disease resistance protein. EMBO J. **22,** 5679–5689.

Hubert, D.A., He, Y., McNulty, B.C., Tornero, P., and Dangl, J.L. (2009). Specific *Arabidopsis* HSP90.2 alleles recapitulate RAR1 cochaperone function in plant NB-LRR disease resistance protein regulation. Proc. Natl Acad. Sci. U S A. **106,** 9556–9563.

Hulo, N., et al. (2006). The PROSITE database. Nucleic Acids Res. **34,** D227–D230.

Jarvis, P. (2008). Targeting of nucleus-encoded proteins to chloroplasts in plants. New Phytol. **179,** 257–285.

Kerk, D., et al. (2006). A chloroplast-localized dual-specificity protein phosphatase in *Arabidopsis* contains a phylogenetically dispersed and ancient carbohydrate-binding domain, which binds the polysaccharide starch. Plant J. **46,** 400–413.

Klein, R.R., and Salvucci, M.E. (1992). Photoaffinity labeling of mature and precursor forms of the small subunit of ribulose-1,5-bisphosphate carboxylase/oxygenase after expression in *Escherichia coli*. Plant Physiol. **98,** 546–553.

Krishna, P., and Gloor, G. (2001). The Hsp90 family of proteins in *Arabidopsis thaliana*. Cell Stress Chaperones. **6,** 238–246.

Kurek, I., Aviezer, K., Erel, N., Herman, E., and Breiman, A. (1999). The wheat peptidyl prolyl *cis- trans*-isomerase FKBP77 is heat induced and developmentally regulated. Plant Physiol. **119,** 693–704.

Kurek, I., Pirkl, F., Fischer, E., Buchner, J., and Breiman, A. (2002). Wheat FKBP73 functions *in vitro* as a molecular chaperone independently of its peptidyl prolyl *cis-trans* isomerase activity. Planta. **215,** 119–126.

Leon, S., Touraine, B., Ribot, C., Briat, J.F., and Lobreaux, S. (2003). Iron–sulphur cluster assembly in plants: distinct NFU proteins in mitochondria and plastids from *Arabidopsis thaliana*. Biochem. J. **371,** 823–830.

Lezhneva, L., Amann, K., and Meurer, J. (2004). The universally conserved HCF101 protein is involved in assembly of [4Fe–4S]-cluster-containing complexes in *Arabidopsis thaliana* chloroplasts. Plant J. **37,** 174–185.

Lintala, M., et al. (2007). Structural and functional characterization of ferredoxin-$NADP^+$-oxidoreductase using knock-out mutants of *Arabidopsis*. Plant J. **49,** 1041–1052.

Martin, T., Sharma, R., Sippel, C., Waegemann, K., Soll, J., and Vothknecht, U.C. (2006). A protein kinase family in *Arabidopsis* phosphorylates chloroplast precursor proteins. J. Biol. Chem. **281,** 40216–40223.

Martin, W., Stoebe, B., Goremykin, V., Hapsmann, S., Hasegawa, M., and Kowallik, K.V. (1998). Gene transfer to the nucleus and the evolution of chloroplasts. Nature. **393,** 162–165.

May, T., and Soll, J. (2000). 14–3–3 proteins form a guidance complex with chloroplast precursor proteins in plants. Plant Cell. **12,** 53–64.

Meiri, D., and Breiman, A. (2009). *Arabidopsis* ROF1 (FKBP62) modulates thermotolerance by interacting with HSP90.1 and affecting the accumulation of HsfA2-regulated sHSPs. Plant J. **59,** 387–399.

Meiri, D., et al. (2010). Involvement of *Arabidopsis* ROF2 (FKBP65) in thermotolerance. Plant Mol. Biol. **72,** 191–203.

Meurer, J., Grevelding, C., Westhoff, P., and Reiss, B. (1998). The PAC protein affects the maturation of specific chloroplast mRNAs in *Arabidopsis thaliana*. Mol. Gen. Genet. **258,** 342–351.

Muramoto, T., Kohchi, T., Yokota, A., Hwang, I., and Goodman, H.M. (1999). The *Arabidopsis* photomorphogenic mutant *hy1* is deficient in phytochrome chromophore biosynthesis as a result of a mutation in a plastid heme oxygenase. Plant Cell. **11,** 335–348.

Noel, L.D., et al. (2007). Interaction between SGT1 and cytosolic/nuclear HSC70 chaperones regulates *Arabidopsis* immune responses. Plant Cell. **19,** 4061–4076.

Owens-Grillo, J.K., Stancato, L.F., Hoffmann, K., Pratt, W.B., and Krishna, P. (1996). Binding of immunophilins to the 90 kDa heat shock protein (hsp90) via a tetratricopeptide repeat domain is a conserved protein interaction in plants. Biochemistry. **35,** 15249–15255.

Pearl, L.H., and Prodromou, C. (2006). Structure and mechanism of the Hsp90 molecular chaperone machinery. Annu. Rev. Biochem. **75,** 271–294.

Peltier, J.B., et al. (2002). Central functions of the lumenal and peripheral thylakoid proteome of *Arabidopsis* determined by experimentation and genome-wide prediction. Plant Cell. **14,** 211–236.

Prasad, B.D., Goel, S., and Krishna, P. (2010). *In silico* identification of carboxylate clamp type tetratricopeptide repeat proteins in *Arabidopsis* and rice as putative cochaperones of Hsp90/Hsp70. PLoS One. **5,** e12761.

Qbadou, S., Becker, T., Mirus, O., Tews, I., Soll, J., and Schleiff, E. (2006). The molecular chaperone Hsp90 delivers precursor proteins to the chloroplast import receptor Toc64. EMBO J. **25,** 1836–1847.

Qbadou, S., et al. (2007). Toc64—a preprotein-receptor at the outer membrane with bipartide function. J. Mol. Biol. **367,** 1330–1346.

Queitsch, C., Sangster, T.A., and Lindquist, S. (2002). Hsp90 as a capacitor of phenotypic variation. Nature. **417,** 618–624.

Reddy, R.K., Kurek, I., Silverstein, A.M., Chinkers, M., Breiman, A., and Krishna, P. (1998). High-molecular-weight FK506-binding proteins are components of heat-shock protein 90 heterocomplexes in wheat germ lysate. Plant Physiol. **118,** 1395–1401.

Reinbothe, C., et al. (2006). A role for chlorophyllide a oxygenase in the regulated import and stabilization of light-harvesting chlorophyll a/b proteins. Proc. Natl Acad. Sci. U S A. **103,** 4777–4782.

Rial, D.V., Arakaki, A.K., and Ceccarelli, E.A. (2000). Interaction of the targeting sequence of chloroplast precursors with Hsp70 molecular chaperones. Eur. J. Biochem. **267,** 6239–6248.

Rudiger, S., Buchberger, A., and Bukau, B. (1997). Interaction of Hsp70 chaperones with substrates. Nat. Struct. Biol. **4,** 342–349.

Ruprecht, M., Bionda, T., Sato, T., Sommer, M.S., Endo, T., and Schleiff, E. (2010). On the impact of precursor unfolding during protein import into chloroplasts. Mol. Plant. **3,** 499–508.

Sangster, T.A., et al. (2007). Phenotypic diversity and altered environmental plasticity in *Arabidopsis thaliana* with reduced Hsp90 levels. PLoS One. **2,** e648.

Sangster, T.A., et al. (2008). HSP90 affects the expression of genetic variation and developmental stability in quantitative traits. Proc. Natl Acad. Sci. U S A. **105,** 2963–2968.

Schiene-Fischer, C., and Yu, C. (2001). Receptor accessory folding helper enzymes: the functional role of peptidyl prolyl *cis/trans* isomerases. FEBS Lett. **495,** 1–6.

Shanklin, J., DeWitt, N.D., and Flanagan, J.M. (1995). The stroma of higher plant plastids contain ClpP and ClpC, functional homologs of *Escherichia coli* ClpP and ClpA: an archetypal two-component ATP-dependent protease. Plant Cell. **7,** 1713–1722.

Shirasu, K. (2009). The HSP90–SGT1 chaperone complex for NLR immune sensors. Annu. Rev. Plant Biol. **60,** 139–164.

Simpson, J.P., et al. (2008). Identification and characterization of a plastid-localized *Arabidopsis* glyoxylate reductase isoform: comparison with a cytosolic isoform and implications for cellular redox homeostasis and aldehyde detoxification. J. Exp. Bot. **59,** 2545–2554.

Smith, D.F. (2004). Tetratricopeptide repeat cochaperones in steroid receptor complexes. Cell Stress Chaperones. **9,** 109–121.

Stettler, M., Eicke, S., Mettler, T., Messerli, G., Hortensteiner, S., and Zeeman, S.C. (2009). Blocking the metabolism of starch breakdown products in *Arabidopsis* leaves triggers chloroplast degradation. Mol. Plant. **2,** 1233–1246.

Stuttmann, J., Parker, J.E., and Noel, L.D. (2008). Staying in the fold: the SGT1/chaperone machinery in maintenance and evolution of leucine-rich repeat proteins. Plant Signal Behav. **3,** 283–285.

Sun, Q., Zybailov, B., Majeran, W., Friso, G., Olinares, P.D., and van Wijk, K.J. (2009). PPDB, the Plant Proteomics Database at Cornell. Nucleic Acids Res. **37,** D969–D974.

Taipale, M., Jarosz, D.F., and Lindquist, S. (2010). HSP90 at the hub of protein homeostasis: emerging mechanistic insights. Nat. Rev. Mol. Cell Biol. **11,** 515–528.

Waegemann, K., and Soll, J. (1996). Phosphorylation of the transit sequence of chloroplast precursor proteins. J. Biol. Chem. **271,** 6545–6554.

Wandinger, S.K., Richter, K., and Buchner, J. (2008). The Hsp90 chaperone machinery. J. Biol. Chem. **283,** 18473–18477.

Wang, Q., et al. (2004). Deletion of the chloroplast-localized Thylakoid formation1 gene product in *Arabidopsis* leads to deficient thylakoid formation and variegated leaves. Plant Physiol. **136,** 3594–3604.

Watkins, K.P., Rojas, M., Friso, G., van Wijk, K.J., Meurer, J., and Barkan, A. (2011). APO1 promotes the splicing of chloroplast group II introns and harbors a plant-specific zinc-dependent RNA binding domain. Plant Cell. in press.

Young, J.C., Hoogenraad, N.J., and Hartl, F.U. (2003). Molecular chaperones Hsp90 and Hsp70 deliver preproteins to the mitochondrial import receptor Tom70. Cell. **112,** 41–50.

Zhang, X.P., and Glaser, E. (2002). Interaction of plant mitochondrial and chloroplast signal peptides with the Hsp70 molecular chaperone. Trends Plant Sci. **7,** 14–21.

Zhang, Z., Quick, M.K., Kanelakis, K.C., Gijzen, M., and Krishna, P. (2003). Characterization of a plant homolog of hop, a cochaperone of hsp90. Plant Physiol. **131,** 525–535.

4 Publication II

Schweiger R., Müller N.C., Schmitt M.J., Soll J. and Schwenkert S., (2012). *AtTPR7 is a chaperone-docking protein of the Sec translocon in Arabidopsis.* J Cell Sci. **125**, 5196-5207.

AtTPR7 is a chaperone-docking protein of the Sec translocon in *Arabidopsis*

Regina Schweiger[1], Nina C. Müller[2], Manfred J. Schmitt[2], Jürgen Soll[1,3] and Serena Schwenkert[1,3,*]

[1]Department of Biology I, Botany, Ludwig-Maximilians-Universität München, Großhaderner Strasse 2–4, D-82152 Planegg-Martinsried, Germany
[2]Molecular and Cell Biology, Department of Biosciences, Universität des Saarlandes, Campus A 1.5., D-66041 Saarbrücken, Germany
[3]Munich Center for Integrated Protein Science CiPSM, Ludwig-Maximilians-Universität München, Feodor-Lynen-Strasse 25, D-81377 Munich, Germany

*Author for correspondence (serena.schwenkert@lmu.de)

Accepted 12 July 2012
Journal of Cell Science 125, 5196–5207

doi: 10.1242/jcs.111054

Summary

Chaperone-assisted sorting of post-translationally imported proteins is a general mechanism among all eukaryotic organisms. Interaction of some preproteins with the organellar membranes is mediated by chaperones, which are recognised by membrane-bound tetratricopeptide repeat (TPR) domain containing proteins. We have characterised AtTPR7 as an endoplasmic reticulum protein in plants and propose a potential function for AtTPR7 in post-translational protein import. Our data demonstrate that AtTPR7 interacts with the heat shock proteins HSP90 and HSP70 via a cytosol-exposed TPR domain. We further show by *in vitro* and *in vivo* experiments that AtTPR7 is associated with the *Arabidopsis* Sec63 homologue, AtERdj2. Interestingly, AtTPR7 can functionally complement a Δ*sec71* yeast mutant that is impaired in post-translational protein transport. These data strongly suggest that AtTPR7 not only has a role in chaperone binding but also in post-translational protein import into the endoplasmic reticulum, pointing to a general mechanism of chaperone-mediated post-translational sorting between the endoplasmic reticulum, mitochondria and chloroplasts in plant cells.

Key words: Endoplasmic reticulum, HSP90, Post-translational import, *Arabidopsis thaliana*

Introduction

Most proteins localised to cellular compartments are translated in the cytosol and have to be targeted to the destined compartments where they are translocated post- or co-translationally across the organellar membranes (Schleiff and Becker, 2011). Post-translational import occurs predominantly into the endosymbiotic organelles chloroplasts and mitochondria, whereas proteins of the endoplasmic reticulum (ER) are imported either co- or post-translationally. Despite the co-translational pathway being the predominant one in mammals, yeast utilises both pathways equally (Rapoport, 2007; Wang et al., 2010; Zimmermann et al., 2011). In both cases the preproteins are transported across the membrane through the channel protein Sec61. During post-translational translocation in mammals the Sec61 channel associates with additional components, the Sec62/63 complex and the luminal HSP70 chaperone BiP, which assists in translocating the peptide across the membrane (Osborne et al., 2005; Zimmermann et al., 2006). For both pathways cytosolic components are indispensable. During co-translational transport the nascent polypeptide emerging from the ribosome in the cytosol is recognised at a signal or transmembrane sequence by the signal recognition particle. This complex associates first with the signal recognition particle receptor at the ER membrane and subsequently with the Sec translocation channel. The post-translational pathway is predominantly used by more hydrophobic proteins (Ng et al., 1996) and thus requires the assistance of molecular chaperones to prevent molecular crowding and to facilitate interaction with the translocon complex. Members of the HSP70 and HSP40 chaperone family have been described to aid the translocation of ER localised proteins (Ngosuwan et al., 2003; Zimmermann et al., 1988). Likewise, the insertion of tail-anchored ER membrane proteins is facilitated by HSP70 or by components of the so called 'guided entry for tail anchored proteins' (GET) pathway (Abell et al., 2007; Wang et al., 2010). HSP70 not only participates in ER protein translocation but also interacts with preproteins targeted to chloroplasts and mitochondria (Young et al., 2003; Zhang and Glaser, 2002). HSP70 can either function alone or in concert with HSP90. HSP90 and HSP70 together with cochaperones associate with a large population of chloroplast preproteins as well as with hydrophobic carrier proteins destined to the inner mitochondrial membrane in mammals (Fan et al., 2006; Fellerer et al., 2011; Qbadou et al., 2006; Young et al., 2003; Zara et al., 2009).

Preproteins can be recognised at the membrane surfaces either directly by receptor proteins or indirectly via their bound chaperones. Remarkably, all chaperone recognising docking proteins contain one or more tetratricopeptide repeat (TPR) motif facing the cytosol. These docking proteins are found throughout eukaryotic organisms and are distributed among all cellular compartments, suggesting a general mechanism for preprotein recognition through HSP90 and HSP70 (Kriechbaumer et al., 2012; Schlegel et al., 2007). TPR domains mediating interaction with chaperones, so called clamp-type TPR motifs, generally consist of at least three tandemly arranged TPR motifs which are highly degenerate 34 amino acid repeats without any strictly conserved residues. Proteins containing three TPR repeats are organised in a right-handed super helical structure capped by a so called solvation helix at the C-terminal end. This helix turn helix motif is packed into a regular series of antiparallel alpha helices. They form a

dicarboxylate clamp coordinating the conserved aspartate residue in the C-terminus of HSP90 and HSP70 (D'Andrea and Regan, 2003; Scheufler et al., 2000). In addition to the chaperone-mediated pathway, TPR domains of some receptor proteins facilitate direct interaction with preproteins. Tom20 of the yeast and mammalian mitochondrial translocon binds to N-terminal presequences with its clamp-type TPR domain (Abe et al., 2000; Saitoh et al., 2007). Pex5, a component found in the peroxisomal import apparatus of plants, animals and fungi contains seven non-clamp-type TPR domains allowing recognition of the peroxisomal C-terminal targeting signal (Erdmann and Schliebs, 2005; Gatto et al., 2000; Lee et al., 2006). Tom70 is another well described TPR docking protein in the outer membrane of yeast and mammalian mitochondria containing seven TPR motifs and interacts with both, chaperones and preproteins. The C-terminal TPR motifs of Tom70 directly bind to internal targeting signals of mitochondrial preproteins (Young et al., 2003), whereas the N-terminal motifs interact with chaperone–preprotein complexes. In yeast, preproteins associated with HSP70 are recognised by Tom70, whereas mammalian Tom70 interacts additionally with HSP90–preprotein complexes (Young et al., 2003). Tom34 is an additional component in mammalian mitochondria and has recently been shown to associate with HSP70– and HSP90–preprotein complexes (Faou and Hoogenraad, 2012). In plant mitochondria Tom70 may functionally be replaced by OM64 (Chew et al., 2004; Lister et al., 2007) which is closely related to the chloroplast outer envelope TPR domain containing protein Toc64. Toc64 likewise mediates interaction with HSP90-bound chloroplast preproteins in the cytosol and is associated with the Toc translocon (Qbadou et al., 2006). A TPR containing component associated to the ER membrane, Sec72, which is involved in post-translational import of some ER proteins, has so far only been identified in yeast (Fang and Green, 1994; Feldheim and Schekman, 1994; Harada et al., 2011). Sec72 does not contain a transmembrane domain, but is anchored to the ER membrane by the integral membrane protein Sec71 and both associate with Sec62/63 and the channel protein Sec61 (Harada et al., 2011) to form a translocon complex for post-translational protein import. However, no functional homologues of Sec72 or Sec71 have been identified in higher eukaryotes so far.

The mechanisms of ER protein import in plants have not been analysed in great detail up to date, although the major components of the Sec translocon show a high homology to their mammalian and yeast counterparts. The *Arabidopsis thaliana* orthologue of the channel protein Sec61α is present as three isoforms and orthologues of the two associated membrane compounds Sec62 and Sec63 are also found in the *Arabidopsis* genome. AtSec62 is a single copy gene, whereas two isoforms of the J-domain containing AtSec63 exist, which are referred to as AtERdj2A and AtERdj2B (Yamamoto et al., 2008). However, neither co- nor post-translational import into plant ER has been investigated so far.

In this study we describe a TPR domain-containing plant-specific protein, termed AtTPR7 (At5g21990), which was previously identified by Prasad et al. (Prasad et al., 2010). The protein was previously described as a protein of the outer envelope in chloroplast [OEP61 (von Loeffelholz et al., 2011)] and proposed to function as a chaperone receptor for preproteins. However, we could show that the protein resides most likely exclusively in the ER membrane. AtTPR7 associates with AtERdj2 in membrane complexes of 140 and 200 kDa and it specifically interacts with the HSP70 and HSP90 chaperones via its TPR domain. Moreover, we could functionally complement a yeast Δ*sec71* mutant which is deficient in post-translational protein translocation. We thus propose AtTPR7 to function as chaperone docking protein with a possible role during post-translational protein translocation into the ER in *Arabidopsis*.

Results

AtTPR7 contains a TPR and a transmembrane domain and is localised to the ER membrane

A search for tail-anchored TPR domain containing proteins identified AtTPR7 as a plant specific TPR protein. The TPR motif of AtTPR7 is a carboxylate clamp-type domain and consists of a triple repeat of 34 amino acid long TPR degenerate consensus motif, which is located near the N-terminus (amino acids 104–212; Fig. 1A). AtTPR7 further contains a predicted hydrophobic transmembrane region at its C-terminus reaching from amino acids 531–551 (Fig. 1A; supplementary material Fig. S1) and probably spans the membrane once, which classifies it as a so called tail-anchored protein, found in many cellular compartments. Blast searches against the genomes of various organisms revealed that AtTPR7 homologues are represented in the unicellular green algae *Chlamydomonas* as well as in mosses, ferns, mono- and dicotyledonous plants, but are absent from bacteria, yeast and mammals. A complete sequence alignment of AtTPR7 homologues in land plants and algae showing the conserved TPR repeat domain as well as the conserved C-terminus containing the transmembrane domain is presented in

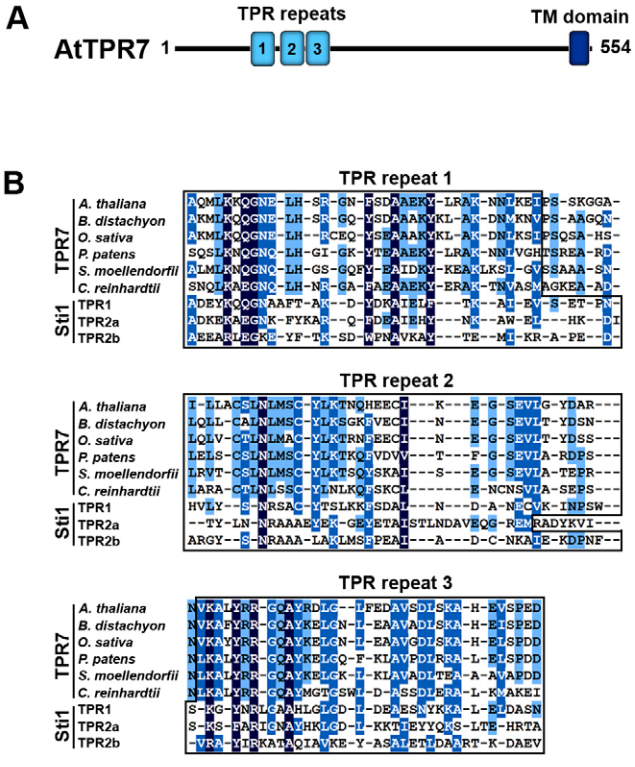

Fig. 1. AtTPR7 domain organisation. (**A**) Diagram of the TPR domain consisting of three degenerate 34 amino acid TPR repeats and the transmembrane (TM) domain. (**B**) The TPR domain of AtTPR7 was aligned with homologues in *B. distachyon, O. sativa, P. patens, S. moellendorfii* and *C. reinhardtii* as well as with the three TPR domains of Sti1 (TPR1, TPR2a and TPR2b), each also consisting of three TPR repeats. Conserved amino acids are shaded in blue.

supplementary material Fig. S1. AtTPR7 was also recently identified in an in silico search for potential HSP90/HSP70 interactors in plants (Prasad et al., 2010). An alignment comparing the TPR domain structure of AtTPR7 in plants with the three triple TPR repeats of the yeast HSP90 cochaperone Sti1/HOP is shown in Fig. 1B. Sti1 is known to bind selectively to HSP90 as well as HSP70 via its individual TPR domains (Schmid et al., 2012). TPR1 of Sti1 is mostly responsible for HSP70 binding, whereas TPR2a associates preferably with HSP90. The third domain TPR2b can bind to both, HSP90 and HSP70. Since the amino acid sequence of the TPR domain of AtTPR7 is 25% identical to TPR1 as well as to TPR2a, AtTPR7 likely binds both chaperones.

We have investigated the localisation of AtTPR7 using expression of a GFP fusion protein as well as cell fractionation. Since AtTPR7 does not contain a predicted N-terminal signal sequence its C-terminal transmembrane domain most likely functions as a targeting signal, as is common for tail-anchored proteins (Borgese et al., 2001; Hegde et al., 2007). In order to prevent masking of the transmembrane anchor by GFP we generated a N-terminal GFP-*AtTPR7* construct using full-length *AtTPR7*.

This construct as well as constructs encoding marker proteins for ER and Golgi fused to mCherry (see Materials and Methods and Nelson et al. for detailed information) were transformed into agrobacteria (Nelson et al., 2007). Agrobacteria carrying the GFP-*AtTPR7* construct and either ER or Golgi marker constructs were co-infiltrated into tobacco leaves. We analysed intact tobacco leaves (Fig. 2A) as well as protoplasts (Fig. 2B,C), which were isolated from tobacco leaves two days after infiltration. Fluorescent signals were observed by confocal laser scanning microscopy. Chlorophyll autofluorescence is false coloured in blue. As can be seen in merged pictures of GFP–AtTPR7 and an ER marker, as well as merged pictures of GFP–AtTPR7 and chloroplasts, signals clearly overlap with the ER marker fluorescence pattern in both, intact leaves and protoplasts.

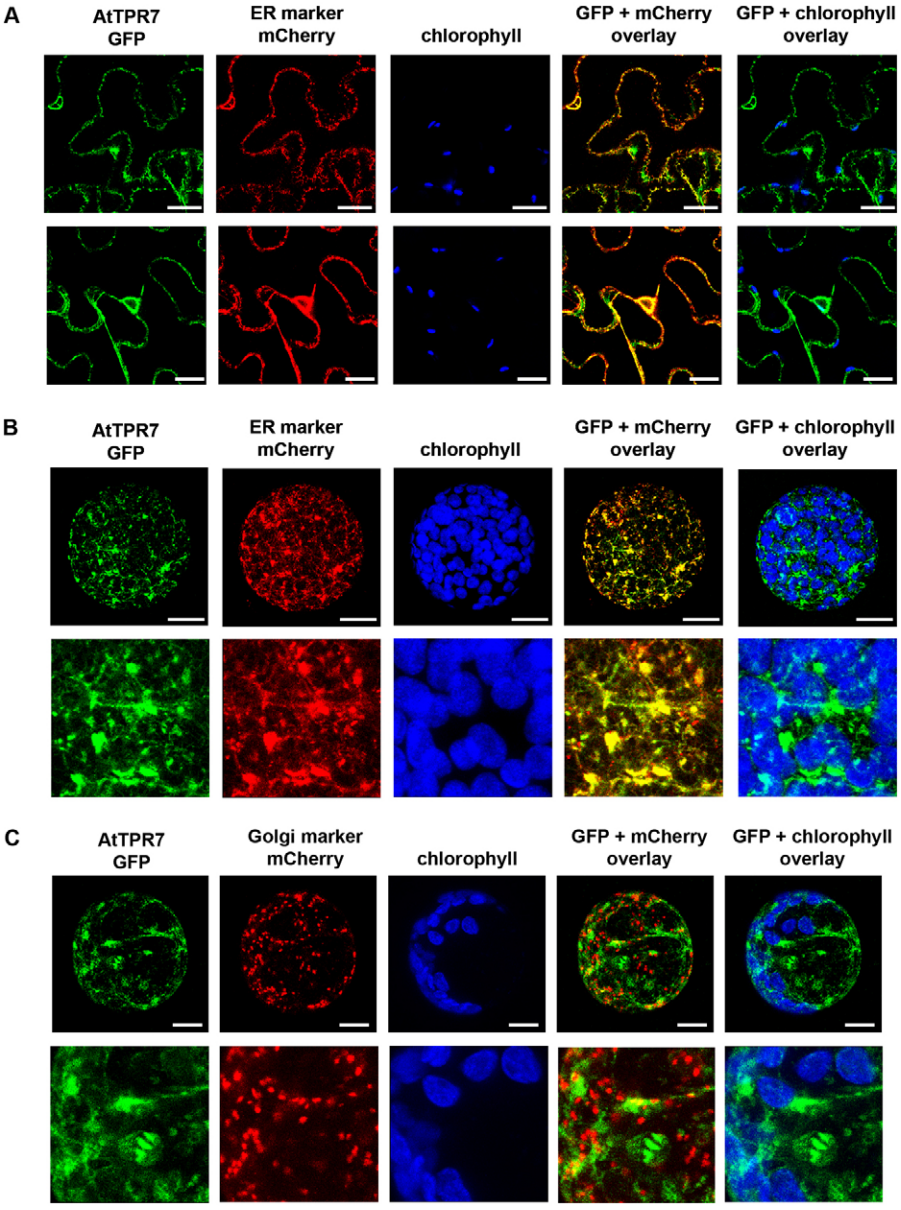

Fig. 2. AtTPR7 is localised to the ER membrane. (**A**) Tobacco leaves were co-transformed with agrobacteria carrying constructs for AtTPR7 (GFP) and an ER marker (mCherry). Fluorescence was monitored in intact leaves by confocal laser scanning microscopy. Chlorophyll autofluorescence is false coloured in blue. Two representative leaf sections are shown. Scale bars: 10 µm. (**B**) Protoplasts of leaves expressing GFP–AtTPR7 and an ER marker were isolated and fluorescence was monitored by confocal laser scanning microscopy as in A. A section, 10×10 µm, of each image is magnified in the lower panels. Scale bars: 10 µm. (**C**) Protoplasts of leaves expressing GFP–AtTPR7 and a Golgi marker are shown. Fluorescence was monitored by confocal laser scanning microscopy as in A. A section, 10×10 µm, of each image is magnified in the lower panels. Scale bars: 10 µm.

Magnifications (lower panels Fig. 2B,C) show that although ER structures and chloroplasts overlap at some points (see also merged pictures of chloroplasts and ER marker in supplementary material Fig. S2A), no clear ring around the chloroplasts of the GFP signal is visible as would be expected for a chloroplast envelope localisation. Also, no colocalisation of GFP–AtTPR7 with the Golgi marker is visible (Fig. 2C). Immunoblot analysis with membrane proteins extracted from infiltrated tobacco leaves detects a clear signal at 88 kDa, which is the expected size of the GFP–AtTPR7 fusion protein (supplementary material Fig. S2B). No signal is detected at 27 kDa, which would correspond to GFP alone. Therefore the fluorescent signal is derived from the fusion protein. Moreover, we generated a YFP-AtTPR7 construct (as was used by von Loeffelholz et al.) and co-expressed it in tobacco leaves together with the mCherry Marker. Again, the AtTPR7 signal is visible in the ER membrane (supplementary material Fig. S2C) (von Loeffelholz et al., 2011).

As a next step we aimed to further asses the localisation of the endogenous AtTPR7. To separate the individual membranes of different cellular compartments a membrane preparation of *Arabidopsis* leaves was loaded onto a sucrose density gradient (density: 1.05–1.25 g/ml). Gradients were fractionated and proteins were detected by immunodecoration with specific polyclonal AtTPR7 and AtToc64 antisera (Fig. 3A, upper panels). Toc64 was mainly found in fractions with a density of 1.08 g/ml, as it is expected for chloroplast outer envelope membranes (Cline et al., 1981). AtTPR7 in contrast was found in fractions with a sucrose density of 1.17 g/ml, corresponding to ER membranes (Ceriotti et al., 1995). The AtTPR7 antisera showed cross reactivity with the pea homologue and we therefore additionally performed the same experiment with a membrane preparation from pea leaves. Again, AtTPR7 was found in fractions corresponding to the ER membrane, clearly separated from PsToc64 (Fig. 3A, lower panels). Fractions 16–19 of the gradients containing *Arabidopsis* proteins, corresponding to ER membranes of wild-type *Arabidopsis*, pea and a *attpr7* T-DNA mutant (supplementary material Fig. S3A–C) were subjected to SDS-PAGE and immunodecorated with AtTPR7 antisera (Fig. 3B). Intact and pure *Arabidopsis* and pea chloroplasts, isolated with a Percoll step gradient, were used additionally as a control. A signal for AtTPR7 was only obtained in wild-type *Arabidopsis* and pea ER membranes and no signal was detected in the chloroplast fractions or the *attpr7* mutant. To test the purity of the ER membranes and chloroplasts and to provide a loading control we probed the samples with antisera against ER localised AtERdj2 as well as antisera against AtToc64/PsToc64.

Two isoforms of the yeast Sec63 orthologue are found in the *Arabidopsis* genome, AtERdj2A and AtERdj2B, sharing 71% identity. The antibody used in this study was raised against AtERdj2B although it has been shown to recognise both, AtERdj2A and AtERdj2B (Yamamoto et al., 2008). However, we could detect only a single band either representing AtERdj2B or both proteins were not separated sufficiently. Nevertheless, AtERdj2 was only detected in the ER fractions, whereas Toc64 was mainly detected in the chloroplasts, showing a high degree of purity of the fractions, apart from a slight contamination of the ER with chloroplast membranes.

To test whether AtTPR7 is an integral membrane protein, a total microsomal membrane preparation was treated with high salt, urea, Na_2CO_3 (pH 11), SDS and buffer as a control. AtTPR7 was only extracted from the membrane by SDS, clearly

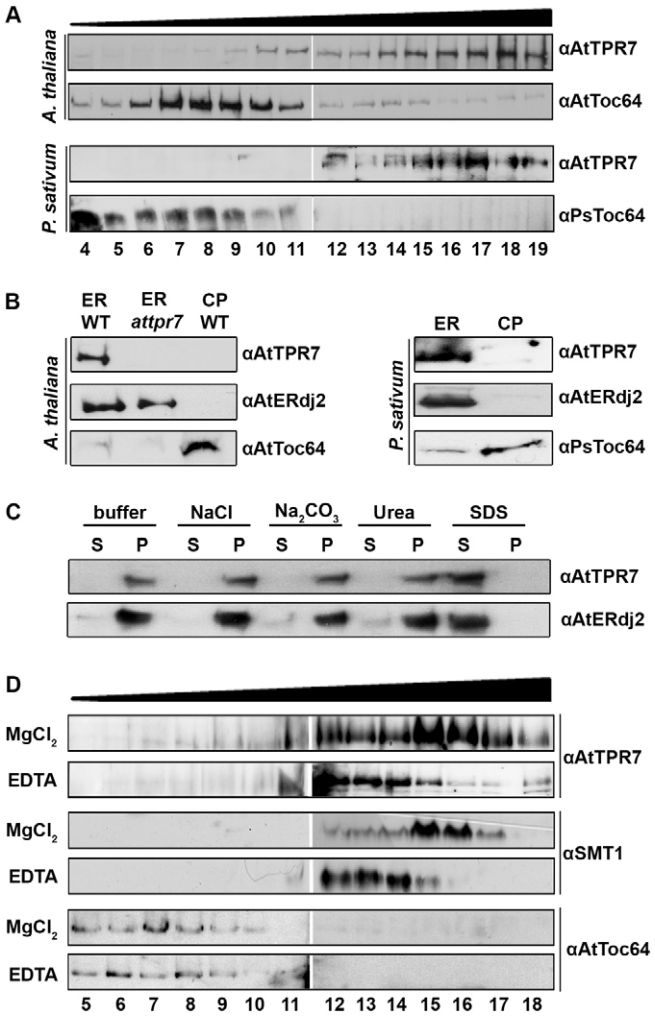

Fig. 3. (**A**) Total membranes of *A. thaliana* (upper panels) and *P. sativum* (lower panels) were separated by sucrose density gradients (1.05–1.25 g/ml) and fractions were probed with antisera against the chloroplast outer envelope protein Toc64 as well as AtTPR7. (**B**) ER membranes (ER) from wild type (*A. thaliana* and *P. sativum*) and *attpr7* mutants (*A. thaliana*) as well as isolated chloroplasts (CP) were probed with antisera against AtTPR7, AtERdj2 and Toc64. (**C**) A microsomal membrane preparation was treated with buffer, 1 M NaCl, 0.1 M Na_2CO_3, 4 M urea and 1% SDS for 30 min as indicated. The proteins were separated into supernatant and pellet after the treatment and probed with AtTPR7 and AtERdj2A antisera. (**D**) Microsomal membranes were loaded on sucrose density gradients (1.05 1.25 g/ml) containing either 1 mM EDTA or 2 mM $MgCl_2$. Fractions were separated by SDS-PAGE and probed with the ER membrane protein SMT1 and AtTPR7 antisera as well as with antisera against the chloroplast outer envelope protein Toc64.

demonstrating that it is a membrane protein (Fig. 3C). AtERdj2 was monitored as a control integral membrane protein and showed similar behaviour.

Next, we applied a magnesium-induced-shift assay, which is frequently used as an indicator of ER membrane localisation (Ceriotti et al., 1995; Levitan et al., 2005). Ribosomes are released from the ER membrane upon treatment with EDTA. This in turn leads to a shift in migration of ER membranes in sucrose density gradients to a lower density in contrast to other membranes. In the presence of Mg^{2+}, however, the small and the large subunit of the ribosome remain associated. Therefore, ER

proteins are found in different fractions depending on the addition of EDTA in sucrose gradients. Total leaf extract was loaded on sucrose density gradients (1.05–1.25 g/ml) with 1 mM EDTA or with 2 mM $MgCl_2$, fractions were separated by SDS-PAGE and probed with AtTPR7 antisera as well as antisera against the ER specific protein SMT1 [sterol methyltransferase 1 (Boutté et al., 2010)] and the chloroplast outer envelope protein AtToc64 as a control. A clear shift is visible for AtTPR7 as well as SMT1 (Fig. 3E) confirming the localisation of AtTPR7 in the ER membrane, whereas Toc64 as a non-ER protein does not shift to lighter density fractions.

von Loeffelholz et al. showed that AtTPR7 is imported in an *in vitro* assay into isolated chloroplasts, also in competition with mitochondria (von Loeffelholz et al., 2011). We have therefore performed a competitive import assay with chloroplasts and ER and found that in this case AtTPR7 inserts preferentially into the ER membrane, although a minor amount of the protein is inserted into the chloroplast as was previously observed (von Loeffelholz. et al., 2011). AtToc64, which was used as a control, is predominantly targeted to chloroplasts (supplementary material Fig. S4). However, our cell fractionation assays analysing the endogenous AtTPR7 clearly point to an exclusive localisation in the ER.

AtTPR7 is post-translationally inserted into the ER and has a cytosolic exposed TPR domain

Tail-anchored proteins are known to be inserted preferably post-translationally into the ER, where the transmembrane domain usually functions as a signal sequence (Borgese et al., 2001). We therefore investigated whether AtTPR7 is integrated post- or co-translationally into the ER. The *Arabidopsis* homologue of the co-translationally inserted luminal ER protein BiP (Denecke et al., 1991; Maruyama et al., 2010), AtBiP2, was used as a control. AtTPR7 and AtBiP2 were translated *in vitro* in a reticulocyte lysate and imported into dog pancreatic microsomes. To monitor post-translational protein import the proteins were added to the microsomes 20 min after the translation reaction. RNase A as well as cycloheximide were added to remove RNA, inhibit translation and prevent co-translational import before addition of microsomes. To observe co-translational translocation, translation was performed directly in the presence of microsomes (Fig. 4A). Indeed, AtTPR7 seems to be imported post-translationally in comparison to AtBiP2, which shows a strong import when allowing co-translational translocation and no import during post-translational import conditions. AtBiP2 is protected from digestion by proteinase K after co-translational import, demonstrating efficient import of AtBiP2, since AtBiP2 is not predicted to be glycosylated the processed signal peptide is only 3 kDa in size. Solubilisation of the membrane with 1% Triton (v/v) results in proteolysis of AtBiP2 by proteinase K. AtTPR7 in contrast is degraded by proteinase K in the absence of detergent, thus suggesting that the major part of the protein faces the cytosol. To ensure insertion of AtTPR7 microsomal membranes were treated after AtTPR7 import with buffer, 1 M NaCl or 4 M urea (Fig. 4B).

To further test the topology of the endogenous AtTPR7, we analysed *Arabidopsis* microsomal membranes. The membranes were likewise treated with proteinase K and probed with antisera against AtTPR7 and SMT1 as a control. AtTPR7 is again degraded in contrast to SMT1, which is a transmembrane protein facing the lumenal side (Boutté et al., 2010) and only proteolysed

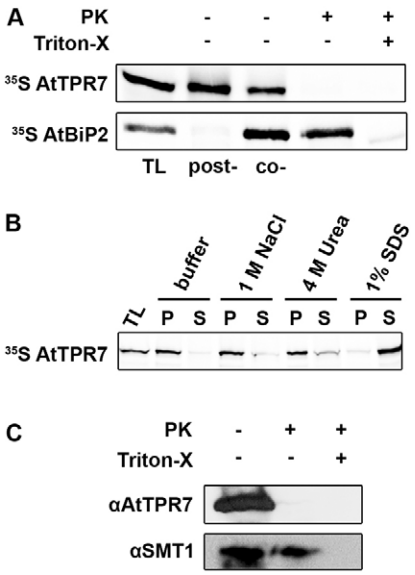

Fig. 4. Post-translational import of AtTPR7 into the ER, and topology. (**A**) Radiolabelled AtTPR7 and AtBiP2 were either imported into dog pancreatic microsomes after the translation reaction (post-) or translation was carried out in the presence of dog pancreatic microsomes (co-). Samples were treated with proteinase K (PK) and Triton X-100 as indicated. ^{35}S-labelled proteins were detected by autoradiography. (**B**) Microsomal membranes were treated with buffer, 1 M NaCl, 4 M urea and 1% SDS after import of AtTPR7. ^{35}S-labelled proteins were detected by autoradiography. (**C**) Microsomal membranes of *Arabidopsis* (100 µg) were treated with proteinase K (PK) and Triton X-100 as indicated. Proteins were separated by SDS-PAGE and immunodecorated with AtTPR7 and SMT1 antisera.

upon prior solubilisation of the membranes with Triton (Fig. 4C). Moreover, we performed the same experiment with membranes isolated from tobacco leaves transiently transformed with GFP–AtTPR7. Like the endogenous AtTPR7 GFP–AtTPR7 is rapidly degraded, thus confirming the predicted topology (supplementary material Fig. S5).

We therefore conclude that the N-terminal TPR domain of AtTPR7 is facing the cytosol, thus fulfilling an important prerequisite for a possible function as a chaperone receptor.

The TPR domain of AtTPR7 specifically interacts with HSP70 and HSP90

In the following experiment we aimed to elucidate whether AtTPR7 is able to interact with the cytosolic chaperones HSP90 and/or HSP70. We showed previously that the chloroplast TPR domain containing protein Toc64 interacts with HSP90–preprotein complexes (Qbadou et al., 2007). Therefore we tested whether the TPR domain of AtTPR7 could interact with HSP90 and/or HSP70. Since there are four isoforms of HSP90 present in the *Arabidopsis* cytosol (Krishna and Gloor, 2001), we tested whether any of them can interact with AtTPR7 in an *in vitro* pull-down assay.

The coding sequence of *AtTPR7* lacking the C-terminal transmembrane domain was fused to a His tag replacing the transmembrane domain and recombinant AtTPR7–His was overexpressed in *E. coli* and purified via Ni-NTA. HSP90 isoforms were fused to an N-terminal Strep tag, which does not interfere with binding of the C-terminal EEVD motif to the TPR domain and purified accordingly. AtTPR7–His was incubated

with either Strep–AtHSP90.1, Strep–AtHSP90.2, Strep–AtHSP90.3 or Strep–AtHSP90.4 and recovered by Ni-NTA. A sample without AtTPR7–His served as a control. Associated HSP90 was detected by immunoblotting with HSP90 antisera (Fig. 5A,B upper panel). All isoforms are able to interact with AtTPR7–His, although HSP90.2 and HSP90.3 showed a slightly increased binding.

Moreover, we tested the association of AtTPR7–His with Strep–AtHSP70.1, which is an abundant and constitutively expressed HSP70 isoform of the five HSP70 isoforms found in the *Arabidopsis* cytosol (Lin et al., 2001) (Fig. 5B, lower panel). Interaction with this chaperone was even stronger compared to HSP90 and is in line with previous results (von Loeffelholz et al., 2011). In addition to the ability of AtTPR7–His to interact with recombinant chaperones we tested whether AtTPR7–His could co-purify the chaperones from wheat germ lysate. AtTPR7–His was incubated with wheat germ lysate, re-purified by Ni-NTA and associated chaperones were again detected by immunoblotting. The results showed that AtTPR7–His is indeed also able to interact with wheat germ lysate HSP90 and HSP70 (Fig. 5B).

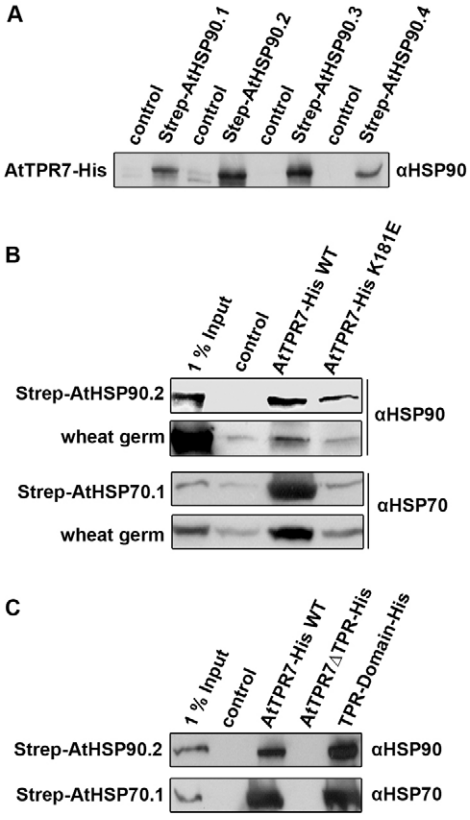

Fig. 5. Interaction of AtTPR7 with HSP70 and HSP90. (**A**) Recombinant AtTPR7–His (60 µg) was incubated with four cytosolic HSP90 isoforms (1 mM) and AtTPR7–His was affinity purified with Ni-NTA subsequently. Association of HSP90 was detected by immunoblotting with HSP90 antisera. A sample without AtTPR7–His was used as a control. (**B**) Recombinant AtTPR7–His wild type (60 µg) as well as AtTPR7–His K181E (60 µg) were incubated with recombinant Strep–AtHSP70.1 (1 mM), Strep–HSP90.2 (1 mM) or 100 µl wheat germ lysate (20 µg/µl) and subsequently affinity purified via the His tag. Eluted proteins were probed with antisera against HSP90 (upper panels) and HSP70 (lower panels). 1% of the HSP90/70 amount was loaded in lane 1 (input). (**C**) Recombinant AtTPR7–His wild type, AtTPR7ΔTPR–His and TPR-Domain–His (60 µg) were incubated with recombinant Strep–AtHSP70.1 (1 mM) and Strep–HSP90.2 (1 mM) and further treated as described in B. 1% of the HSP90/70 amount was loaded in lane 1 (input).

Since association of HSP70 among other factors with post-translationally inserted tail-anchored proteins is often observed during their membrane insertion (Abell et al., 2007; Rabu et al., 2008), we aimed to ensure that chaperone interaction is mediated specifically via the TPR domain. Therefore, an AtTPR7 mutant with a point mutation in the TPR region was generated. Comparison of the TPR domain of AtTPR7 with the well analysed TPR domains of the yeast HSP70 HSP90 organising protein (HOP), of which the TPR domain TPR1 is known to interact with HSP70 and the TPR domain TPR2a with HSP90, revealed a conserved lysine in position 181, which has been shown to be essential for HSP70 binding in HOP (Smith, 2004). The lysine was mutated by site-directed mutagenesis to a glutamic acid, thus introducing a negative charge in the protein binding pocket, which interferes with the chaperone EEVD peptide interaction. Recombinant AtTPR7–His wild-type and AtTPR7–His K181E proteins were incubated with (i) Strep–AtHSP70.1, (ii) Strep AtHSP90.2 and (iii) wheat germ lysate. AtTPR7–His was recovered with Ni-NTA (Fig. 5B) and the interacting chaperones were detected with antisera against HSP70 and HSP90. Association of Strep–AtHSP70.1 to AtTPR7–His was strongly reduced in the AtTPR7–His K181E mutant, indicating a specific interaction via the TPR region. Likewise, interaction with Strep–AtHSP90.2 was affected in the mutant. Nevertheless, residual binding was observed for both, HSP70 and HSP90, indicating that a single inserted negatively charged amino acid does not change the structure of the TPR domain drastically and thus still allows a weak chaperone association.

To ensure the specific interaction with chaperones via the TPR domain of AtTPR7 we generated a deletion mutant of AtTPR7 lacking the TPR domain (amino acids 104–212, AtTPR7ΔTPR–His). Furthermore, we tested chaperone association solely with the TPR domain (TPR-Domain–His). Wild-type AtTPR7–His as well as the two constructs were incubated with Strep–AtHSP70.1 and Strep–AtHSP90.2 and His-tagged AtTPR7 constructs were recovered and immunodecorated as described earlier. Binding of Strep–AtHSP70.1 as well as Strep–AtHSP90.2 to AtTPR7ΔTPR–His was completely abolished. In contrast to that association of Strep–AtHSP70.1 and Strep–AtHSP90.2 to TPR-Domain–His was comparable to wild-type AtTPR7–His (Fig. 5C).

AtTPR7 is a component of a higher molecular weight complex and interacts with AtERdj2 *in vivo*

Next, we wanted to elucidate whether AtTPR7 is part of a higher molecular weight complex possibly containing components of the Sec translocon. Therefore we analysed the composition of ER membrane complexes by blue native gel electrophoresis (BN-PAGE). Microsomal membranes were solubilized with 0.4% *n*-decyl-β-maltoside (DeMa) and complexes were separated on a native 5–12% gel in the first dimension. The composition of the separated protein complexes was further analysed by SDS-PAGE and immunoblotting in the second dimension. Fig. 6A (upper panel) shows that AtTPR7 is found in at least two higher molecular weight complexes of ~140 and ~200 kDa. Intriguingly, AtTPR7 co-migrates with AtERdj2, which is found in complexes of almost identical running behaviour (Fig. 6A, lower panel). Moreover, we subjected microsomal membranes of wild type and the *attpr7*

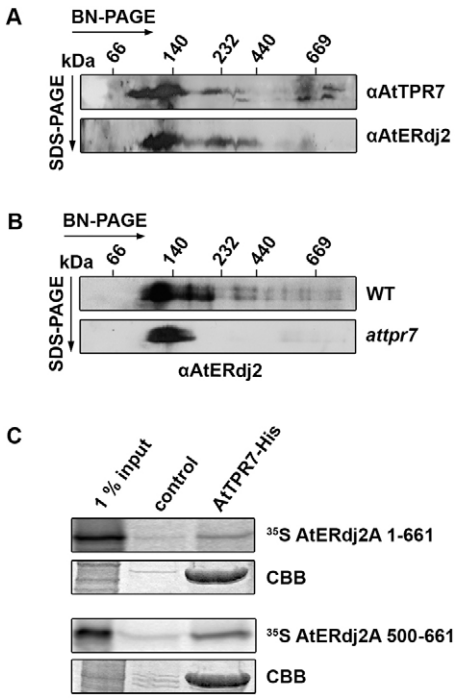

Fig. 6. AtTPR7 co-migrates with AtERdj2. (**A**) Microsomal membranes of wild-type leaves were solubilized with 0.4% DeMa and protein complexes were separated in a first dimension (BN-PAGE) on a 5–12% gel and in second dimension (SDS-PAGE) on a 12% gel. The second dimension was probed with antisera against AtTPR7 and AtERdj2A. (**B**) Microsomal membranes of wild type and *attpr7* mutant were separated by BN- and SDS-PAGE as in A and probed with AtERdj2A antisera. Protein content of microsomal membranes of wild type and mutant was determined using a Bradford assay and equal amounts of protein equivalent to 100 µg were loaded. (**C**) Recombinant AtTPR7–His (60 µg) was incubated with full-length radiolabelled AtERdj2A (upper panel) and the C-terminus of AtERdj2A, comprising amino acids 500–661 (lower panel) translated in reticulocyte lysate in a 10 µl reaction. In both cases AtERdj2A could be re-purified with AtTPR7–His and detected by autoradiography. Coomassie-stained eluted AtTPR7–His (CBB) is shown as a control.

mutant to BN-PAGE. Interestingly, the higher molecular weight complexes at ~200 kDa disappear in the mutant, which again points to an interaction between the two proteins, which cannot be formed in the mutant any longer (Fig. 4B). These data suggest that AtTPR7 and AtERdj2 form complexes, possibly containing further subunits.

To follow this line of evidence we tested whether a direct interaction between AtTPR7 and AtERdj2 could be observed. We chose AtERdj2A for these experiments, since AtERdj2A mutants are lethal in comparison to AtERdj2B and therefore seems to represent the physiologically more relevant isoform (Yamamoto et al., 2008). Purified AtTPR7–His was bound to Ni-NTA and incubated with radiolabelled AtERdj2A translated in reticulocyte lysate. Ni-NTA without bound protein was used as a control (Fig. 6C, upper panel). Indeed, AtERdj2A could be co-purified with AtTPR7–His. We could moreover show that the association seems to involve the C-terminal 161 amino acids of AtERdj2A, since AtTPR7–His was also able to interact with this peptide of AtERdj2A (Fig. 6C, lower panel).

To further test whether this interaction also persists *in vivo*, BiFC (bimolecular fluorescence complementation) analysis was applied. Full-length *AtERdj2A* and *AtTPR7* were fused to complementary portions of fluorescent tags and expressed simultaneously in tobacco leaves resulting in a reconstituted fluorescence signal upon physical interaction (Gehl et al., 2009). The C-terminal part of SCFP was fused to the N-terminus of *TPR7* to avoid interference with targeting. The N-terminal part of Venus was fused to the C-terminus of *AtERdj2A*, according to its likely topology as described for the homologue yeast Sec63 (Feldheim et al., 1992) (Fig. 7A). The vectors additionally contain either a HA or a c-myc tag, respectively, to monitor expression on protein level by immunoblotting with specific antisera. Both constructs were co-transformed with the ER mCherry marker protein described earlier in agrobacteria infiltrated tobacco leaves under the expression of the *CaMV 35S* promoter. Reconstituted fluorescence at 515 nm was clearly observed upon simultaneous expression of *AtTPR7* and *AtERdj2A* (Fig. 7B, upper and middle left panels), indicating that the two proteins indeed interact physically *in vivo*. Comparison with the fluorescence of the ER marker protein shows clearly overlapping signals, as confirmed by colocalisation analysis, representing colocalised ER and BiFC signals in white (Fig. 7B, upper and middle right panels). This confirms an interaction within the ER membrane. As a negative control *AtTPR7* was expressed together with the luminal protein *AtBiP2*, which should not be able to interact and prevent reconstitution of a fluorescent signal. The negative control shows slight background fluorescence not comparable to the AtERdj2A/AtTPR7 sample, even though pictures were taken with identical microscope settings. Fluorescent pixels were quantified and relative fluorescent values after background subtraction from 10 individual pictures are shown (Fig. 7C). Coexpression of AtTPR7 and AtERdj2A results in a relative fluorescence of 50% in contrast to coexpression of AtTPR7 and AtBiP2, which only reaches 10% relative fluorescence. To ensure proper expression of proteins in the negative control immunoblotting was performed. Signals were obtained with HA antisera, recognising SCFP– HA–AtTPR7 and with c-myc antisera recognising the AtERdj2A–c-myc–Venus and AtBiP2–c-myc–Venus protein (Fig. 7D, left and middle panel). No proteins were detected with the same antisera in untransformed tobacco leaves (Fig. 7D, right panel). Coomassie staining is shown as a loading control for all samples.

AtTPR7 fully restores post-translational ER import in a yeast Δ*sec71* mutant

To investigate a possible *in vivo* function of AtTPR7 in post-translational ER import we asked whether AtTPR7 could complement a Δ*sec71* phenotype in yeast. Sec71 recruits the TPR domain containing component Sec72 to the ER membrane and Δ*sec71* mutants have been shown to lack accumulation of Sec72 due to rapid degradation (Feldheim and Schekman, 1994). Both proteins are required for post-translational import and we therefore tested the functional complementation of Δ*sec71* with *AtTPR7* expressing the unprocessed precursor of a viral A/B toxin in mutant and complemented yeast cells. In *S. cerevisiae*, K28 killer strains are naturally infected by a double-stranded (ds)RNA killer virus which stably persists in the cytosol and encodes an unprocessed precursor (preprotoxin; pptox) of a secreted α/β heterodimeric protein toxin (Schmitt and Breinig, 2006; Schmitt and Tipper, 1990). After post-translational pptox import into the lumen of the ER, the toxin preprotein is processed during passage through the yeast secretory pathway, resulting in a

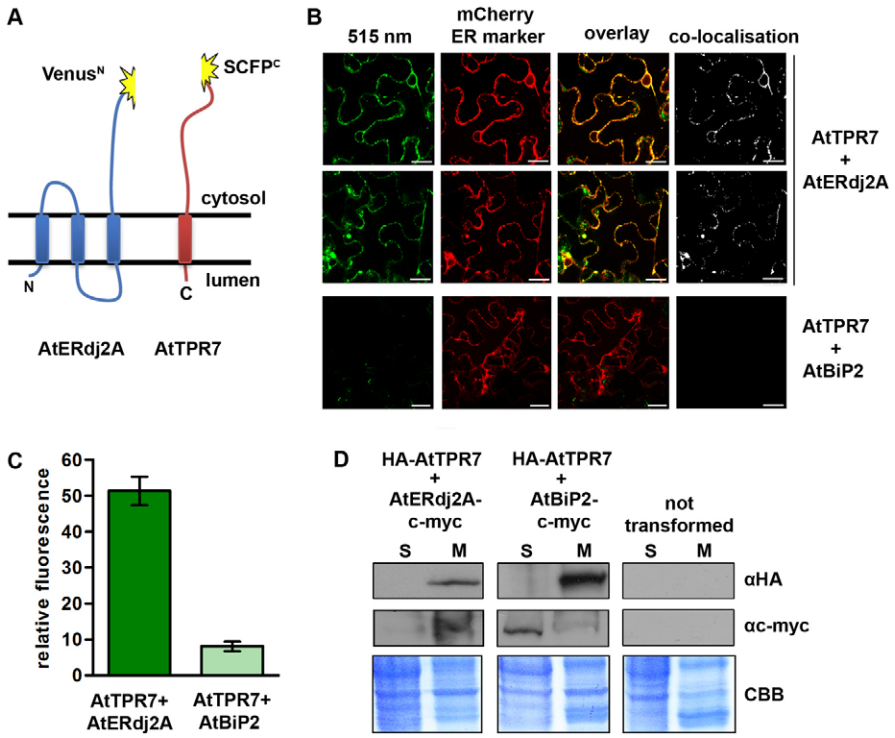

Fig. 7. AtTPR7 associates with AtERdj2A *in vivo* as visualised by BiFC analysis in tobacco leaf cells. (**A**) Diagram of the likely topology of AtERdj2A as deduced from the yeast homologue and the experimentally verified topology of AtTPR7. The N-terminal part of Venus was fused to the C-terminus of AtERdj2A and the C-terminal part of SCFP to the cytosol-exposed N-terminus of AtTPR7. (**B**) Constructs shown in A were co-transformed with the ER mCherry marker (second column) and expressed in tobacco. AtTPR7 was co-transformed with AtBiP2 as a negative control (lower panel). Images of tobacco leaf cells were obtained by confocal laser scanning microscopy. Reconstituted fluorescence obtained by close proximity of the Venus and the SCFP parts was monitored at 515 nm (left panel). Overlay of the signal at 515 nm and the mCherry marker is shown as well as colocalisation of both signals (right panel; in white). Scale bars: 10 µm. (**C**) Fluorescent pixels at 515 nm in 10 separate images as in B were quantified. (**D**) Expression of the proteins was confirmed by immunoblotting. Proteins were extracted from transformed and untransformed tobacco leaves, separated into a soluble (S) and a membrane (M) fraction and probed with HA antisera (detection of HA–AtTPR7) and c-myc antisera (detection of AtERdj2A–c-myc and AtBiP2–c-myc). Proteins from untransformed leaves were likewise probed with the respective antisera (right panels). Coomassie staining (CBB) is shown as a loading control (lower panels).

disulfide-bonded α/β toxin which arrests sensitive cells at the G1/S boundary of the cell cycle and finally kills by causing cell death (Reiter et al., 2005). Post-translational pptox import into the ER is assisted by cytosolic chaperones and mediated through the Sec61 complex, the major import channel in the ER membrane. Since we previously demonstrated that pptox import into the ER and subsequent K28 toxin secretion is severely blocked in the genetic background of a Δ*sec71* knockout (Breinig et al., 2006), we asked whether *AtTPR7* expression can complement this phenotypic defect by restoring post-translational pptox import into the ER and subsequent secretion of biologically active K28 toxin. The experimental setup for such complementation analysis is schematically illustrated in Fig. 8A; wild-type strain BY4742 and its isogenic Δ*sec71* knockout mutant were transformed with a vector constitutively expressing a V5 epitope-tagged version of the K28 toxin precursor (pptox–V5) from the phosphoglyceratkinase (PGK1) promoter. Thereafter, cells were co-transformed with a second plasmid expressing either (i) full-length *AtTPR7*, (ii) a C-terminal truncated variant (*AtTPR7*ΔTM) lacking its transmembrane domain, or (iii) wild-type *SEC71*. In each case, aliquots of cell-free culture supernatants adjusted to 2×10^8 cells/ml were subjected to SDS-PAGE and probed with monoclonal V5 antisera. As shown in Fig. 8B, toxin secretion was blocked in a yeast Δ*sec71* mutant, confirming our previous data on post-translational pptox import into the ER (Breinig et al., 2006). In contrast, K28 toxin secretion was fully restored to wild-type level after co-expression of either wild-type *SEC71* from *S. cerevisiae* (positive control) or full-length *AtTPR7* from *A. thaliana*. Interestingly and as expected, C-terminal truncated *AtTPR7*ΔTM was not capable to complement the pronounced defect in post-translational pptox import into the ER of a Δ*sec71* mutant, as illustrated by the unaffected block in toxin secretion after *AtTPR7*ΔTM expression. Additionally, expression of both TPR constructs is shown on protein level (Fig. 8C) in the soluble and membrane fraction of transformed Δ*sec71* yeast cells by immunoblotting with AtTPR7 antisera. Full-length AtTPR7 is found in the membrane fraction, which is in accordance with the successful complementation, whereas AtTPR7ΔTM is found in the cytosol as expected.

Discussion

Our study characterises AtTPR7 as a novel ER membrane protein in *Arabidopsis* that interacts with the Sec translocon and has a potential function in post-translational protein transport into the ER. A working hypothesis, summarising the data obtained on AtTPR7 in this work is presented in Fig. 9. The TPR domain of AtTPR7 is exposed in the cytosol thus allowing a specific interaction with HSP90 and/or HSP70. Moreover, interaction with AtERdj2A, as

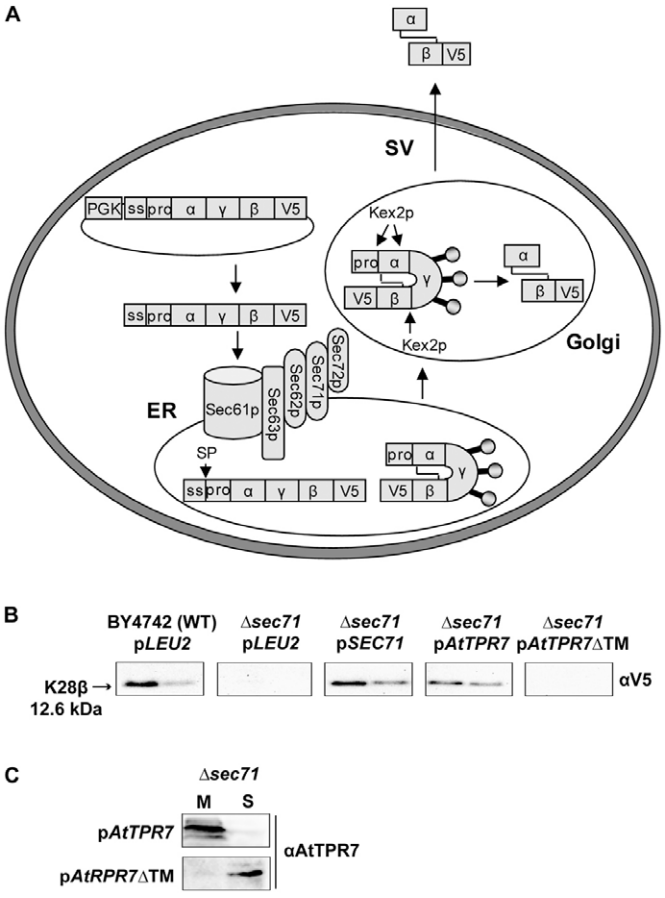

Fig. 8. AtTPR7 complements a Δ*sec71* knockout in yeast and restores post-translational preprotoxin (pptox) import into the ER. (**A**) Experimental setup and schematic outline of post-translational pptox import into the yeast ER. Unprocessed pptox consisting of an N-terminal signal sequence (SS) followed by a pro-, α-, β- and γ-sequence is constitutively expressed from a multi-copy plasmid under PGK1 promoter control. After *in vivo* translation, the toxin precursor enters the secretory pathway post-translationally through the major ER import channel (Sec61 complex), aided by the indicated components of the ER membrane. Subsequent processing through signal peptidase (SP) and Kex2 endopeptidase cleavage generates a disulfide-bonded α/β-heterodimeric toxin which is packaged into secretory vesicles (SV) and finally released into the cell-free culture medium. (**B**) Immunoblot of secreted K28 toxin in cell-free culture supernatants of the indicated wild-type strain BY4742 and its isogenic Δ*sec71* null mutant after co-transformation with a plasmid expressing either (i) *LEU2* (vector control), (ii) wild-type *SEC71* (positive control), (iii) full-length *AtTPR7* or (iv) C-terminal truncated *AtTPR7*ΔTM. In each case, culture supernatants of two independent yeast transformants were adjusted to aliquots of 2×10^8 cells/ml, separated by SDS-PAGE under reducing conditions and subsequently probed with anti-V5 (position of the V5-tagged β-subunit of the toxin is indicated; note that slight differences in protein expression level that can be seen in some yeast transformants are due to different and individual copy numbers of the episomal expression vector in each clone). (**C**) Δ*sec71* yeast cells transformed with full-length *AtTPR7* and *AtTPR7*ΔTM were separated into a membrane (M) and a soluble (S) fraction and probed with AtTPR7 antisera.

observed in this study, strongly suggests an association with a hypothetical plant Sec translocon for post-translational protein import composed of AtSec61 as a channel, AtERdj2 and possibly AtSec62 as it is found in yeast (Harada et al., 2011).

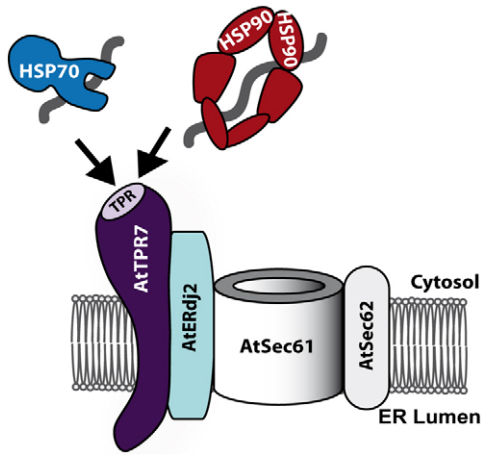

Fig. 9. Working hypothesis. AtTPR7 associates with the Sec translocon via AtERdj2 and has a cytosolic TPR domain that interacts with HSP70 and HSP90, which may be involved in delivering post-translationally imported preproteins.

Several experiments in this study clearly demonstrate that AtTPR7 is localised to the ER, although previous data presented by von Loeffelholz et al., 2011 suggested AtTPR7 to reside in the outer membrane of chloroplasts. We have performed additional experiments to those presented by von Loeffelholz et al., 2011 showing the specificity of our antibody with a T-DNA insertion mutant and characteristic behaviour of AtTPR7 in a magnesium-induced-shift assay, which is widely used as an indicator for ER localised proteins (Ceriotti et al., 1995; Levitan et al., 2005). Although our data strongly imply that AtTPR7 predominantly – if not exclusively – resides in the ER, we cannot exclude that a minor amount of AtTPR7 is associated with the chloroplast outer membrane. Von Loeffelholz et al. show in their *in vitro* experiments that AtTPR7 interacts with a number of chloroplast preproteins and that soluble AtTPR7 can inhibit the import of these preproteins (von Loeffelholz et al., 2011). Since interaction with the preproteins is mostly mediated by HSP70, this might result in unspecific binding of AtTPR7 to chloroplast preproteins, although the authors could not observe a similar effect when using HOP TPR1 as a control TPR protein. Nevertheless, further careful analysis is necessary to explore whether AtTPR7 indeed plays a role in chloroplast import *in vivo*.

Intriguingly, several lines of evidence imply a function in post-translational protein translocation for AtTPR7. TPR domain containing proteins, which are found in all organisms and cellular compartments are known to contribute to post-translational protein import by the interaction with chaperones (Feldheim and Schekman, 1994; Qbadou et al., 2006; Schlegel et al., 2007; Young et al., 2003). HSP90 and HSP70 interact with preproteins in the cytosol and subsequently mediate a first contact between preproteins and membrane surfaces. In plants, the TPR domain containing protein Toc64 is associated with the chloroplast Toc translocon and has been shown to interact with HSP90 bound to preproteins (Qbadou et al., 2007). OM64 is a TPR protein in the outer mitochondrial membrane in *Arabidopsis*, which might functionally replace Tom70 and is involved in the import of some mitochondrial preproteins (Chew et al., 2004; Lister et al., 2007). Mammalian Tom70 and Tom34 also play a role in the delivery of chaperone-bound preproteins to mitochondria (Faou and

Hoogenraad, 2012; Young et al., 2003). Although post-translationally imported proteins in the ER remain to be identified in plants, a mechanism involving chaperones seems likely. Many ER proteins are known to interact with cytosolic HSP70 (Ngosuwan et al., 2003) in yeast, and cytosolic and membrane associated chaperones have been suggested to assist post-translational import of tail-anchored ER proteins (Abell et al., 2007; Mariappan et al., 2011). So far no TPR domain containing protein has been identified in the ER besides Sec72 in fungi. Whether Sec72 recognises chaperones has not been investigated, however, in some fungi the TPR domain of Sec72 is considered a clamp-type TPR domain and phylogenetic clustering with the TPR1 motif of HOP suggest a potential for HSP70 binding (Schlegel et al., 2007). Involvement of HSP90 next to HSP70 in ER protein translocation remains to be elucidated in the future.

Our studies revealed that AtTPR7 exposes its clamp-type TPR domain to the cytosol, a prerequisite for its interaction with cytosolic chaperones. Indeed, AtTPR7 interacts with all cytosolic *Arabidopsis* HSP90 isoforms, most strongly with AtHSP90.2 and AtHSP90.3, which are constitutively expressed in *Arabidopsis* (Krishna and Gloor, 2001). Possibly different HSP90 isoforms might participate in chloroplast and ER protein sorting, however, this issue has not been addressed so far. A clear interaction was likewise observed with AtHSP70.1, which is also a constitutively expressed and highly abundant HSP70 isoform of the five cytosolic isoforms found in *Arabidopsis* (Lin et al., 2001). Interaction of recombinant AtTPR7 with both chaperones was additionally observed in wheat germ lysate. Preferential interaction with either of the chaperones remains to be analysed by biophysical measurements. HSP70 interaction with AtTPR7 was described previously (Kriechbaumer et al., 2011; von Loeffelholz et al., 2011); however, both these studies reported that no HSP90 interaction could be detected. Possibly variations in the reaction setup and/or experimental conditions favoured HSP90 binding in our experiments. For example in the previous work an N-terminal His-tagged AtTPR7 was used and HSP90 was treated with protease to cleave the His tag. In contrast to this, we used an N-terminal His tag, replacing the transmembrane domain and Strep-tagged HSP90. Nevertheless, interaction with HSP90 and HSP70 via the cytosolic TPR domain strongly suggests a possible interaction with cytosolic preprotein–chaperone complexes. However, to identify such target preproteins in plants, which are imported post-translationally into the ER, is challenging and remains to be elucidated. Moreover, a possible direct interaction of potential post-translationally imported ER preproteins with AtTPR7, as it is known from Tom20 and Pex5, remains to be analysed. The notion of AtTPR7 being involved in post-translational protein import was further strengthened by the successful complementation of a yeast Δ*sec71* mutant by full-length AtTPR7, which fully restored the defect in toxin secretion in Δ*sec71*, which is due to a less efficient post-translational import process. Importantly, Sec71 recruits the TPR domain containing protein Sec72 to the membrane, which also plays a role in post-translational import, and is rapidly degraded in Δ*sec71*. We therefore suggest that AtTPR7 functionally replaces both yeast proteins, since it comprises not only a cytosolic TPR domain but also a transmembrane anchor. AtTPR7 may therefore represent the first ER TPR docking protein in higher eukaryotes.

However, AtTPR7 *Arabidopsis* loss-of-function mutants do not show a visible phenotype under standard growth conditions, indicating that the chaperone recognition process can be bypassed, as it is also the case for the chloroplast receptor Toc64 and the mitochondrial TPR protein OM64 in *Arabidopsis* (Aronsson et al., 2007; Lister et al., 2007). Likewise, neither the loss of Sec71/Sec72 nor deletion of the yeast/mammalian mitochondrial TPR receptors Tom70 and Tom34 results in a lethal phenotype (Fang and Green, 1994; Faou and Hoogenraad, 2012; Young et al., 2003).

Since AtTPR7 might functionally replace Sec72 we would expect it to be associated with components of the Sec translocon of *Arabidopsis* to transfer potential substrate proteins to the channel Sec61. In yeast, Sec63 and Sec62 participate in post-translation protein import next to the Sec61 channel and Sec71/Sec72 (Harada et al., 2011). Indeed, our data present the interaction of AtTPR7 with AtERdj2, the *Arabidopsis* homologue of yeast Sec63. This interaction was observed not only by *in vitro* experiments, but also *in vivo* with the help of BiFC analysis and co-migration of the two proteins in native gels. Again this supports our hypothesis concerning the function of AtTPR7 as part of the Sec translocon. In addition, it provides a first insight into the architecture of the Sec complex in plants, which has not been analysed so far, although several essential components showing homology to yeast/mammalian components have been identified (Yamamoto et al., 2008).

In summary, AtTPR7 presents a third chaperone docking protein, next to Toc64 and OM64, which implies a general mechanism in recognition of post-translationally imported proteins in plant cells and presents an intriguing and exciting system to explore ER, mitochondrial and chloroplast protein translocation in a single cellular context.

Materials and Methods

Plant material

Wild-type *Arabidopsis thaliana* (ecotype Columbia) and the *attpr7* mutant line were grown on soil under 16 h light/8 h dark in the climate chamber at 22℃ at 120 μE/m^2/s. *Nicotiana benthamiana* was grown in soil under greenhouse conditions. *Pisum sativum* (var. Arvica) were grown under a 14 h light/10 h dark regime at 20℃/15℃. The *attpr7* T-DNA insertion line with an insertion in exon 9 (SALK_057977) was obtained from the SALK collection (http://signal.salk.edu) and homozygous lines were isolated by PCR using the oligonucleotides *AtTPR7*-Ex9-f, *AtTPR7*-Ex11-rev and LBa1 (supplementary material Table S1).

Agrobacterium-mediated transient expression of fluorescent proteins in tobacco

Leaves of 4- to 6-week-old *Nicotiana benthamiana* were infiltrated with agrobacteria for transient expression of gene constructs. The *Agrobacterium tumefaciens* strain Agl1 was transformed with the respective gene constructs and cell cultures were resuspended in infiltration medium [10 mM $MgCl_2$, 10 mM MES/KOH (pH 5.7), 150 μM acetosyringone] to a final OD_{600} of 1.0 and incubated for 2 h in the dark. Protein expression was monitored after 2 days. Protoplasts were prepared as described previously (Koop et al., 1996), however, cell walls were digested for 90 min at 40 rpm in 1% cellulase R10 and 0.3% macerase R10 after vacuum infiltration. Fluorescence was observed with a confocal laser scanning microscope at 20℃ (Leica, Type: TCS SP5; objective lens: HCX PL APO CS, magnification: 63×, numerical aperture: 1.3; imaging medium: glycerol, software: Leica Application Suite/Advanced Fluorescence).

For localisation experiments the *AtTPR7* coding sequence was cloned into the binary gateway vector pK7WGF2 (Plant Systems Biology, Gent). The Golgi marker is composed of the cytoplasmic tail and transmembrane domain of soybean α-1,2-mannosidase I and the ER marker consists of the signal peptide of *Arabidopsis thaliana* wall-associated kinase 2 at the N-terminus of the fluorescent protein and the ER retention signal His-Asp-Glu-Leu at its C-terminus (Nelson et al., 2007). Construction of the plant binary gateway vector pAM-PAT-35S-YFP-GW used for the YFP fusion construct is described elsewhere (Lefebvre et al., 2010). Constructs for fluorescence and BiFC analysis were cloned into appropriate entry and destination vectors with the gateway system (Invitrogen; see supplementary material Table S1) (Gehl et al., 2009). Quantification of fluorescent pixels and colocalisation analysis was performed with ImageJ (http://imagej.nih.gov/ij/).

Preparation of microsomal membranes

Three week old *Arabidopsis thaliana* leaves were homogenised in a buffer containing 0.05 M Tris-HCl (pH 7.5), 0.5 M sucrose, 1 mM EDTA using an ultra

turrax. The filtrated lysate was centrifuged twice to remove thylakoids, intact chloroplasts and mitochondria (first centrifugation 4200 ***g***, 10 min; second centrifugation 10,000 ***g***, 10 min, 4℃). To pellet the microsomal membranes the remaining lysate was centrifuged at 100 000 ***g*** for 1 h. Microsomes were resuspended in appropriate buffers and either loaded on sucrose density gradients or directly subjected to further experiments.

SDS-PAGE and immunoblotting

Proteins were separated on 10 or 12% polyacrylamide gels and immunodetection was performed as described previously (Lamberti et al., 2011). *Arabidopsis* chloroplasts were isolated on percoll gradients as described previously (Benz et al., 2009). AtERdj2A Antisera were kindly provided by Shuh-ichi Nishikawa. SMT1 antiserum was obtained from Agrisera (Vännäs, Sweden), GFP and HA antisera from Roche (Grenzach-Wyhlen, Germany) and c-myc antisera from Santa Cruz Biotechnology (Santa Cruz, USA). HSP90 and HSP70 antisera were generated against wheat chaperones and are described elsewhere (Fellerer et al., 2011). Polyclonal PsToc64 antisera were raised against pea PsToc64.

BN-PAGE

100 µg microsomes were resuspended in 50 µl ACA buffer (750 mM aminocaproic acid, 50 mM Bis Tris (pH 7), 0.5 mM EDTA) and solubilized with 0.4% DeMa for 10 min on ice. After centrifugation (10 min, 16,100 ***g***, 4℃) the supernatant was loaded on a 5–12% native gel. The first dimension gel stripes were incubated for 15 min in 62.5 mM Tris-HCl (pH 6.8), 1% SDS, 1% β-mercaptoethanol, and 15 min in the same buffer without β-mercaptoethanol. The gel stripes were applied on a second dimension 12% SDS-PAGE and analysed by immunoblotting.

Sucrose density gradients

Microsomal fractions or total plant lysate ground in homogenisation buffer (100 mM Tris-HCl pH 7.8, 10 mM KCl, 12% sucrose) was applied on a linear sucrose gradient (1.05–1.25 g/ml sucrose) and centrifuged for 2 h at 166,900 ***g*** and 4℃ in a swing-out rotor.

In vitro transcription, translation and import of radiolabelled proteins

Templates for *in vitro* transcription were cloned into pF3A (Promega, Madison, USA; see supplementary material Table S1 for oligonucleotides) and *in vitro* transcription was performed with SP6 polymerase (Fermentas, St-Leon-Rot, Germany). *In vitro* translation in reticulocyte lysate (Promega) was performed according to manufacturer's instructions. Co-translational import of radiolabelled proteins into dog pancreatic microsomes was achieved by incubation of the microsomes with the translation mix at 30℃ for 60 min. Post-translational import was achieved by incubation of the microsomes with freshly translated protein after RNase A digest for 5 min at 30℃ (80 µg/ml) and cycloheximide treatment (100 µg/ml) as described elsewhere (Lang et al., 2012), except that ER membranes were washed with 100 mM Na_2CO_3 and pelleted prior to SDS-PAGE to remove residual uninserted protein. Triton X-100 was added in a concentration of 1% (v/v). Proteinase K (50 µg/ml final concentration) digest was performed for 30 min on ice and the reaction was stopped with 200 mM PMSF and addition of SDS loading buffer.

Purification and overexpression of proteins

AtTPR7 lacking the transmembrane domain of AtTPR7 (amino acids 1–500) used for pull down experiments was cloned into pET21a$^+$ (Novagen, Darmstadt, Germany), expressed in M9ZB medium at 25℃ for 5 h and purified via Ni-NTA-affinity chromatography (GE Healthcare). For production of polyclonal antisera full length *AtTPR7* and *TOC64* were cloned with a C-terminal StrepII tag into pET21a$^+$ and expressed in M9ZB medium over night at 18℃ and purified accordingly. Antibodies against the purified proteins were generated by Biogenes (Berlin, Germany). *AtHSP90* isoforms were initially amplified from *Arabidopsis* cDNA using oligonucleotides recognising the 3′ and 5′ UTR to ensure amplification of the correct isoform. In a second step the genes were cloned into pET51b with an N-terminal StrepII tag. Site-directed mutagenesis of *AtTPR7* was performed as described previously (Kunkel et al., 1987). Sequences of all clones were controlled by DNA sequencing. Oligonucleotides and constructs are summarised in supplementary material Table S1.

In vitro pull-down experiments

AtTPR7–His was incubated with Strep-tagged chaperones, wheat germ lysate or proteins translated in reticulocyte lysate as indicated for 1 h at RT. AtTPR7–His was subsequently re-purified by incubation with Ni-NTA for 1 h at RT and proteins were eluted with 300 mM imidazol and either probed with HSP70 or HSP90 antisera or detected by autoradiography.

Yeast strains and complementation

The *S. cerevisiae* wild-type strain BY4742 and its isogenic Δ*sec71* knockout mutant were derived from the *Saccharomyces* Genome Deletion Consortium and obtained from Open Biosystems. Yeast transformations and immunoblot analysis of secreted K28 toxin in cell-free culture supernatants of wild-type and Δ*sec71* cells before and after co-transformation with the expression vectors p*AtTPR7*, p*AtTPR7*ΔTM, p*SEC71* or p*LEU2* were performed as previously described (see supplementary material Table S1 for constructs and oligonucleotides) (Breinig et al., 2006; Breinig et al., 2002; Heiligenstein et al., 2006; Schmitt and Tipper, 1990).

Competitive chloroplast and ER import

Chloroplasts from *P. sativum* were isolated as described previously (Waegemann and Soll, 1995). Chloroplasts (corresponding to 10 µg chlorophyll) and 1 µl dog pancreatic microsomes were mixed in a 100 µl reaction volume in a buffer containing (50 mM HEPES, pH 8.0, 330 mM sorbitol, 8.4 mM methionine, 13 mM ATP, 13 mM $MgCl_2$) and incubated at 30℃ for 20 min with radiolabelled translation products synthesised in reticulocyte lysate. After the import reaction chloroplasts were separated from ER membranes by centrifugation through a 40% percoll cushion and pelleted at 3000 ***g***. ER membranes were pelleted by centrifugation at 200,000 ***g***. Both membranes were washed with 100 mM Na_2CO_3 to remove uninserted protein.

Sequence analysis and accession numbers

Sequence data from this article can be found in the NCBI data libraries under accession numbers: At5g21990 (*AtTPR7*), At3g17970 (*TOC64*), At1g79940 (AtERdj2A), At5g42020 (*AtBiP2*), At5g02500 (*AtHSP70.1*). At5g52640 (*AtHSP90.1*), At5g56030 (*AtHSP90.2*), At5g56010 (*AtHSP90.3*), At5g56000 (*AtHSP90.4*), SPAC4D7.01c (*SEC71*), Bd1g56980 (*Brachypodium distachyon TPR7*), NP_001058942 (*Oryza sativa TPR7*), *XP_001765981* (*Physcomitrella patens TPR7*), XP_002977395 (*Selaginella moellendorfii TPR7*), XP_001701985 (*Chlamydomonas reinhardtii TPR7*), YOR027W (*STI1*). TPR and transmembrane domains were predicted by NCBI conserved domain search and Aramemnon, respectively (http://www.ncbi.nlm.nih.gov/Structure/cdd/wrpsb.cgi and http://aramemnon.botanik.uni-koeln.de). Alignments were generated using ClustalW.

Acknowledgements

Richard Zimmermann is acknowledged for the generous gift of dog pancreatic microsomes and advice on ER import experiments. AtERdj2 antisera were a kind gift from Shuh-ichi Nishikawa. Vectors and strains for tobacco infiltration were kindly provided by Norbert Mehlmer and Thomas Ott. Katharina Schöngruber and Stefanie Rapp are acknowledged for excellent technical assistance. We further thank Sandra Ring for the construction of AtTPR7 plasmids and WaiLing Chang for preparation of chloroplasts.

Funding

This work was supported by Deutsche Forschungsgemeinschaft [grants numbers SFB 1035, project A04 to J.S. and S.S., GRK 845 to M.J.S.]; and Fonds der chemischen Industrie [grant number Do 187/22 to R.S.]

Supplementary material available online at
http://jcs.biologists.org/lookup/suppl/doi:10.1242/jcs.111054/-/DC1

References

Abe, Y., Shodai, T., Muto, T., Mihara, K., Torii, H., Nishikawa, S., Endo, T. and Kohda, D. (2000). Structural basis of presequence recognition by the mitochondrial protein import receptor Tom20. *Cell* **100**, 551-560.

Abell, B. M., Rabu, C., Leznicki, P., Young, J. C. and High, S. (2007). Post-translational integration of tail-anchored proteins is facilitated by defined molecular chaperones. *J. Cell Sci.* **120**, 1743-1751.

Aronsson, H., Boij, P., Patel, R., Wardle, A., Töpel, M. and Jarvis, P. (2007). Toc64/OEP64 is not essential for the efficient import of proteins into chloroplasts in *Arabidopsis thaliana*. *Plant J.* **52**, 53-68.

Benz, M., Bals, T., Gügel, I. L., Piotrowski, M., Kuhn, A., Schünemann, D., Soll, J. and Ankele, E. (2009). Alb4 of *Arabidopsis* promotes assembly and stabilization of a non chlorophyll-binding photosynthetic complex, the CF1CF0-ATP synthase. *Mol. Plant* **2**, 1410-1424.

Borgese, N., Gazzoni, I., Barberi, M., Colombo, S. and Pedrazzini, E. (2001). Targeting of a tail-anchored protein to endoplasmic reticulum and mitochondrial outer membrane by independent but competing pathways. *Mol. Biol. Cell* **12**, 2482-2496.

Boutté, Y., Frescatada-Rosa, M., Men, S., Chow, C. M., Ebine, K., Gustavsson, A., Johansson, L., Ueda, T., Moore, I., Jürgens, G. et al. (2010). Endocytosis restricts *Arabidopsis* KNOLLE syntaxin to the cell division plane during late cytokinesis. *EMBO J.* **29**, 546-558.

Breinig, F., Tipper, D. J. and Schmitt, M. J. (2002). Kre1p, the plasma membrane receptor for the yeast K1 viral toxin. *Cell* **108**, 395-405.

Breinig, F., Sendzik, T., Eisfeld, K. and Schmitt, M. J. (2006). Dissecting toxin immunity in virus-infected killer yeast uncovers an intrinsic strategy of self-protection. *Proc. Natl. Acad. Sci. USA* **103**, 3810-3815.
Ceriotti, A., Pedrazzini, E., De Silvestris, M. and Vitale, A. (1995). Import into the endoplasmic reticulum. *Methods Cell Biol.* **50**, 295-308.
Chew, O., Lister, R., Qbadou, S., Heazlewood, J. L., Soll, J., Schleiff, E., Millar, A. H. and Whelan, J. (2004). A plant outer mitochondrial membrane protein with high amino acid sequence identity to a chloroplast protein import receptor. *FEBS Lett.* **557**, 109-114.
Cline, K., Andrews, J., Mersey, B., Newcomb, E. H. and Keegstra, K. (1981). Separation and characterization of inner and outer envelope membranes of pea chloroplasts. *Proc. Natl. Acad. Sci. USA* **78**, 3595-3599.
D'Andrea, L. D. and Regan, L. (2003). TPR proteins: the versatile helix. *Trends Biochem. Sci.* **28**, 655-662.
Denecke, J., Goldman, M. H., Demolder, J., Seurinck, J. and Botterman, J. (1991). The tobacco luminal binding protein is encoded by a multigene family. *Plant Cell* **3**, 1025-1035.
Erdmann, R. and Schliebs, W. (2005). Peroxisomal matrix protein import: the transient pore model. *Nat. Rev. Mol. Cell Biol.* **6**, 738-742.
Fan, A. C., Bhangoo, M. K. and Young, J. C. (2006). Hsp90 functions in the targeting and outer membrane translocation steps of Tom70-mediated mitochondrial import. *J. Biol. Chem.* **281**, 33313-33324.
Fang, H. and Green, N. (1994). Nonlethal sec71-1 and sec72-1 mutations eliminate proteins associated with the Sec63p-BiP complex from S. cerevisiae. *Mol. Biol. Cell* **5**, 933-942.
Faou, P. and Hoogenraad, N. J. (2012). Tom34: a cytosolic cochaperone of the Hsp90/Hsp70 protein complex involved in mitochondrial protein import. *Biochim. Biophys. Acta* **1823**, 348-357.
Feldheim, D. and Schekman, R. (1994). Sec72p contributes to the selective recognition of signal peptides by the secretory polypeptide translocation complex. *J. Cell Biol.* **126**, 935-943.
Feldheim, D., Rothblatt, J. and Schekman, R. (1992). Topology and functional domains of Sec63p, an endoplasmic reticulum membrane protein required for secretory protein translocation. *Mol. Cell. Biol.* **12**, 3288-3296.
Fellerer, C., Schweiger, R., Schöngruber, K., Soll, J. and Schwenkert, S. (2011). Cytosolic HSP90 cochaperones HOP and FKBP interact with freshly synthesized chloroplast preproteins of *Arabidopsis*. *Mol. Plant* **4**, 1133-1145.
Gatto, G. J., Jr, Geisbrecht, B. V., Gould, S. J. and Berg, J. M. (2000). Peroxisomal targeting signal-1 recognition by the TPR domains of human PEX5. *Nat. Struct. Biol.* **7**, 1091-1095.
Gehl, C., Waadt, R., Kudla, J., Mendel, R. R. and Hänsch, R. (2009). New GATEWAY vectors for high throughput analyses of protein-protein interactions by bimolecular fluorescence complementation. *Mol. Plant* **2**, 1051-1058.
Harada, Y., Li, H., Wall, J. S., Li, H. and Lennarz, W. J. (2011). Structural studies and the assembly of the heptameric post-translational translocon complex. *J. Biol. Chem.* **286**, 2956-2965.
Hegde, S., Lenox, L. E., Lariviere, A., Porayette, P., Perry, J. M., Yon, M. and Paulson, R. F. (2007). An intronic sequence mutated in flexed-tail mice regulates splicing of Smad5. *Mamm. Genome* **18**, 852-860.
Heiligenstein, S., Eisfeld, K., Sendzik, T., Jimenéz-Becker, N., Breinig, F. and Schmitt, M. J. (2006). Retrotranslocation of a viral A/B toxin from the yeast endoplasmic reticulum is independent of ubiquitination and ERAD. *EMBO J.* **25**, 4717-4727.
Koop, H. U., Steinmüller, K., Wagner, H., Rössler, C., Eibl, C. and Sacher, L. (1996). Integration of foreign sequences into the tobacco plastome via polyethylene glycol-mediated protoplast transformation. *Planta* **199**, 193-201.
Kriechbaumer, V., Tsargorodskaya, A., Mustafa, M. K., Vinogradova, T., Lacey, J., Smith, D. P., Abell, B. M. and Nabok, A. (2011). Study of receptor-chaperone interactions using the optical technique of spectroscopic ellipsometry. *Biophys. J.* **101**, 504-511.
Kriechbaumer, V., von Löffelholz, O. and Abell, B. M. (2012). Chaperone receptors: guiding proteins to intracellular compartments. *Protoplasma* **249**, 21-30.
Krishna, P. and Gloor, G. (2001). The Hsp90 family of proteins in *Arabidopsis thaliana*. *Cell Stress Chaperones* **6**, 238-246.
Kunkel, T. A., Roberts, J. D. and Zakour, R. A. (1987). Rapid and efficient site-specific mutagenesis without phenotypic selection. *Methods Enzymol.* **154**, 367-382.
Lamberti, G., Gügel, I. L., Meurer, J., Soll, J. and Schwenkert, S. (2011). The cytosolic kinases STY8, STY17, and STY46 are involved in chloroplast differentiation in *Arabidopsis*. *Plant Physiol.* **157**, 70-85.
Lang, S., Benedix, J., Fedeles, S. V., Schorr, S., Schirra, C., Schäuble, N., Jalal, C., Greiner, M., Hassdenteufel, S., Tatzelt, J. et al. (2012). Different effects of Sec61α, Sec62 and Sec63 depletion on transport of polypeptides into the endoplasmic reticulum of mammalian cells. *J. Cell Sci.* **125**, 1958-1969.
Lee, J. R., Jang, H. H., Park, J. H., Jung, J. H., Lee, S. S., Park, S. K., Chi, Y. H., Moon, J. C., Lee, Y. M., Kim, S. Y. et al. (2006). Cloning of two splice variants of the rice PTS1 receptor, OsPex5pL and OsPex5pS, and their functional characterization using pex5-deficient yeast and *Arabidopsis*. *Plant J.* **47**, 457-466.
Lefebvre, B., Timmers, T., Mbengue, M., Moreau, S., Hervé, C., Tóth, K., Bittencourt-Silvestre, J., Klaus, D., Deslandes, L., Godiard, L. et al. (2010). A remorin protein interacts with symbiotic receptors and regulates bacterial infection. *Proc. Natl. Acad. Sci. USA* **107**, 2343-2348.
Levitan, A., Trebitsh, T., Kiss, V., Pereg, Y., Dangoor, I. and Danon, A. (2005). Dual targeting of the protein disulfide isomerase RB60 to the chloroplast and the endoplasmic reticulum. *Proc. Natl. Acad. Sci. USA* **102**, 6225-6230.
Lin, B. L., Wang, J. S., Liu, H. C., Chen, R. W., Meyer, Y., Barakat, A. and Delseny, M. (2001). Genomic analysis of the Hsp70 superfamily in *Arabidopsis thaliana*. *Cell Stress Chaperones* **6**, 201-208.
Lister, R., Carrie, C., Duncan, O., Ho, L. H., Howell, K. A., Murcha, M. W. and Whelan, J. (2007). Functional definition of outer membrane proteins involved in preprotein import into mitochondria. *Plant Cell* **19**, 3739-3759.
Mariappan, M., Mateja, A., Dobosz, M., Bove, E., Hegde, R. S. and Keenan, R. J. (2011). The mechanism of membrane-associated steps in tail-anchored protein insertion. *Nature* **477**, 61-66.
Maruyama, D., Endo, T. and Nishikawa, S. (2010). BiP-mediated polar nuclei fusion is essential for the regulation of endosperm nuclei proliferation in *Arabidopsis thaliana*. *Proc. Natl. Acad. Sci. USA* **107**, 1684-1689.
Nelson, B. K., Cai, X. and Nebenführ, A. (2007). A multicolored set of *in vivo* organelle markers for co-localization studies in *Arabidopsis* and other plants. *Plant J.* **51**, 1126-1136.
Ng, D. T., Brown, J. D. and Walter, P. (1996). Signal sequences specify the targeting route to the endoplasmic reticulum membrane. *J. Cell Biol.* **134**, 269-278.
Ngosuwan, J., Wang, N. M., Fung, K. L. and Chirico, W. J. (2003). Roles of cytosolic Hsp70 and Hsp40 molecular chaperones in post-translational translocation of presecretory proteins into the endoplasmic reticulum. *J. Biol. Chem.* **278**, 7034-7042.
Osborne, A. R., Rapoport, T. A. and van den Berg, B. (2005). Protein translocation by the Sec61/SecY channel. *Annu. Rev. Cell Dev. Biol.* **21**, 529-550.
Prasad, B. D., Goel, S. and Krishna, P. (2010). In silico identification of carboxylate clamp type tetratricopeptide repeat proteins in *Arabidopsis* and rice as putative co-chaperones of Hsp90/Hsp70. *PLoS ONE* **5**, e12761.
Qbadou, S., Becker, T., Mirus, O., Tews, I., Soll, J. and Schleiff, E. (2006). The molecular chaperone Hsp90 delivers precursor proteins to the chloroplast import receptor Toc64. *EMBO J.* **25**, 1836-1847.
Qbadou, S., Becker, T., Bionda, T., Reger, K., Ruprecht, M., Soll, J. and Schleiff, E. (2007). Toc64—a preprotein-receptor at the outer membrane with bipartide function. *J. Mol. Biol.* **367**, 1330-1346.
Rabu, C., Wipf, P., Brodsky, J. L. and High, S. (2008). A precursor-specific role for Hsp40/Hsc70 during tail-anchored protein integration at the endoplasmic reticulum. *J. Biol. Chem.* **283**, 27504-27513.
Rapoport, T. A. (2007). Protein translocation across the eukaryotic endoplasmic reticulum and bacterial plasma membranes. *Nature* **450**, 663-669.
Reiter, J., Herker, E., Madeo, F. and Schmitt, M. J. (2005). Viral killer toxins induce caspase-mediated apoptosis in yeast. *J. Cell Biol.* **168**, 353-358.
Saitoh, T., Igura, M., Obita, T., Ose, T., Kojima, R., Maenaka, K., Endo, T. and Kohda, D. (2007). Tom20 recognizes mitochondrial presequences through dynamic equilibrium among multiple bound states. *EMBO J.* **26**, 4777-4787.
Scheufler, C., Brinker, A., Bourenkov, G., Pegoraro, S., Moroder, L., Bartunik, H., Hartl, F. U. and Moarefi, I. (2000). Structure of TPR domain-peptide complexes: critical elements in the assembly of the Hsp70-Hsp90 multichaperone machine. *Cell* **101**, 199-210.
Schlegel, T., Mirus, O., von Haeseler, A. and Schleiff, E. (2007). The tetratricopeptide repeats of receptors involved in protein translocation across membranes. *Mol. Biol. Evol.* **24**, 2763-2774.
Schleiff, E. and Becker, T. (2011). Common ground for protein translocation: access control for mitochondria and chloroplasts. *Nat. Rev. Mol. Cell Biol.* **12**, 48-59.
Schmid, A. B., Lagleder, S., Gräwert, M. A., Röhl, A., Hagn, F., Wandinger, S. K., Cox, M. B., Demmer, O., Richter, K., Groll, M. et al. (2012). The architecture of functional modules in the Hsp90 co-chaperone Sti1/Hop. *EMBO J.* **31**, 1506-1517.
Schmitt, M. J. and Breinig, F. (2006). Yeast viral killer toxins: lethality and self-protection. *Nat. Rev. Microbiol.* **4**, 212-221.
Schmitt, M. J. and Tipper, D. J. (1990). K28, a unique double-stranded RNA killer virus of Saccharomyces cerevisiae. *Mol. Cell. Biol.* **10**, 4807-4815.
Smith, D. F. (2004). Tetratricopeptide repeat cochaperones in steroid receptor complexes. *Cell Stress Chaperones* **9**, 109-121.
von Loeffelholz, O., Kriechbaumer, V., Ewan, R. A., Jonczyk, R., Lehmann, S., Young, J. C. and Abell, B. M. (2011). OEP61 is a chaperone receptor at the plastid outer envelope. *Biochem. J.* **438**, 143-153.
Waegemann, K. and Soll, J. (1995). Characterization and isolation of the chloroplast protein import machinery. *Methods Cell Biol.* **50**, 255-267.
Wang, F., Brown, E. C., Mak, G., Zhuang, J. and Denic, V. (2010). A chaperone cascade sorts proteins for posttranslational membrane insertion into the endoplasmic reticulum. *Mol. Cell* **40**, 159-171.
Yamamoto, M., Maruyama, D., Endo, T. and Nishikawa, S. (2008). *Arabidopsis thaliana* has a set of J proteins in the endoplasmic reticulum that are conserved from yeast to animals and plants. *Plant Cell Physiol.* **49**, 1547-1562.
Young, J. C., Hoogenraad, N. J. and Hartl, F. U. (2003). Molecular chaperones Hsp90 and Hsp70 deliver preproteins to the mitochondrial import receptor Tom70. *Cell* **112**, 41-50.
Zara, V., Ferramosca, A., Robitaille-Foucher, P., Palmieri, F. and Young, J. C. (2009). Mitochondrial carrier protein biogenesis: role of the chaperones Hsc70 and Hsp90. *Biochem. J.* **419**, 369-375.
Zhang, X. P. and Glaser, E. (2002). Interaction of plant mitochondrial and chloroplast signal peptides with the Hsp70 molecular chaperone. *Trends Plant Sci.* **7**, 14-21.
Zimmermann, R., Sagstetter, M., Lewis, M. J. and Pelham, H. R. (1988). Seventy-kilodalton heat shock proteins and an additional component from reticulocyte lysate stimulate import of M13 procoat protein into microsomes. *EMBO J.* **7**, 2875-2880.
Zimmermann, R., Müller, L. and Wullich, B. (2006). Protein transport into the endoplasmic reticulum: mechanisms and pathologies. *Trends Mol. Med.* **12**, 567-573.
Zimmermann, R., Eyrisch, S., Ahmad, M. and Helms, V. (2011). Protein translocation across the ER membrane. *Biochim. Biophys. Acta* **1808**, 912-924.

Journal of Cell Science

5 Publication III

Schweiger R. and Schwenkert S., (2013). *AtTPR7 as part of the Arabidopsis Sec post-translocon.* Plant Signaling & Behavior; 8:e25286; PMID: 23759546; http://dx.doi.org/10.4161/psb.25286.

Plant Signaling & Behavior 8:8, e25286; August 2013; © 2013 Landes Bioscience

AtTPR7 as part of the *Arabidopsis* Sec post-translocon

Regina Schweiger and Serena Schwenkert*

Department of Biology I, Botany; Ludwig-Maximilians-Universität München; Planegg-Martinsried, Germany

Keywords: endoplasmic reticulum, HSP70, HSP90, post-translational import, *Arabidopsis thaliana*, Sec translocon, AtTPR7

Abbreviations: ER, endoplasmic reticulum; TPR, tetratricopeptide repeat; HSP, heat shock protein; SRP, signal recognition particle; BiFC, bimolecular fluorescence complementation

The secretory system in eukaryotic organisms ensures targeting of proteins to their place of function after they entered the endoplasmic reticulum either co- or post-translationally. Thereby proteins are translocated through the Sec translocon into the endoplasmic reticulum. In the *Arabidopsis* genome homologs for the three major components of the Sec translocon, the central pore Sec61α and the auxiliary proteins Sec62 and Sec63 are present. Phylogenetic analyses show Sec61α to be the most conserved subunit within the Sec translocon whereas Sec62 and Sec63 show less homology but contain the same functional domains among all organisms. We recently characterized a novel tetratricopeptide repeat domain containing protein, AtTPR7, as part of the *Arabidopsis* Sec translocon which is probably involved in chaperone assisted post-translational import. In this study we investigated the interaction of AtTPR7 with Sec62 as well as the cytosolic chaperones HSP70 and HSP90 not only in vitro but also in vivo to further strengthen the hypothesis of AtTPR7 being a chaperone docking protein of the Sec translocon for secretory preproteins in *Arabidopsis*.

The secretory pathway regulates proper targeting of proteins synthesized on cytosolic ribosomes to their destined compartments through the endoplasmic reticulum (ER) and the golgi apparatus as well as via the plasma membrane to the extracellular matrix. The first step in this pathway is the translocation of the newly synthesized proteins into the ER which can occur either co- or post-translationally.[1,2] During co-translational translocation elongation of the protein is arrested due to binding of the signal recognition particle (SRP) to the freshly synthesized nascent polypeptide chain appearing at the ribosome. Translation continues after binding of the SRP to the SRP receptor at the ER membrane and the polypeptide is translocated through the Sec61 channel into the ER.[3]

In the post-translational pathway proteins are first fully synthesized in the cytosol and therefore released from the ribosomes before being translocated. It was shown that predominantly small secretory proteins are translocated post-translationally into the ER in yeast and mammals. These small proteins are expected to be inefficiently recognized by the SRP at the ribosome since translation is completed only shortly after exposure of the N-terminal signal sequence.[4] This post-translational transport is typically facilitated by molecular chaperones such as the heat shock protein 70 (HSP70) in the cytosol.[5] In yeast post-translational translocation requires a heptameric Sec complex at the ER membrane, consisting of a tetrameric Sec62/63p complex (containing Sec62p, Sec63p, Sec71p and Sec72p) in addition to the heterotrimeric Sec61p complex (containing Sec61p, Sbh1p and Sss1p).[6] The Sec61 protein-conducting channel and Sec63p are involved in both, co- and post-translational translocation into the ER.[7] Sec62 as well as the two nonessential proteins Sec71p and Sec72p are specifically associated with the post-translational translocon in yeast. Sec62p is suggested to form a signal peptide receptor together with the proteins Sec71p and Sec72p.[8,9] Sec72p is a soluble protein which is anchored to the ER membrane via the integral membrane protein Sec71p.[6] Moreover, Sec72p contains a tetratricopeptide repeat (TPR) domain, facilitating interaction with HSP70 associated preproteins.[10] Homologs of the yeast Sec62p and Sec63p proteins are also present in mammals and it was shown that these proteins form complexes with each other as well as with Sec61.[11] However, mammalian Sec62 can additionally bind in close proximity to the ribosomal exit tunnel suggesting that it gained a function in comparison to the yeast homolog.[12] Sec71p as well as Sec72p are exclusively found in yeast.

Post-translational translocation into the ER in plants has not been investigated up to date, although homologs for the major components of the Sec translocon can also be identified in plant genomes. The *Arabidopsis thaliana* counterpart of the major channel subunit Sec61α is present as three isoforms, Sec62 occurs as a single gene in *Arabidopsis thaliana* whereas two isoforms of Sec63

*Correspondence to: Serena Schwenkert; Email: serena.schwenkert@lmu.de
Submitted: 05/13/13; Revised: 06/05/13; Accepted: 06/05/13
Citation: Schweiger R, Schwenkert S. AtTPR7 as part of the *Arabidopsis* Sec post-translocon. Plant Signal Behav 2013; 8: e25286; http://dx.doi.org/10.4161/psb.25286

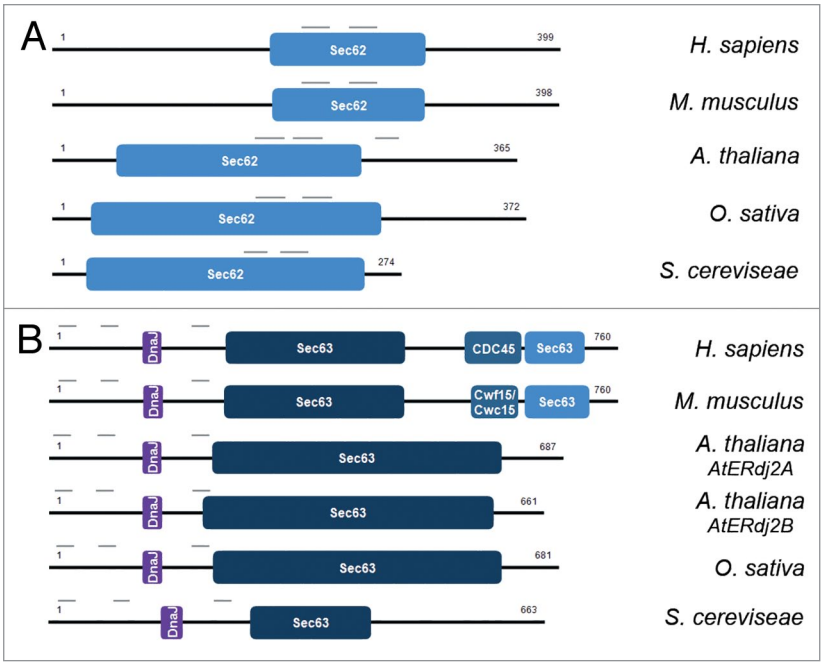

Figure 1. Domain structure of Sec62 and Sec63 in mammals, plants and yeast. (**A**) Comparison of the Sec62 protein of *Homo sapiens*, NP_003253.1; *Mus musculus*, NP_081292.1; *Arabidopsis thaliana*, At3g20920; *Oryza sativa*, Os02 g0435000; *Saccharomyces cereviseae*, NP_015231.2. (**B**) Comparison of the Sec63 protein of *Homo sapiens*, NP_009145.1; *Mus musculus*, NP_694695.3; *Arabidopsis thaliana*, At1g79940, At4g21180; *Oryza sativa*, Os04 g0307200; *Saccharomyces cereviseae*, NP_014897.1. Specific domains are indicated in colors. Predicted transmembrane domains are indicated as gray bars. Homolog genes were identified by "HomoloGene" (NCBI), conserved domains by "Conserved Domain Search" (NCBI) and transmembrane domains were predicted with the help of TMHMM (CBS).

have been identified, AtERdj2A and AtERdj2B.[13] Phylogenetic analyses revealed that the homology of the *Arabidopsis* Sec62 protein to the yeast and mammalian counterparts is comparatively low with a sequence identity of 12% and 15%, respectively. In contrast to yeast and mammals the plant Sec62 homologs show one additional hydrophobic stretch at the C-terminal part reaching from amino acids 254–271 which is predicted as a potential third transmembrane domain in *Arabidopsis* (**Fig. 1A**). In the *Arabidopsis* Sec62 protein the conserved domain of the Sec62 superfamily is reaching from amino acids 50–242 similar to the yeast homolog, whereas in the mammalian homologs this domain reaches only from amino acids 170–293 and is therefore significantly shorter. The two Sec63 isoforms in *Arabidopsis thaliana*, AtERdj2A and AtERdj2B, show 74% identity to each other and only 19% to the human and 22% to the yeast counterparts, respectively (**Fig. 1B**). Both, AtERdj2A and AtERdj2B have three predicted transmembrane domains within the N-terminal region and a J-domain located between the second and the third transmembrane domain, therefore showing the same characteristics as the yeast and mammalian homologs. All Sec63 homologs contain a domain of unknown function conserved in the Sec63 superfamily. The mammalian homologs have two additional domains at the C-terminus lacking in the plant Sec63 proteins, a CDC45-like domain in *Homo sapiens* replaced by a Cwf15/Cwc15 domain in *Mus musculus* and a Sec63 Brl domain which is known to be required for assembly of functional ER translocons[14] conserved in both. Deletion of AtERdj2A in *Arabidopsis* leads to a lethal phenotype and causes defects in pollen function, whereas AtERdj2B mutants grow normally without obvious developmental defect.[13] The β-barrel forming Sec61α subunit is the most highly conserved component of the Sec translocon with all three *Arabidopsis* isoforms bearing 67% identity to the human Sec61α subunit and 52% to the yeast Sec61p. The three *Arabidopsis* Sec61α isoforms share 89% identical amino acids among each other, indicating functional redundancy. Structural features as well as conserved domains such as the Plug- and the SecY-domain were compared between different organisms and showed no significant differences.

In our recent studies we analyzed the composition of the *Arabidopsis* Sec post-translocon and we identified a novel TPR domain containing protein, AtTPR7, which is interacting with AtERdj2A at the ER membrane.[15] Further analyses suggest Sec62 as additional interaction partner of AtTPR7 not only by in vitro pull down experiments but also in vivo performing a bimolecular fluorescence complementation assay (BiFC) (**Fig. 2**). For the pull down experiment recombinant AtTPR7 (amino acids 1–500) carrying a His-tag at the C-terminus replacing the transmembrane domain was purified as described previously.[15] By this deletion unspecific interactions between hydrophobic transmembrane domains of AtTPR7 and Sec62 are avoided. ATPR7 was incubated with radiolabeled Sec62 translated in reticulocyte lysate and recovered by Ni-NTA sepharose. As a control translated Sec62 was incubated with Ni-NTA sepharose without any AtTPR7-His construct and visualized by autoradiography. Sec62 specifically binds to AtTPR7-His and not to the empty beads (**Fig. 2A**). Hereby, we could show that AtTPR7 directly interacts with Sec62 in vitro.

In a second approach AtTPR7 and Sec62 were expressed in tobacco leaves, both linked to complementary parts of fluorescent tags only giving a signal at 515 nm when both fluorescent tags get in close proximity in the cell.[16] An ER mCherry marker protein was co-transformed to determine the location of the interaction.[15] As a negative control Venus^{N}-AtTPR7 was expressed together with the soluble C-terminal part of SCFP alone (empty vector), which should not be able to interact. This in vivo experiment revealed close proximity of AtTPR7 and Sec62 at the ER membrane (**Fig. 2B**), suggesting that AtTPR7 and Sec62 are part of the same protein complex. In combination with the in vitro results a direct interaction of AtTPR7 and Sec62 can be considered. An interaction of Venus^{N}-AtTPR7 with the soluble C-terminus of SCFP at the ER membrane could not be detected. This in vivo approach strengthens the idea that both, not only Sec62 but also AtTPR7, are part of the *Arabidopsis* Sec post-translocon, forming a similar complex to the yeast post-translocon.

Since Sec72 homologs are only present in fungi[17] AtTPR7 might functionally replace yeast Sec72p and its membrane anchor Sec71p in plants. The TPR domain of AtTPR7 seems to replace Sec72p whereas the transmembrane domain of AtTPR7 might compensate for Sec71p. AtTPR7 is a plant specific protein[15] not present in other higher eukaryotes. Among plants, however, AtTPR7 is conserved from the unicellular green algae *Chlamydomonas* to mosses, ferns, mono- and dicotyledonous plants.

TPR domain containing docking proteins are distributed among all cellular compartments associated with the membrane translocons and thereby facilitating post-translational translocation.[18] In yeast the TPR domain containing docking protein Sec72p has been described to bind HSP70 during post-translational translocation of preproteins into the ER.[10] Furthermore, Toc64, a TPR domain containing docking protein at the chloroplast outer envelope, plays a role in chloroplast import by recognizing HSP70/HSP90 bound preproteins.[19] In mammals and yeast Tom70 is the most prominent TPR domain containing receptor in the outer membrane of mitochondria. In yeast Tom70 binds to HSP70, whereas in mammals additional HSP90 binding was demonstrated. Furthermore, the mitochondrial membrane associated protein Tom34, which carries two TPR domains, is shown to interact with HSP70 and HSP90 suggesting a possible function as co-chaperone of HSP70 and HSP90 and thereby playing a role in mitochondrial preprotein delivery.[20,21] Tom70 seems to be functionally replaced by OM64 in plants, a close homolog to Toc64 in chloroplast.[22] We already investigated HSP70 and HSP90 binding to AtTPR7 in vitro in our recent study.[15] To strengthen our hypothesis of HSP70 as well as HSP90 involvement in ER preprotein delivery we performed an in vivo analysis using a BiFC approach (**Fig. 3**). As representative of the HSP70 family in *Arabidopsis* HSP70.1 was used for the interaction studies since it is demonstrated to be an abundant and constitutively expressed isoform.[23] A pull down experiment with all four cytosolic HSP90 isoforms of *Arabidopsis* revealed HSP90.2 to be the isoform with the strongest binding affinity[15] to AtTPR7 in vitro and therefore HSP90.2 was chosen as representative of the HSP90 family in *Arabidopsis* for the BiFC approach. We could show that AtHSP70.1 as well as AtHSP90.2 are interacting with AtTPR7 at the ER membrane in tobacco leaves in vivo since the signal at 515 nm was reconstituted. Expression of the soluble C-terminus of SCFP in the cytosol and Venus^{N}-AtTPR7 at the ER membrane shows no reconstitution of the fluorescent signal showing specificity of the AtTPR7-chaperone interaction. This additional in vivo data supports the idea of AtTPR7 functionally replacing yeast Sec71/72p in *Arabidopsis*. AtTPR7 is strongly assumed to be the docking protein for chaperone bound preproteins during post-translational translocation into the ER in plants. The TPR domain of yeast Sec72p is shown to cluster together with the HSP70 recognizing TPR domains (Hop1 and Hop2b) of the HSP70/HSP90 organizing protein (HOP) and not with the HSP90 binding one (Hop2a) and only HSP70 binding to its TPR domain was investigated so far.[17,24] Therefore, the involvement of HSP90 in addition to HSP70 adds more complexity to the plant translocon machinery in comparison to yeast. Moreover, since neither Sec71p/72p nor AtTPR7 are conserved in mammals, the question arises whether and how chaperone mediated post-translational translocation occurs in these organisms. As a next step it will be of high interest for us to investigate plant proteins as potential chaperone assisted post-translationally translocated preproteins of the ER to gain further insight into the function of AtTPR7 as part of the Sec post-translocon in plants.

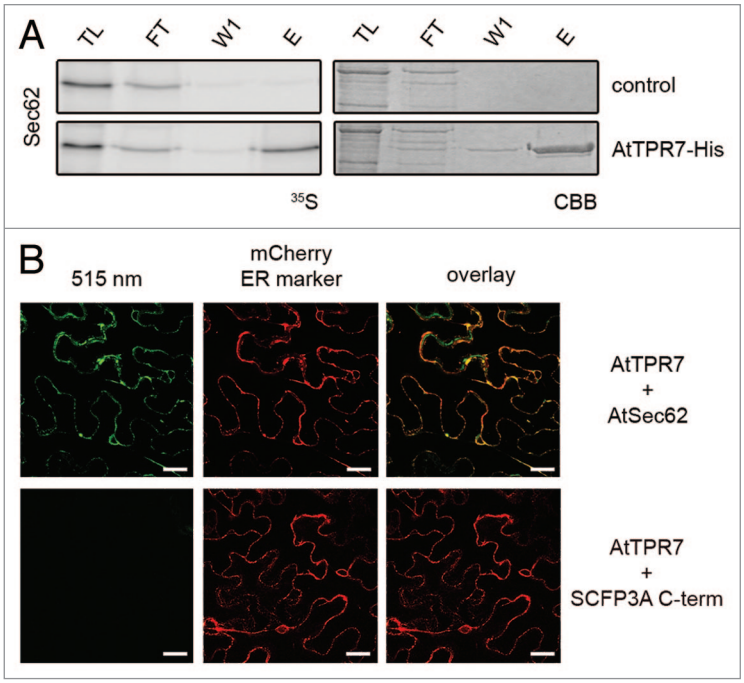

Figure 2. Interaction of AtTPR7 with Sec62. (**A**) Recombinant AtTPR7-His (20 μg) (At5g21990) was incubated for 1 h with 15 μl of radiolabeled Sec62 translation product in 300 μl 1× PBS buffer (140 mM NaCl, 2.7 mM KCl, 10 mM Na_2HPO_4, 1.8 mM KH_2PO_4; pH 7.3). AtTPR7-His was re-purified by incubation with 20 μl Ni-NTA sepharose for 1 h at RT. the Ni-NTA sepharose was washed for three times with 1 ml of 1× PBS buffer containing 50 mM imidazole and samples were subsequently eluted with 20 μl of 1× PBS containing 300 mM imidazole. Five percent of the translation (TL), 2% of the flow through (FT), 2% of the first washing step (W1) and the total eluates (E) were subjected on a 10% SDS-PAGE. Association of Sec62 was detected by autoradiography. A sample without AtTPR7-His constructs was used as a control. (**B**) For bimolecular fluorescence complementation experiments the N-terminal part of Venus was fused to the N-terminus of AtTPR7 and the C-terminal part of SCFP to the N-terminus of Sec62. The constructs were co-transformed with the ER mCherry marker (middle panel) and transiently expressed in tobacco leaves. As a control Venus^{N}-AtTPR7 was cotransformed with SCFP3A^{C} alone (empty vector) and the ER mCherry marker (bottom panels). Images of tobacco leaf cells were obtained by confocal laser scanning microscopy (Leica, Type: TCS SP5; objective lense: HCX PL APO CS; magnification: 63×; numerical aperatur: 1.3; imaging medium: glycerol; software: Leica Application Suite/Advanced Fluorescence). Reconstituted fluorescence obtained by close proximity of the Venus and the SCFP parts was monitored at 515 nm (left panel). Overlay of the signal at 515 nm and the mCherry marker is shown (right panel). Scale bars: 10 μm.

Disclosure of Potential Conflicts of Interest

No potential conflicts of interest were disclosed.

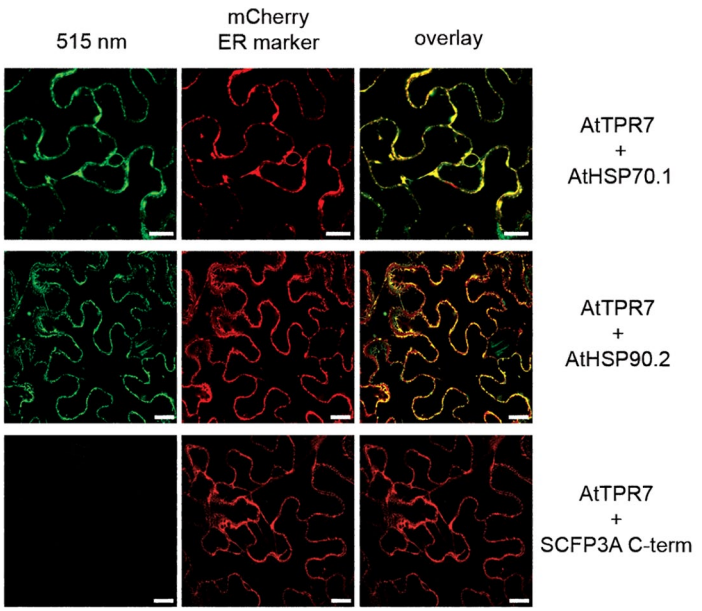

Figure 3. Interaction of AtTPR7 with AtHSP70.1 and AtHSP90.2. For bimolecular fluorescence complementation experiments the N-terminal part of Venus was fused to the N-terminus of AtTPR7 and the C-terminal part of SCFP to the N-terminus of AtHSP70.1 (At5g02500) and AtHSP90.2 (At5g56030), respectively. The constructs were cotransformed with the ER mCherry marker (middle panel) and transiently expressed in tobacco leaves. As a control $Venus^{N}$-AtTPR7 was cotransformed with $SCFP3A^{C}$ alone and the ER mCherry marker (bottom panels). Images of tobacco leaf cells were obtained by confocal laser scanning microscopy. Reconstituted fluorescence was monitored at 515 nm (left panel). Overlay of the signal at 515 nm and the mCherry marker is shown (right panel). Scale bars: 10 μm.

Acknowledgments

We would like to thank Jürgen Soll for helpful discussions. Vectors and strains for tobacco infiltration were kindly provided by Norbert Mehlmer. This project was funded by the DFG and Fonds der chemischen Industrie (grants numbers SFB 1035, project A04 to S.S. and Do 187/22 to R.S.).

References

1. Cross BC, Sinning I, Luirink J, High S. Delivering proteins for export from the cytosol. Nat Rev Mol Cell Biol 2009; 10:255-64; PMID:19305415; http://dx.doi.org/10.1038/nrm2657
2. Rapoport TA. Protein translocation across the eukaryotic endoplasmic reticulum and bacterial plasma membranes. Nature 2007; 450:663-9; PMID:18046402; http://dx.doi.org/10.1038/nature06384
3. Saraogi I, Shan SO. Molecular mechanism of cotranslational protein targeting by the signal recognition particle. Traffic 2011; 12:535-42; PMID:21291501; http://dx.doi.org/10.1111/j.1600-0854.2011.01171.x
4. Ast T, Schuldiner M. All roads lead to Rome (but some may be harder to travel): SRP-independent translocation into the endoplasmic reticulum. Crit Rev Biochem Mol Biol 2013; 48:273-88; PMID:23530742; http://dx.doi.org/10.3109/10409238.2013.782999
5. Dierks T, Klappa P, Wiech H, Zimmermann R. The role of molecular chaperones in protein transport into the endoplasmic reticulum. Philos Trans R Soc Lond B Biol Sci 1993; 339:335-41; PMID:8098538; http://dx.doi.org/10.1098/rstb.1993.0032
6. Harada Y, Li H, Wall JS, Li H, Lennarz WJ. Structural studies and the assembly of the heptameric posttranslational translocon complex. J Biol Chem 2011; 286:2956-65; PMID:20826819; http://dx.doi.org/10.1074/jbc.M110.159517
7. Brodsky JL, Goeckeler J, Schekman R. BiP and Sec63p are required for both co- and posttranslational protein translocation into the yeast endoplasmic reticulum. Proc Natl Acad Sci USA 1995; 92:9643-6; PMID:7568189; http://dx.doi.org/10.1073/pnas.92.21.9643
8. Lyman SK, Schekman R. Binding of secretory precursor polypeptides to a translocon subcomplex is regulated by BiP. Cell 1997; 88:85-96; PMID:9019409; http://dx.doi.org/10.1016/S0092-8674(00)81861-9
9. Plath K, Mothes W, Wilkinson BM, Stirling CJ, Rapoport TA. Signal sequence recognition in posttranslational protein transport across the yeast ER membrane. Cell 1998; 94:795-807; PMID:9753326; http://dx.doi.org/10.1016/S0092-8674(00)81738-9
10. Fang H, Green N. Nonlethal sec71-1 and sec72-1 mutations eliminate proteins associated with the Sec63p-BiP complex from S. cerevisiae. Mol Biol Cell 1994; 5:933-42; PMID:7841522
11. Meyer HA, Grau H, Kraft R, Kostka S, Prehn S, Kalies KU, et al. Mammalian Sec61 is associated with Sec62 and Sec63. J Biol Chem 2000; 275:14550-7; PMID:10799540; http://dx.doi.org/10.1074/jbc.275.19.14550
12. Müller L, de Escauriaza MD, Lajoie P, Theis M, Jung M, Müller A, et al. Evolutionary gain of function for the ER membrane protein Sec62 from yeast to humans. Mol Biol Cell 2010; 21:691-703; PMID:20071467; http://dx.doi.org/10.1091/mbc.E09-08-0730
13. Yamamoto M, Maruyama D, Endo T, Nishikawa S. Arabidopsis thaliana has a set of J proteins in the endoplasmic reticulum that are conserved from yeast to animals and plants. Plant Cell Physiol 2008; 49:1547-62; PMID:18718935; http://dx.doi.org/10.1093/pcp/pcn119
14. Jermy AJ, Willer M, Davis E, Wilkinson BM, Stirling CJ. The Brl domain in Sec63p is required for assembly of functional endoplasmic reticulum translocons. J Biol Chem 2006; 281:7899-906; PMID:16368690; http://dx.doi.org/10.1074/jbc.M511402200
15. Schweiger R, Müller NC, Schmitt MJ, Soll J, Schwenkert S. AtTPR7 is a chaperone-docking protein of the Sec translocon in Arabidopsis. J Cell Sci 2012; 125:5196-207; PMID:22899711; http://dx.doi.org/10.1242/jcs.111054
16. Gehl C, Waadt R, Kudla J, Mendel RR, Hänsch R. New GATEWAY vectors for high throughput analyses of protein-protein interactions by bimolecular fluorescence complementation. Mol Plant 2009; 2:1051-8; PMID:19825679; http://dx.doi.org/10.1093/mp/ssp040
17. Schlegel T, Mirus O, von Haeseler A, Schleiff E. The tetratricopeptide repeats of receptors involved in protein translocation across membranes. Mol Biol Evol 2007; 24:2763-74; PMID:17905998; http://dx.doi.org/10.1093/molbev/msm211
18. Kriechbaumer V, von Löffelholz O, Abell BM. Chaperone receptors: guiding proteins to intracellular compartments. Protoplasma 2012; 249:21-30; PMID:21461941; http://dx.doi.org/10.1007/s00709-011-0270-9
19. Qbadou S, Becker T, Mirus O, Tews I, Soll J, Schleiff E. The molecular chaperone Hsp90 delivers precursor proteins to the chloroplast import receptor Toc64. EMBO J 2006; 25:1836-47; PMID:16619024; http://dx.doi.org/10.1038/sj.emboj.7601091
20. Young JC, Hoogenraad NJ, Hartl FU. Molecular chaperones Hsp90 and Hsp70 deliver preproteins to the mitochondrial import receptor Tom70. Cell 2003; 112:41-50; PMID:12526792; http://dx.doi.org/10.1016/S0092-8674(02)01250-3
21. Faou P, Hoogenraad NJ. Tom34: a cytosolic cochaperone of the Hsp90/Hsp70 protein complex involved in mitochondrial protein import. Biochim Biophys Acta 2012; 1823:348-57; PMID:22178133
22. Chew O, Lister R, Qbadou S, Heazlewood JL, Soll J, Schleiff E, et al. A plant outer mitochondrial membrane protein with high amino acid sequence identity to a chloroplast protein import receptor. FEBS Lett 2004; 557:109-14; PMID:14741350; http://dx.doi.org/10.1016/S0014-5793(03)01457-1
23. Lin BL, Wang JS, Liu HC, Chen RW, Meyer Y, Barakat A, et al. Genomic analysis of the Hsp70 superfamily in Arabidopsis thaliana. Cell Stress Chaperones 2001; 6:201-8; PMID:11599561; http://dx.doi.org/10.1379/1466-1268(2001)006<0201:GAOTHS>2.0.CO;2
24. Feldheim D, Schekman R. Sec72p contributes to the selective recognition of signal peptides by the secretory polypeptide translocation complex. J Cell Biol 1994; 126:935-43; PMID:8051213; http://dx.doi.org/10.1083/jcb.126.4.935

6 Publication IV

Schweiger R. and Schwenkert S., (2013). *Protein-Protein Interactions Visualized by Bimolecular Fluorescence Complementation in Tobacco Protoplasts and Leaves.* JoVE (accepted).

17 Sellers Street
Cambridge, MA 02139
tel. +1.617.945.9051
www.JoVE.com

TITLE: Protein-Protein Interactions Visualized by Bimolecular Fluorescence Complementation in Tobacco Protoplasts and Leaves

AUTHORS:
Schweiger, Regina
Department Biologie I, Botanik
Ludwig-Maximilians-Universität München
Großhadernerstr. 2-4
82152 Planegg-Martinsried, Bavaria, Germany
phone +49 (0)89 2180 74760
fax +49 (0)89 2180 74752
regina.schweiger@biologie.uni-muenchen.de

Schwenkert, Serena
Department Biologie I, Botanik
Ludwig-Maximilians-Universität München
Großhadernerstr. 2-4
82152 Planegg-Martinsried, Bavaria, Germany
phone +49 (0)89 2180 74760
fax +49 (0)89 2180 74752
serena.schwenkert@lmu.de

CORRESPONDING AUTHOR:
Schwenkert, Serena

KEYWORDS:
Tetratricopeptide repeat domain, chaperone, chloroplasts, endoplasmic reticulum, HSP90, Toc complex, Sec translocon, BiFC

SHORT ABSTRACT:
Formation of protein complexes *in vivo* can be visualized by bimolecular fluorescence complementation. Interaction partners are fused to complementary parts of fluorescent tags and transiently expressed in tobacco leaves, resulting in a reconstituted fluorescent signal upon close proximity of the two proteins.

LONG ABSTRACT:
Many proteins interact transiently with other proteins or are integrated into multi-protein complexes to perform their biological function. Bimolecular fluorescence complementation (BiFC) is an *in vivo* method to monitor such interactions in plant cells. In the presented protocol

the investigated candidate proteins are fused to complementary halves of fluorescent proteins and the respective constructs are introduced into plant cells via agrobacterium-mediated transformation. Subsequently, the proteins are transiently expressed in tobacco leaves and the restored fluorescent signals can be detected with a confocal laser scanning microscope in the intact cells. This allows not only visualization of the interaction itself, but also the subcellular localization of the protein complexes can be determined. For this purpose, marker genes containing a fluorescent tag can be co-expressed along with the BiFC constructs, thus visualizing cellular structures such as the endoplasmic reticulum, mitochondria, the Golgi apparatus or the plasma membrane. The fluorescent signal can be monitored either directly in epidermal leaf cells or in single protoplasts, which can be easily isolated from the transformed tobacco leaves. BiFC is ideally suited to study protein-protein interactions in their natural surroundings within the living cell. However, it has to be considered that the expression has to be driven by strong promotors and that the interaction partners are modified due to fusion of the relatively large fluorescence tags, which might interfere with the interaction mechanism. Nevertheless, BiFC is an excellent complementary approach to other commonly applied methods investigating protein-protein interactions, such as co-immunoprecipitation, *in vitro* pull-down assays or yeast-two-hybrid experiments.

INTRODUCTION:

Studying the formation of protein complexes and their localization in plant cells *in vivo* is essential to investigate cellular networks, signaling and metabolic processes. BiFC allows visualization of protein-protein interactions in their natural environment directly within the living plant cell[1-5].

In the BiFC approach the complementation of two non-fluorescent N- and C-terminal fragments of a fluorescent protein lead to a reconstituted fluorescent protein. Fragments of many different fluorescent proteins have been used to detect protein interactions, e.g. the green fluorescent protein (GFP) the chromophore of which is chemically formed by three distinct residues[6]. Fluorescent proteins can be halved within a loop or ß-strand to result in the two non-fluorescent fragments which can be fused to both proteins of interest. The assay can be used to detect interactions in any subcellular compartment in any aerobically growing organism or cells that can be genetically modified to express the fusion proteins. If the two proteins come into close proximity within the cell, fluorescence is reconstituted and can be monitored by microscopy without the addition of exogenous fluorophores or dyes[3].

Tobacco (*Nicotiana benthamiana*) has proven to be a convenient model organism to visualize the interaction of plant proteins, since proteins can easily be expressed by utilizing agrobacterium-mediated transformation of tobacco leaves with the generated constructs. Agrobacteria use a so-called Ti plasmid (Tumor inducing) coding for enzymes which mediate the transduction of the gene of interest into plant cells. BiFC is well applicable for soluble as well as for membrane proteins within all cellular compartments and has been successfully used over the past years to identify interacting proteins *in vivo* as well as to analyze interaction sites within the proteins[7-9]. Upon expression of the introduced genes, the interaction of the fluorescent proteins can be visualized directly in leaves, which is suitable for larger cellular structures, such as the endoplasmic reticulum (ER), the plasma membrane or chloroplasts.

However, to monitor the localization in more refined structures, for e.g. the chloroplast envelope, it is advisable to visualize the fluorescence in protoplasts isolated from transformed tobacco leaves. A set of BiFC vectors containing either a C-terminal or an N-terminal fluorescent tag has to be used for the BiFC approach in plants[10]. The hereafter described protocol was used to study the interaction of cytosolic heat shock protein 90 (HSP90) with the tetratricopeptide domain containing docking proteins Toc64 and AtTPR7 residing in the chloroplast outer envelope and the endoplasmic reticulum, respectively[11-13]. For this purpose, HSP90 was fused to the C-terminal part of SCFP ($SCFP^C$). The tag was N-terminally fused to the chaperone to ensure accessibility of the C-terminal MEEVD binding motif of HSP90 to clamp-type TPR domains. In parallel, the N-terminal part of Venus ($Venus^N$) was fused to the cytosolic domains of the TPR domain containing docking proteins Toc64 and AtTPR7, respectively. For a negative control we cloned the soluble C-terminal part of $SCFP^C$ solely which resides in the cytosol and is therefore an appropriate control.
The fluorescent tags of the studied proteins have to face the same cellular compartment to allow close proximity and thereby reconstitution of the fluorescent signal. To determine the localization of the reconstituted fluorescent signal a marker protein fused to a different fluorescent tag can be cotransformed to demonstrate the subcellular localization of the interaction. An ER marker protein fused to mCherrry was transformed simultaneously in the case of the ER located AtTPR7[14]. The autofluorescence of chlorophyll served as chloroplast marker in case of Toc64. By this not only the *in vivo* interaction of Toc64 and AtTPR7, respectively, with the cytosolic HSP90 chaperone can be monitored directly in the tobacco leaves but also the subcellular localization of the interaction can be investigated.
BiFC is well suited as a complementary approach to other methods studying protein-protein interactions. Compared to co-immunoprecipitation or *in vitro* pull-down experiments, for e.g., no specific antibodies have to be available for the proteins of interest and the proteins do not have to be recombinantly expressed *in vitro* which can be challenging, especially for membrane proteins. Moreover, also transient interactions can be monitored using BiFC, since the proteins are captured by the interaction of the fused fluorescent tags[15].

PROTOCOL:

1. Transformation of BiFC constructs in Agrobacteria

1.1 Cloning of BiFC constructs

1.1.1 Amplify the gene of interest from an appropriate template using oligonucleotides containing flanking *attB*-sites. Perform a PCR using a proofreading polymerase. Adapt the length of the annealing step to the designed primer combination and the length of the elongation step according to the fragment size. Check the PCR product by agarose gel electrophoresis and purify it by using a PCR Clean-up Kit.

1.1.2 Perform the BP reaction with the obtained fragment and the entry vector using a BP recombinase. Mix 15-150 ng of the *att*B-PCR product with 150 ng of the entry vector, add 2 µl of the BP recombinase and fill up with TE buffer to a total volume of 8 µl. Incubate the reaction for 1 hr at RT and stop the reaction by adding 2 µl proteinaseK for 10 min at 37 °C.

1.1.3 Transform the entire reaction into competent *E. coli* DH5α cells and screen the obtained colonies by colony PCR for correct insertion of the DNA fragment into the vector. DNA sequencing of positive plasmids is performed to verify the absence of mutations.

1.1.4 Use the obtained entry clone for LR recombination with the appropriate destination vector[10] using a LR recombinase. Mix 50-150 ng of the entry vector with 150 ng of the destination vector, add 1 µl LR recombinase and fill up with TE buffer to a total volume of 5 µl. Incubate the reaction for 1 hr at RT and stop the reaction by adding 1 µl Proteinase K for 10 min at 37 °C.

1.1.5 Transform the entire reaction into competent *E. coli* DH5α cells and screen obtained colonies by colony PCR for correct insertion of the DNA fragment into the vector. DNA sequencing is not necessary at this step.

1.1.6 Isolate plasmid DNA with a plasmid Mini kit to ensure a high degree of purity.

1.2 Preparation of chemically competent Agrobacteria (strain AGL1, Rifampicin and Carbenicillin resistance)

1.2.1 Streak out agrobacteria from a stock culture and grow for 24 hr at 28 °C.

1.2.2 Inoculate 5 ml LB medium with a single colony and incubate overnight at 28 °C.

1.2.3 Inoculate 50 ml LB medium with 2 ml of the over-night culture and grow for approx. 4 hr at 28 °C to an OD_{600} of 1.0.

1.2.4 Centrifuge the cells at 3000 x g for 15 min at 4 °C and resuspend the pellet in 1 ml sterilized ice-cold $CaCl_2$ (10 mM). Keep cells on ice after this step.

1.2.5 Prepare aliquots (100 µl) of the cells, freeze immediately in liquid nitrogen and store at -80 °C.

1.3 Transformation of chemically competent Agrobacteria

1.3.1 Thaw one aliquot of competent AGL1 cells on ice. Add 1-2 µg of plasmid DNA to the cells. Incubate for 5 min on ice, 5 min in liquid nitrogen and 5 min at 37 °C. Add 600 µl LB medium to the cells and shake at 650 rpm for 4 hr at 28 °C.

1.3.2 Centrifuge the cells for 1 min at 8000 x g and discard the supernatant. Resuspend the pellet in 50 µl of the remaining LB medium and plate on LB plates containing the appropriate antibiotics. Seal the plates and incubate for 2 days at 28 °C. Screen colonies for the presence of the plasmid by colony PCR.

1.3.3 Inoculate one positive colony in 5 ml LB medium containing the appropriate antibiotics and incubate at 28 °C over night. Mix 500 µl of the overnight culture with 500 µl 50 % sterilized glycerol and freeze at -80 °C.

1.3.4 Inoculate the agrobacteria in LB medium containing the appropriate antibiotics directly from the glycerol stock for transient transformation of tobacco leaves.

2. Transient transformation of tobacco leaves

2.1 Agrobacteria growth

2.1.1 Prepare the following stock solutions: Acetosyringone (150 mM, dissolve in 70 % EtOH), store as aliquots at -20 °C. MES/KOH (0.1 M) pH 6.5, store at 4 °C (sterile-filter through a 0.2 µM filter to prevent bacterial growth during longer storage). $MgCl_2$ (1 M) stock, store at RT.

2.1.2 Inoculate 10 ml LB medium containing the appropriate antibiotics with 50 µl of the AGL1 glycerol stock culture containing the plasmid of interest in a sterile 50 ml tube and incubate at 28 °C for at least 24 hr shaking at 190 rpm until an OD_{600} between 1.0 and 2.0 is reached.

2.1.3 Centrifuge bacteria at 3000 x g for 15 min. Resuspend the pellet in freshly made infiltration medium [$MgCl_2$ (10 mM), MES/KOH (10 mM) pH 6.5, Acetosyringone (150 µM)] and adjust the suspension to an OD_{600} of 1.0.

2.1.4 Incubate the agrobacteria cells in an over-head shaker for 2 hr in darkness. The cells can then be used for infiltration.

2.1.5 Infiltration of tobacco leaves

2.1.6 Use three week old tobacco *(Nicotiana benthamiana*) plants. Choose several older leaves for infiltration.

2.1.7 Mix equal volumes of the agrobacteria carrying the constructs of interest (3 ml each). Take a 5 ml syringe without a needle for infiltration. Infiltrate the cell suspension carefully into the tobacco leaves by pressing the syringe on the bottom side of the leaves in several places.

2.1.8 Water the plants and leave them in the darkness for two days.

3. Protoplast preparation

Protoplast preparation of tobacco leaves was adapted from Koop et al.[16] and slightly modified.

3.1 Buffer preparation

3.1.1 Prepare F-PCN medium: Macro-salts [KNO_3 (1012 µg/ml), $CaCl_2$ x $2H_2O$ (440 µg/ml), $MgSO_4$ x $7H_2O$ (370 µg/ml), KH_2PO_4 (170 µg/ml), NH_4-succinat (20 mM, prepare a 2 M stock solution (succinate (236 µg/ml) and NH_4Cl (106 µg/ml), adjust to pH 5.8 to dissolve)], Micro-salts [EDTA-Fe(III) x Na-salt (40 µg/ml), KJ (0.75 µg/ml), H_3BO_3 (3 µg/ml), $MnSO_4$ x H_2O (10 µg/ml), $ZnSO_4$ x $7H_2O$ (2 µg/ml), Na_2MoO_4 x $7H_2O$ (0.25 µg/ml), $CuSO_4$ x $5H_2O$ (0.025 µg/ml), $CoCl_2$ x $6H_2O$ (0.025 µg/ml)], MES (390 µg/ml), glucose (approx. 80 µg/ml) osmolarity 550 mOsm, pH 5.8 (KOH). Store in aliquots at -20 °C.

3.1.2 Prepare F-PIN medium: All ingredients as F-PCN but instead of glucose use sucrose (approx. 110 µg/ml), osmolarity 550 mOsm, pH 5.8 (KOH). Store in aliquots at -20 °C.

3.1.3 Prepare W5 medium: 150 mM NaCl, 125 mM $CaCl_2$, 5 mM KCl, 2 mM MES, osmolarity 550-580 mOsm, pH 5.7 (KOH). Store at 4 °C (sterile-filter through a 0.2 µM filter to prevent bacterial growth during longer storage).

3.1.4 Prepare fresh enzyme solution for protoplast isolation (0.1 g cellulase, 0.03 g macerozym in 10 ml F-PIN). Incubate the solution at 55 °C for 10 min and cool to RT. Add 100 µl of 10 % BSA to 10 ml solution.

3.2 Isolation of protoplasts

3.2.1 Place one infiltrated leaf into a petri dish and add the fresh enzyme solution. Use a new razorblade to cut the leaf into approx. 1 cm^2 sized pieces. Transfer the leaf-pieces with the enzyme solution into a vacuum-infiltration flask and vacuum infiltrate for approx. 20 sec until air bubbles emerge from the leaves (release vacuum very carefully).

3.2.2 Shake the flask for 90 min at 40 rpm in darkness.

3.2.3 Release protoplasts by shaking for 1 min at 90 rpm. Filter the solution through gauze (100 µM) into a 15 ml centrifugation tube (round bottom).

3.2.4 Overlay the protoplast solution with 2 ml F-PCN buffer and centrifuge for 10 min at 70 x g (slow acceleration and deceleration) at RT.

3.2.5 Intact protoplasts accumulate at the interface of enzyme solution and F-PCN. Take a wide orifice 1 ml pipette tip to transfer the intact protoplasts into a fresh centrifuge tube and fill up with W5 buffer. Centrifuge for 2 min at 100 x g (slow acceleration and deceleration) to pellet the protoplasts.

3.2.6 Remove the supernatant carefully by using a pipette and resuspend pellet in approx. 200 µl W5 buffer, depending on the amount of protoplasts.

3.2.7 Always use wide orifice tips to prevent rupturing of intact protoplasts.

4. Laser scanning microscopy

4.1 Sample preparation

4.1.1 Paste two small strips of sealant around a microscope slide (2 cm distance). Place 20 µl of the protoplast solution between the strips and carefully place a cover glass on top. The sealant strips make sure that the protoplasts are not squashed by the cover glass.

4.1.2 For total leaf samples cut a 1 cm piece from the leaf and place it onto a microscope slide with the bottom side of the leaf facing upwards. Add approx. 50 µl of H_20, place a cover glass on top and fix it tightly with adhesive tape on both sides.

4.2 Confocal imaging and microscope settings

4.2.1 Imaging is performed with a confocal laser scanning microscope from Leica, Type: TCS SP5. For magnification use an objective lens (HCX PL APO CS) with a magnitude of 63x with glycerol as imaging medium. Set the numerical aperture to 1.3. Use the Leica Application Suite/Advanced Fluorescence software for evaluation (see Supplemental data S1).

4.2.2 Set the Argon laser to 30 % and the laser power at 488 nm to an intensity of 18 % to monitor the reconstituted BiFC signal at 515 nm and set the first PMT detector emission bandwidth from 495 to 550.

4.2.3 To monitor chlorophyll autofluorescence set the second PMT detector emission bandwidth from 650 to 705.

4.2.4 To monitor mCherry signal use the HeNe 561 laser, set the intensity of laser 561 to 18 % and the emission bandwidth of the third PMT detector from 587 to 610.

4.2.5 Make sure that pictures of all PMT detector channels are taken with the same gain settings (gain should be between 800 and 900 to exclude background signals).

4.2.6 Take pictures in a format width/height of 1024x1024 pixels with a scan speed of 100 hrz.

4.2.7 For Z-stackings use a minimum distance of 0.5 µm between each stack.

REPRESENTATIVE RESULTS:

In this example we used the BiFC method to monitor the interaction of the cytosolic molecular chaperone HSP90 with the membrane docking proteins AtTPR7 and Toc64. AtTPR7 is part of the Sec translocon and interacts with cytosolic chaperones, which possibly deliver secretory preproteins for post-translational translocation to the ER membrane. Likewise, Toc64 at the chloroplast outer envelope acts in post-translational import by receiving HSP90 associated chloroplast preproteins[11,12]. Both proteins comprise a cytosolic exposed tetratricopeptide repeat domain, which mediates interaction with the C-terminal MEEVD motif of HSP90.

Proteins were cloned by means of specific recombinases into suitable destination vectors fusing the TPR domain containing docking proteins to $Venus^N$, ensuring that the fluorescent tag is attached to the cytosolic domain and does thus not hinder targeting and membrane insertion of the proteins. In the case of HSP90, $SCFP^N$ was fused to the N-terminus, as not to interfere with the C-terminal MEEVD motif (Figures 1 and 2).

AtTPR7 and HSP90 were co-transformed with an ER marker (mCherry) to verify the localization of the protein complex. The fluorescence was monitored in intact leaves with a laser scanning microscope. As a control $SCFP^C$ alone, which is located in the cytosol (like HSP90), was expressed along with AtTPR7 and the ER mCherry marker. Several leaves were checked for fluorescence and pictures were taken with identical microscope settings. In our experience a typical signal should be visible with gain settings at 800-900, whereas the negative control should only show very slight background fluorescence with these settings (Figure 3). A reconstituted signal for $Venus^N$-AtTPR7 together with $SCFP^N$-HSP90 at 515 nm was monitored overlapping with the mCherry ER marker. No signal for $Venus^N$-AtTPR7 and the negative control $SCFP^N$ could be observed.

In the case of Toc64 and HSP90 expression, as well as Toc64 and $SCFP^C$, protoplasts were isolated from infiltrated tobacco leaves, since in microscopic pictures of the entire leaves the exact localization is difficult to determine, although fluorescence is already visible (Figure 4 and 5). A signal at 515 nm was restored expressing Toc64-$Venus^N$ together with $SCFP^N$-HSP90 at the chloroplast envelope, which could be detected as ring shaped structures surrounding the chloroplasts. As above the control was photographed with identical microscope settings and did not show a fluorescence at 515 nm.

DISCUSSION:

Upon planning a BiFC experiment several points should be considered. Although no structural information about the proteins of interest is required, the topology has to be known when working with membrane spanning proteins. The fluorescent proteins have to reside in the same subcellular compartment or face the same side of a membrane to allow interaction. Naturally, when analyzing proteins which require an N-terminal targeting sequence, only a C-terminal tag can be considered. Since it is possible that the tag interferes with proper targeting or

membrane insertion of the protein of interest it is advisable to test subcellular localization beforehand, for e.g. by expressing a GFP-tagged protein. Moreover, a negative control should always be included. In this example we generated a construct only expressing $SCFP^C$ in the cytosol. However, any protein that is not expected to interact can be used as a negative control. To verify proper expression of the constructs, especially if no fluorescence is visible, protein extracts of infiltrated leaves or protoplasts can be subjected to SDS-PAGE and protein expression can be verified with antibodies directed against the respective tags.

Fluorescent signals can be monitored either in intact leaves or isolated protoplasts. Although detection in entire leaves is faster, signals of more refined structures are better visualized in protoplasts. Moreover, mostly epidermal cells are monitored when looking at the entire leaf, which do not contain chloroplasts. Therefore, when analyzing chloroplast proteins, isolation of protoplasts is advisable.

The major advantage of the technique is the possibility to monitor protein-protein interactions in living plant cells. There is no need to break cells and to solubilize membrane protein complexes, as it is the case for example in co-immunoprecipitation experiments. Moreover, the application is simple since the only required materials are the vectors, agrobacteria and a standard fluorescence microscope (although higher quality images are achieved with a confocal laser scanning microscope). In contrast to *in vitro* pull-down assays with recombinant proteins, which only allow detection of an interaction if both proteins are interacting directly, BiFC can also detect protein complexes which require additional, endogenous proteins present in the cell. However, this also means that BiFC provides no prove of a direct protein-protein interaction, which always has to be verified by other techniques. Moreover, due to overexpression by strong promotors unspecific interactions might occur, which have to be ruled out by appropriate negative controls. To this end a protein not predicted to interact with the protein of interest, but residing in the same compartment, or constructs lacking the protein-protein interaction domains should be used. In addition, a dilution series of the prey cDNA with a non-interacting cDNA as well as observation of the fluorescence in a time dependant manner after transformation can help to validate the results. To ensure discrimination of true fluorescent signals and artifacts the BiFC signals should be quantified and set into relation to another expressed fluorescent protein, for example a marker protein. [7,8] Another drawback of the BiFC method is, that interactions of the proteins may also be hindered sterically by the relatively large fluorescent tags.

Application of agrobacterium-mediated transformation in other plants (for e.g. *Arabidopsis*) is limited, however, it is possible to transform the plasmid DNA directly either into isolated *Arabidopsis* protoplasts or to transform cells using a particle gun. However, plasmid DNA should be isolated using a MAXI Kit, since it should be highly concentrated and as pure as possible for protoplast transformation. Another problem we observed due to high expression of the target proteins was unspecific aggregation in the cytosol, especially when working with mitochondrial membrane proteins. This problem can be overcome by biolistic transformation of onion cells.

ACKNOWLEDGMENTS:

We would like to thank Jürgen Soll for helpful discussions and Chris Carrie for critical reading of the manuscript. This project was funded by the DFG and Fonds der chemischen Industrie

(grants numbers SFB 1035, project A04 to S.S. and Do 187/22 to R.S.).

DISCLOSURES:
The authors have nothing to disclose.

REFERENCES

1 Citovsky, V. *et al.* Subcellular localization of interacting proteins by bimolecular fluorescence complementation in planta. *J Mol Biol* **362**, 1120-1131, doi:S0022-2836(06)01032-1 [pii] 10.1016/j.jmb.2006.08.017 (2006).

2 Schutze, K., Harter, K. & Chaban, C. Bimolecular fluorescence complementation (BiFC) to study protein-protein interactions in living plant cells. *Methods Mol Biol* **479**, 189-202, doi:10.1007/978-1-59745-289-2_12 (2009).

3 Weinthal, D. & Tzfira, T. Imaging protein-protein interactions in plant cells by bimolecular fluorescence complementation assay. *Trends Plant Sci* **14**, 59-63, doi:10.1016/j.tplants.2008.11.002 S1360-1385(09)00002-8 [pii] (2009).

4 Ohad, N., Shichrur, K. & Yalovsky, S. The analysis of protein-protein interactions in plants by bimolecular fluorescence complementation. *Plant Physiol* **145**, 1090-1099, doi:145/4/1090 [pii] 10.1104/pp.107.107284 (2007).

5 Ohad, N. & Yalovsky, S. Utilizing bimolecular fluorescence complementation (BiFC) to assay protein-protein interaction in plants. *Methods Mol Biol* **655**, 347-358, doi:10.1007/978-1-60761-765-5_23 (2010).

6 Tsien, R. Y. The green fluorescent protein. *Annu Rev Biochem* **67**, 509-544, doi:10.1146/annurev.biochem.67.1.509 (1998).

7 Lee, L. Y. *et al.* Screening a cDNA library for protein-protein interactions directly in planta. *Plant Cell* **24**, 1746-1759, doi:10.1105/tpc.112.097998 [pii] (2012).

8 McFarlane, H. E., Shin, J. J., Bird, D. A. & Samuels, A. L. Arabidopsis ABCG transporters, which are required for export of diverse cuticular lipids, dimerize in different combinations. *Plant Cell* **22**, 3066-3075, doi:10.1105/tpc.110.077974 tpc.110.077974 [pii] (2010).

9 Dunschede, B., Bals, T., Funke, S. & Schunemann, D. Interaction studies between the chloroplast signal recognition particle subunit cpSRP43 and the full-length translocase Alb3 reveal a membrane-embedded binding region in Alb3 protein. *J Biol Chem* **286**, 35187-35195, doi:10.1074/jbc.M111.250746 M111.250746 [pii] (2011).

10 Gehl, C., Waadt, R., Kudla, J., Mendel, R. R. & Hansch, R. New GATEWAY vectors for high throughput analyses of protein-protein interactions by bimolecular fluorescence complementation. *Mol Plant* **2**, 1051-1058, doi:ssp040 [pii] 10.1093/mp/ssp040 (2009).

11 Qbadou, S. *et al.* The molecular chaperone Hsp90 delivers precursor proteins to the chloroplast import receptor Toc64. *EMBO J.* **25**, 1836-1847 (2006).

12 Schweiger, R., Muller, N. C., Schmitt, M. J., Soll, J. & Schwenkert, S. AtTPR7 is a chaperone docking protein of the Sec translocon in Arabidopsis. *J Cell Sci*, doi:jcs.111054 [pii] 10.1242/jcs.111054 (2012).

13 Schweiger, R. & S., S. AtTPR7 as part of the Arabidopsis Sec post-translocon. *Plant Signal Behav* **8** (2013).
14 Nelson, B. K., Cai, X. & Nebenfuhr, A. A multicolored set of in vivo organelle markers for co-localization studies in Arabidopsis and other plants. *Plant J* **51**, 1126-1136, doi:TPJ3212 [pii] 10.1111/j.1365-313X.2007.03212.x (2007).
15 Kerppola, T. K. Bimolecular fluorescence complementation (BiFC) analysis as a probe of protein interactions in living cells. *Annu Rev Biophys* **37**, 465-487, doi:10.1146/annurev.biophys.37.032807.125842 (2008).
16 Koop, H. U. *et al.* Integration of foreign sequences into the tobacco plastome via polyethylene glycol-mediated protoplast transformation. *Planta* **199**, 193-201 (1996).

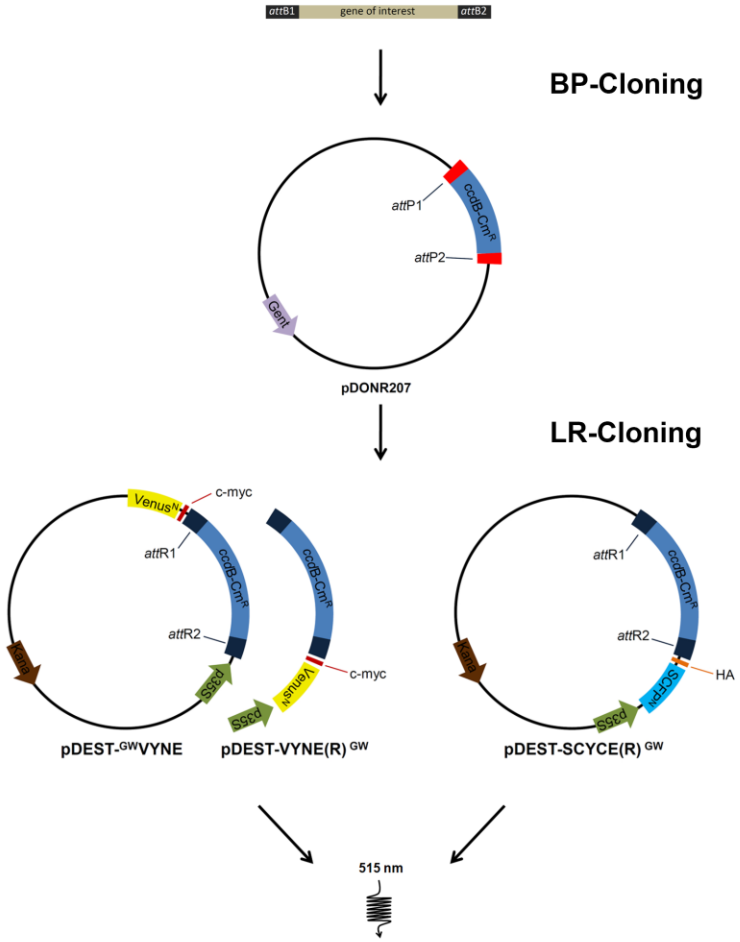

Figure 1: Cloning procedure of BiFC constructs. The genes of interest were amplified with oligonucleotides flanked by *att*B sites to allow BP recombination into an entry vector with *att*P sites, thus replacing the ccdB gene within the vector. Subsequently the entry vector was recombined with appropriate destination vectors using a LR recombinase. Transformation of these constructs into tobacco leaves allows expression of proteins fused to the split fluorescent proteins and to tags for antibody detection.

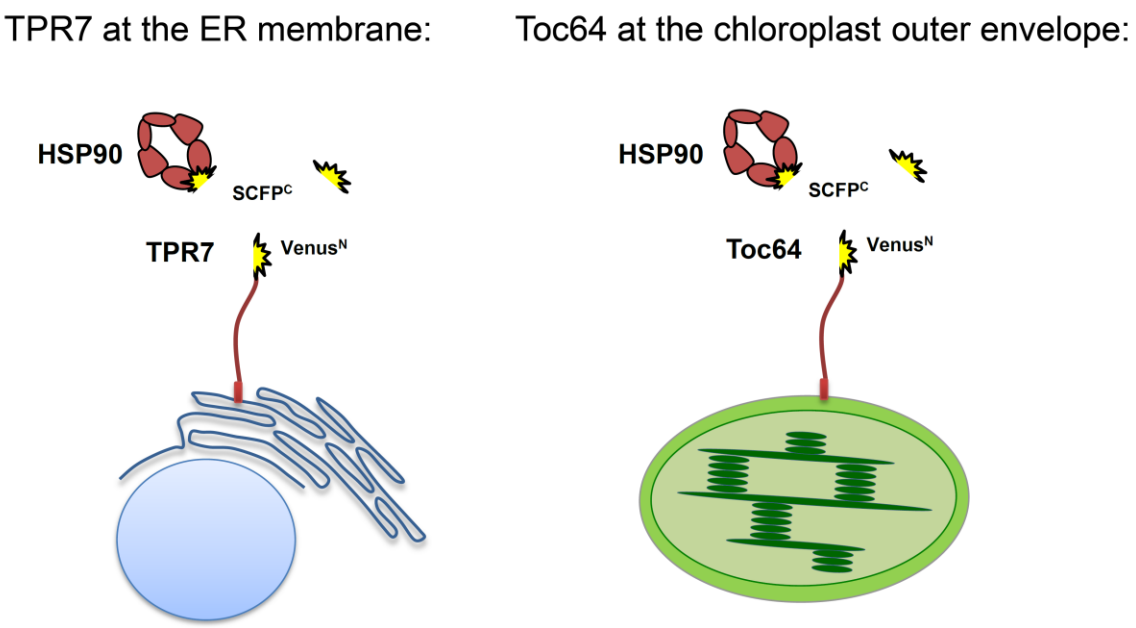

Figure 2: Schematic presentation of the proteins expressed in BiFC experiments. Venus^{N} is coupled to the cytosolic parts of Toc64 or AtTPR7 residing in the chloroplast and ER, respectively. HSP90 is N-terminally fused to SCFP^{C}, enabling interaction of the TPR domains of Toc64 and AtTPR7 with the HSP90 C-terminus. SCFP^{C} alone is expressed in the cytosol as a control.

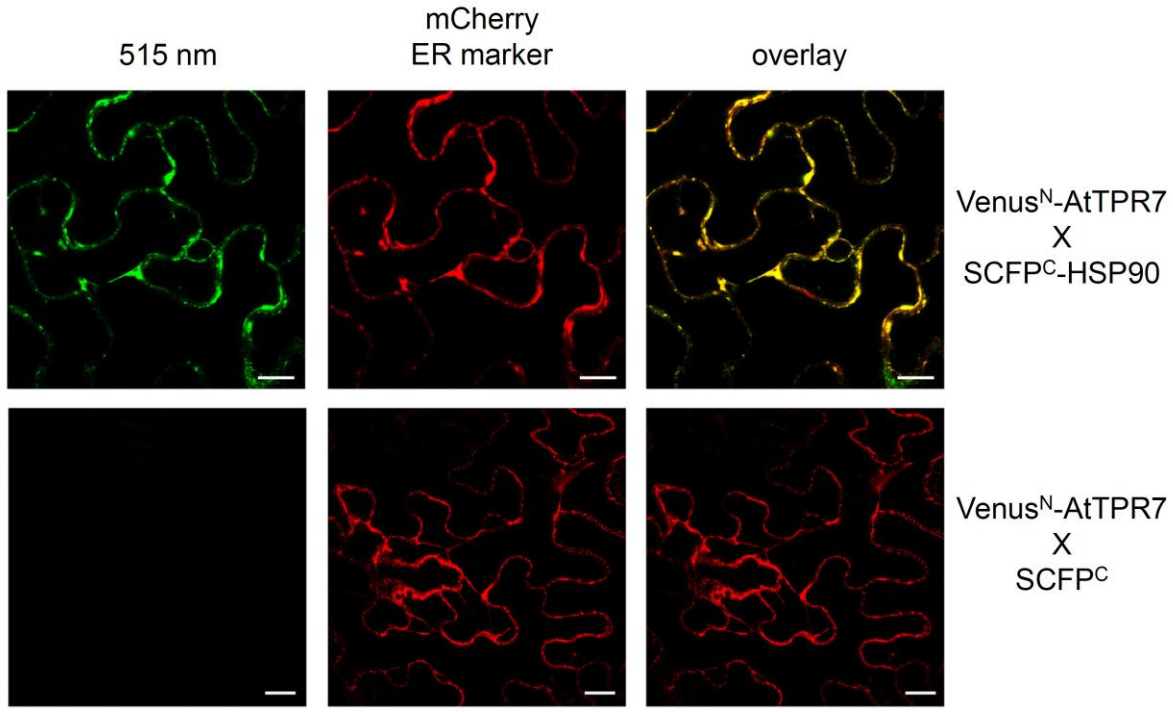

Figure 3: BiFC with AtTPR7 and HSP90 visualized in tobacco epidermal leaf cells. Venus^{N}-AtTPR7 and SCFP^{C}-HSP90 were cotransformed with the ER mCherry marker (middle panel) and transiently expressed in tobacco leaves. As a control Venus^{N}-AtTPR7 was cotransformed with SCFP^{C} alone and the ER mCherry marker (bottom panels). Reconstituted fluorescence was monitored at 515 nm (left panel). Overlay of the signal at 515 nm and the mCherry marker is shown (right panel). Scale bars: 10 µm.

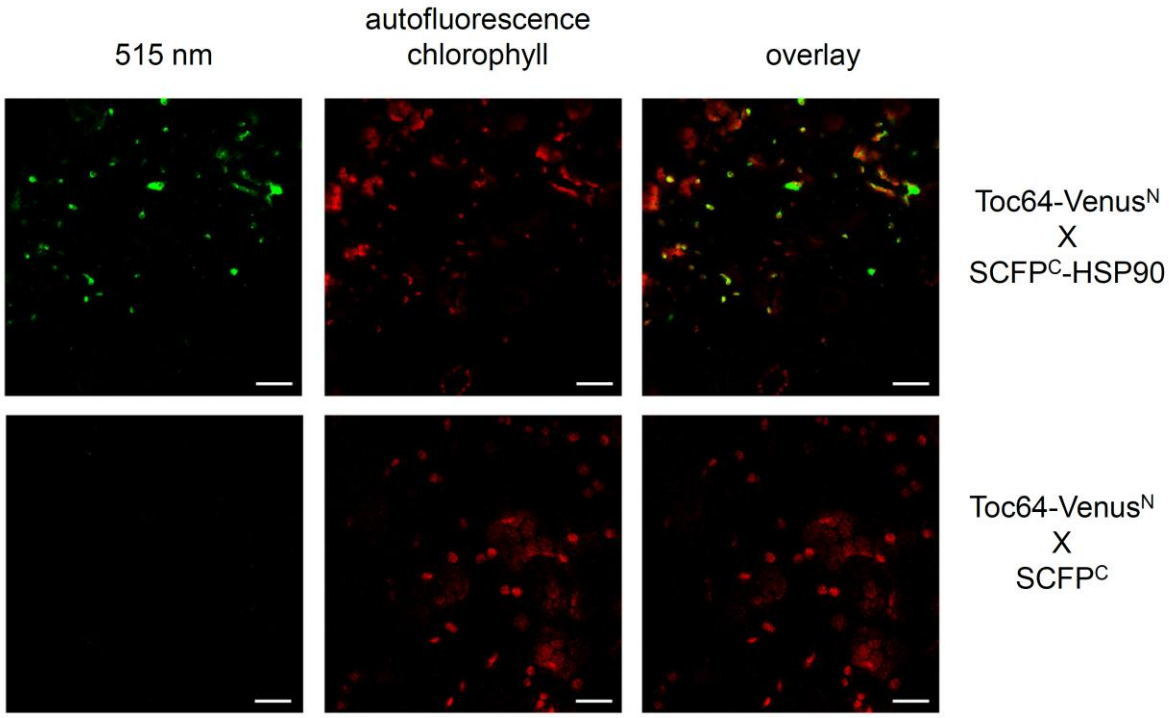

Figure 4: BiFC with Toc64 and HSP90 visualized in tobacco epidermal leaf cells. Toc64-Venus^{N} and SCFP^{C}-HSP90 were transiently expressed in tobacco leaves. As a control Toc64-Venus^{N} was cotransformed with SCFP^{C} alone (bottom panels). Reconstituted fluorescence was monitored at 515 nm (left panel). Overlay of the signal at 515 nm and the chlorophyll autofluorescence is shown (right panel). Chlorophyll autofluorescence is monitored at 480 nm. Scale bars: 10 µm.

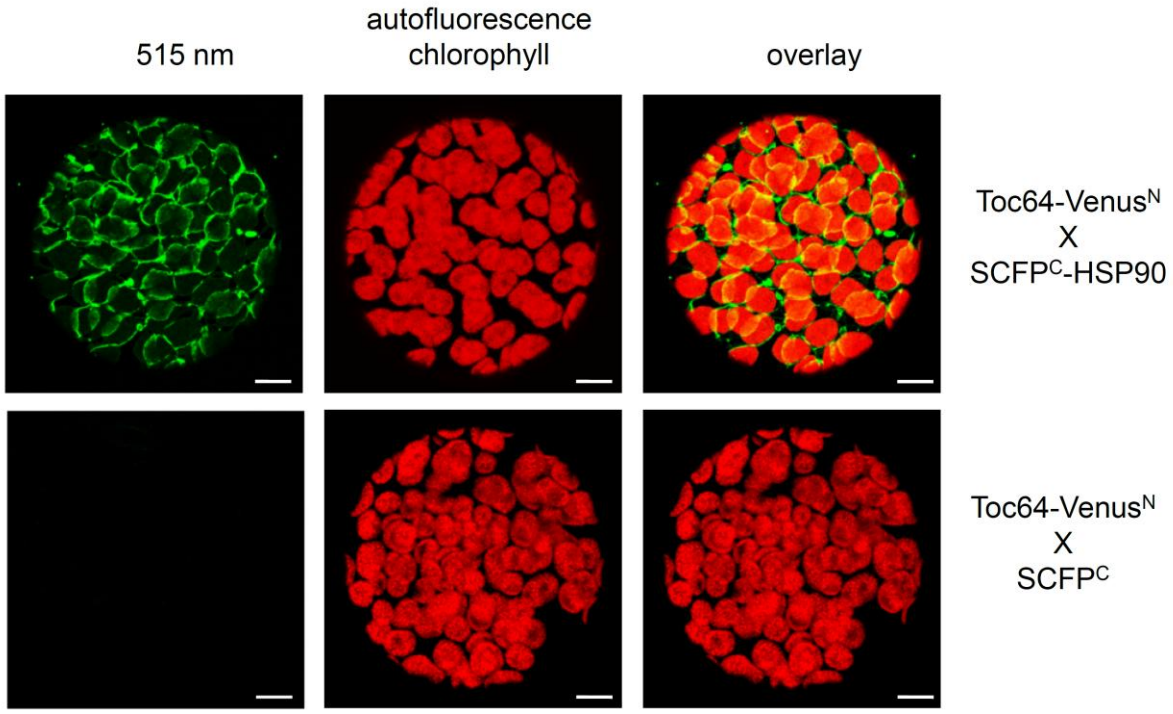

Figure 5: BiFC with Toc64 and HSP90 visualized in tobacco protoplasts. Toc64-Venus^{N} and SCFP^{C}-HSP90 were transiently expressed in tobacco leaves. As a control Toc64-Venus^{N} was cotransformed with SCFP^{C} alone (bottom panels). Reconstituted fluorescence was monitored at 515 nm (left panel) in isolated protoplasts. Overlay of the signal at 515 nm and the chlorophyll autofluorescence is shown (right panel). Chlorophyll autofluorescence is monitored at 480 nm. Scale bars: 10 µm.

7 Publication V

Schweiger R., Soll J., Jung K., Heermann R. and Schwenkert S., (2013). *Quantification of interaction strengths between chaperones and tetratricopeptide repeat domain containing membrane proteins.* JBC; doi:10.1074/jbc.M113.493015jbc.M113.493015.

JBC Papers in Press. Published on September 13, 2013 as Manuscript M113.493015
The latest version is at http://www.jbc.org/cgi/doi/10.1074/jbc.M113.493015

Quantification of interaction strengths between chaperones and tetratricopeptide repeat domain containing membrane proteins

Regina Schweiger[†], Jürgen Soll[†], Kirsten Jung[‡], Ralf Heermann[‡,1] and Serena Schwenkert[†,1]

[†]Munich Center for integrated Protein Science at the Ludwig-Maximilians-Universität München, Department of Biology I, Botany, Großhaderner Straße 2–4, D-82152 Planegg-Martinsried, Germany

[‡]Munich Center for integrated Protein Science at the Ludwig-Maximilians-Universität München, Department of Biology I, Microbiology, Großhaderner Straße 2–4, D-82152 Planegg-Martinsried, Germany

*Running title: *Quantification of TPR docking-chaperone interactions*

To whom correspondence should be addressed: Dr. Serena Schwenkert, Munich Center for integrated Protein Science at the Ludwig-Maximilians-Universität München, Department of Biology I, Botany, Großhaderner Straße 2–4, D-82152 Martinsried, Germany, Tel.: +49 89 2180 74760, Fax: +49 89 2180 74752, E-mail: serena.schwenkert@lmu.de
and PD Dr. Ralf Heermann, Munich Center for integrated Protein Science at the Ludwig-Maximilians-Universität München, Department of Biology I, Microbiology, Großhaderner Straße 2–4, D-82152 Martinsried, Germany, Tel.: +49 89 2180 74506; Fax: +49 89 2180 74520; E-mail: heermann@lmu.de

Keywords: surface plasmon resonance spectroscopy, microscale thermophoresis, chloroplast, mitochondria, endoplasmic reticulum , Interaction Map analysis®, *Arabidopsis*

Background: Tetratricopeptide repeat proteins at organellar surfaces serve as docking proteins for chaperone bound preproteins.
Results: Binding affinities of docking proteins and chaperones were determined using surface plasmon resonance spectroscopy, Interaction Map® analysis and microscale thermophoresis.
Conclusion: Docking proteins of the chloroplast, mitochondrion and endoplasmic reticulum bind differentially to various cytosolic chaperones.
Significance: Tetratricopeptide repeat docking proteins possibly discriminate between chaperones in the cytosol.

ABSTRACT

The three tetratricopeptide repeat domain containing docking proteins Toc64, OM64 and AtTPR7 reside in the chloroplast, mitochondria and endoplasmic reticulum of *Arabidopsis thaliana*, respectively. They are suggested to act during post-translational protein import by association with chaperone bound preprotein complexes. Here we performed a detailed biochemical, biophysical and computational analysis of the interaction between Toc64, OM64 and AtTPR7 and the five cytosolic chaperones HSP70.1, HSP90.1, HSP90.2, HSP90.3 and HSP90.4. We used surface plasmon resonance spectroscopy in combination with Interaction Map® analysis to distinguish between chaperone oligomerization and docking protein-chaperone interactions and to calculate binding affinities for all tested interactions. Complementary to this, we applied pull-down assays as well as microscale thermophoresis as surface immobilization independent techniques. The data revealed that OM64 prefers HSP70 over HSP90, whereas Toc64 binds all chaperones with comparable affinities. We could further show that AtTPR7 is able to bind HSP90 in addition to HSP70. Moreover, differences between the HSP90 isoforms were detected and revealed a weaker binding for HSP90.1 to AtTPR7 and OM64, showing that slight differences in the amino acid composition or structure of the chaperones influence binding to the tetratricopeptide repeat domain. The combinatory approach of several methods provided a powerful toolkit to determine binding affinities of similar interaction partners in a highly quantitative manner.

Targeting of nuclear encoded proteins in plant cells requires regulation at several levels to

ensure efficient biogenesis and maintenance of organelles. All proteins of the endoplasmic reticulum as well as almost the entire proteome of chloroplasts and mitochondria rely on being synthesized in the cytosol and transported to and across the correct membranes. All chloroplast and mitochondrial proteins are imported post-translationally, whereas for the endoplasmic reticulum both co-translational and post-translational import has been described (1-3).

All preprotein-translocon complexes are equipped with a central channel protein embedded into the lipid bilayer thus allowing preproteins to travel from the cytosol into the respective organelles. The translocation process through the pore is assisted by associated docking or receptor proteins, which often harbor large cytosolic domains to mediate interaction with preproteins and cytosolic factors. Docking proteins containing tetratricopeptide repeat (TPR)[4] domains are found in almost all organellar membranes and organisms as parts of the translocon complexes (4). Although they do not represent an essential feature for cell viability, causing only mild defects upon deletion, they act as regulators under stress conditions and in concert with other receptor proteins (5-7). The contact between the TPR domains of membrane docking proteins and cytosolic preproteins can either occur directly or indirectly utilizing chaperones bound to the preproteins as scaffold proteins. The C-terminal EEVD motif conserved in cytosolic chaperones such as HSP70s and HSP90s can be coordinated by the clamp-type TPR domain, which consists of three repetitive motifs of 34 degenerate amino acids together forming a helix-turn-helix structure (8).

In mammals and yeast mitochondrial Tom70 is the most prominent TPR domain containing receptor, which has eleven TPR motifs organized in three distinct domains. The three N-terminal TPR motifs form a clamp-type domain by which it associates with HSP70 in yeast, as well as with HSP90 in mammals. In mammals, Tom70 is assisted by the membrane associated Tom34, which harbors two TPR domains which interact with heat shock protein 70 (HSP70)[4] as well as HSP90, suggesting a possible role as co-chaperone in the cytosol (6,9-12). Recognized chaperone-preprotein complexes are subsequently released to the Tom translocon and preproteins are translocated across the outer mitochondrial membrane. Post-translational import into the ER in yeast is also facilitated with the aid of a TPR domain containing protein - Sec72 - which is soluble by itself, but anchored to the membrane via Sec71, a membrane spanning component of the Sec translocon (13). Recently, several post-translationally imported substrate proteins of the secretory pathway have been identified in yeast (3). However, in plants no preproteins of the post-translational translocation pathway into the ER are known to date which might utilize chaperone guidance. Therefore, it will be interesting to identify candidate proteins in plants in the future and to analyze the role of HSP70 or HSP90 in their delivery to the ER membrane *in vivo*.

In plants, complexity is added to post-translational targeting by the chloroplast as an additional organelle. Likewise cytosolic components have been described to associate with chloroplast preproteins, such as 14-3-3 proteins as well as HSP70 and HSP90. HSP90-binding candidates are recognized indirectly by the TPR domain containing protein Toc64 (5,14-16), a loosely associated component of the chloroplast Toc translocation machinery in the outer envelope membrane. The composition of the Tom complex in plant mitochondria differs distinctively from the complex in yeast and mammals, especially with respect to the receptor proteins. Tom70 is not found in plant genomes, however a close homologue of Toc64 - OM64 - has been identified in the outer mitochondrial membrane. Mutants lacking OM64 show reduced import of some mitochondrial proteins, corroborating the idea of a catalytic function of OM64 in protein import dependent on chaperone assisted translocation (7,17,18). Although plants, yeast and mammals share the central components of the ER Sec translocon Sec61, Sec62 and Sec63, the TPR domain containing Sec72 is only found in yeast. However, we have recently identified AtTPR7 as an interaction partner of *Arabidopsis* Sec63 and Sec62 (19,20). Since we could also show that AtTPR7 can complement for the function of Sec72 in yeast and interacts with both HSP70 and HSP90 in pull-down experiments, AtTPR7 is most likely involved in post-translational translocation into the ER in plants. In the plant cytosol, four HSP90 and five HSP70 isoforms are expressed. Some of these are constitutively produced at high levels, i.e. show a minor response to stress exposure (HSP90.2, HSP90.3, HSP90.4, HSP70.1), whereas other isoforms are heat shock induced and

produced at higher levels under stress conditions (HSP90.1, HSP70.2, HSP70.3, HSP70.4, HSP70.5) (21,22).

In the present study we investigated whether Toc64, OM64 and AtTPR7 exhibit preferences for either HSP70 or any of the HSP90 isoforms to investigate a potential supporting function of chaperones in discrimination between organelles during protein sorting. Individual TPR domains of HSP90 co-chaperones have previously been shown to distinguish between HSP70 and HSP90, for example in the HSP70/90 organizing protein (HOP)[4], which contains three TPR domains all showing different binding affinities for HSP70 and HSP90 (23). Therefore we utilized a combination of several biochemical, biophysical and computational methods to quantify these interactions, including surface plasmon resonance spectroscopy (SPR)[4] with Interaction Map® (IM)[4] evaluation, microscale thermophoresis (MST)[4] as well as *in vitro* pull-down experiments. Interestingly, significant differences were observed with respect to the individual binding affinities of Toc64 and OM64 to HSP70.1 and the HSP90 isoforms. Although the TRP domains are highly similar, OM64 binds preferentially to HSP70.1 whereas Toc64 binds to both HSP70.1 and the HSP90 isoforms. AtTPR7 binds to HSP70.1 and the HSP90 isoforms in the same manner except for HSP90.1, the heat induced isoform, for which it shows a reduced binding affinity. Using a combination of SPR and IM analyses, we were able to determine binding kinetics and to quantify these interactions. MST was used as a novel and surface immobilization independent method to additionally analyze the AtTPR7-chaperone binding affinities.

EXPERIMENTAL PROCEDURES

Cloning and purification of recombinant proteins - Genes encoding the *Arabidopsis* TPR domain containing docking proteins lacking the transmembrane domain (AtTPR7: amino acids 1-500, Toc64: amino acids 50-604, OM64: amino acids 50-590) were cloned into pET21a$^+$ (Novagen, Darmstadt, Germany), over-produced in *E. coli* (BL21-CodonPlus (DE3)-RIPL) cells, grown in M9ZB medium at 25°C for 5 h and purified via Ni-NTA-affinity chromatography (GE Healthcare). HSP90 isoforms were amplified from *Arabidopsis* cDNA using oligonucleotides recognizing the 3´ and 5´ UTR to ensure amplification of the correct isoform. The HSP90 isoforms as well as HSP70.1 were cloned into pET51b (Novagen, Darmstadt, Germany) with an N-terminal StrepII tag. Chaperones were over-produced in *E. coli* (BL21-CodonPlus (DE3)-RIPL) cells, grown in LB medium at 18°C over-night and purified via Strep-Tactin affinity chromatography (GE Healthcare). Sequences of all clones were checked by DNA sequencing. Oligonucleotides for AtTPR7, HSP70.1, HSP90.1, HSP90.2, HSP90.3 and HSP90.4 were described previously (19). The following oligonucleotides were used for the OM64 and Toc64 pET21a$^+$ constructs inserting an N-terminal His-tag, replacing the transmembrane domain: OM64-NheI-for:5'-CGATGCTAGCCACCACCACCACCACTTAGATCGTTTCGAGCTTC-3', OM64-XhoI-rev:5'CGATCTCGAGTCATATGTGTTTTCGGAGTCTC-3', Toc64-NdeI-for: CGATCATATGCACCCCACCACCACCACCACCCTCCCAAAGCTCCTCATC, Toc64-XhoI-rev: CGATCTCGAGTCACTGGAATTTTCTCAGTCTC

Size exclusion chromatography - Size exclusion chromatography (SEC)[4] was performed using a Superdex 200 column and PBS-G buffer (10 mM Na_2HPO_4, 1.8 mM KH_2PO_4, 140 mM NaCl, 2.7 mM KCl, 10 % (v/v) glycerin) as running buffer. 2,000 µM of the receptor protein and 1,000 µM of the respective chaperone were incubated for 1 h at 4°C and centrifuged at 100,000xg for 15 min before loading on the column.

Time dependent ultracentrifugation – Proteins (5 µg in 20 µl) were incubated in PBS buffer (10 mM Na_2HPO_4, 1.8 mM KH_2PO_4, 140 mM NaCl, 2.7 mM KCl) at 25°C for 0.5, 1 and 2 h, respectively, centrifuged at 100,000xg for 15 min and the supernatant as well as the pellet were subjected to SDS-PAGE. Proteins were visualized by Coomassie brilliant blue staining.

SDS-PAGE and immunoblotting - Proteins were separated on 10 % polyacrylamide gels and immunodetection was performed as described previously (24). HSP90 and HSP70 antisera were generated against wheat chaperones and are described elsewhere (25). Polyclonal Toc64 and OM64 antisera were raised against recombinant *Arabidopsis* proteins (Pineda, Berlin, Germany).

In vitro pull-down experiments - His-tagged TPR proteins (30 µg) were incubated with

Strep-tagged chaperones (500 µM) for 1 h at RT in PBS buffer (140 mM NaCl, 2.7 mM KCl, 10 mM Na_2HPO_4, 1.8 mM KH_2PO_4, pH 7.3). His-tagged proteins were subsequently re-purified by incubation with Ni-NTA for 1 h at RT and proteins were eluted with 300 mM imidazol in PBS buffer. Proteins were separated on 10 % polyacrylamid gels and visualized by Coomassie brilliant blue staining.

Surface plasmon resonance spectroscopy - SPR assays were performed in a Biacore T200 using carboxymethyl dextran sensor chips (CM5 Sensor Chip Series S). First, the chips were equilibrated with HBS-EP buffer (10 mM HEPES pH 7.4, 150 mM NaCl, 3 mM EDTA, 0.005 % (v/v) detergent P20) until the dextran matrix was swollen. Then, all four flow cells of the CM5 chips were activated by injecting a one-to-one mixture of N-ethyl-N-(3-dimethylaminopropyl)carbodiimide hydrochloride and N-hydroxysuccinimide using the standard amine-coupling protocol. Flow cells 2, 3, and 4 of each chip were loaded with a final concentration of 10 µg/ml of AtTPR7, OM64 and Toc64, respectively, in 10 mM acetate pH 4.5 (OM64, AtTPR7) or pH 5.5 (Toc64) until surfaces containing densities of 2,000-3,000 resonance units (RU)[4] were generated. High immobilization amounts of the receptors were essential to detect binding of the chaperones, putatively due to low "active" receptor concentrations. As running buffer for immobilization of AtTPR7 HBS-EP buffer was used, for immobilization of OM64 and Toc64 PBS-GTM buffer (10 mM Na_2HPO_4, 1.8 mM KH_2PO_4, 140 mM NaCl, 2.7 mM KCl, 10 % (v/v) glycerin, 0.05 % (v/v) Tween-20, 5 mM β-mercaptoethanol) was used. Free binding sites of all four flow cells were saturated by injection of 1 M ethanolamine/HCl pH 8.0. Preparation of chip surfaces was carried out at a flow rate of 10 µl/min. The interaction kinetics of OM64 or Toc64 with the chaperones was performed in PBS-GTM buffer and for AtTPR7 in Strep-binding buffer (50 mM Tris/HCl pH 8.0, 150 mM NaCl, 1 mM EDTA) at a flow rate of 5 µl/min. Low flow rates emerged best to detect optimal receptor-chaperone binding. The chaperones were diluted in the respective running buffer and passed over all flow cells in different concentrations (0.1 µM-5 µM) using a contact time of 360 sec followed by a 300 sec dissociation time before the next cycle started. After each cycle the surface was regenerated by injection of 50 mM NaOH for 30 sec at 30 µl/min flow rate. All experiments were performed at 25°C. Sensorgrams were recorded using the Biacore T200 Control software 1.0 and analyzed with the Biacore T200 Evaluation software 1.0. The surface of flow cell 1 was used to obtain blank sensorgrams for subtraction of bulk refractive index background. The referenced sensorgrams were normalized to a baseline of 0. Peaks in the sensorgrams at the beginning and the end of the injection emerged from the runtime difference between the flow cells of each chip.

Microscale thermophoresis - MST assays were carried out with a Monolith NT.115 instrument (Nano Temper, Munich, Germany). Purified AtTPR7-His was labeled with L001 Monolith NT.115 Protein Labeling Kit RED-NHS (Amine Reactive) dye. Increasing concentrations (1 nM-80 µM) of non labeled, strep-tagged chaperones were titrated against 30 nM of labeled AtTPR7-His, centrifuged for 5 min at 16,100xg to remove potential aggregates, and the supernatant was soaked into hydrophilic silicon capillaries (K004 Monolith NT.115). Each measurement was taken three times. Experiments were carried out in 40 mM HEPES pH 7.5, 20 mM KCl, 0.5 mg/ml BSA, 0.05 % (w/v) Tween 20. Data evaluation was performed with the Monolith software.

Interaction Map® analysis - IM calculations were performed on the Ridgeview Diagnostic Server (Ridgeview Diagnostics, Uppsala, Sweden). For this, the SPR sensorgrams were exported from the Biacore T200 Evaluation Software 1.0 as *.txt files and imported into the TraceDrawer Software 1.5 (Ridgeview Instruments, Uppsala, Sweden). IM files were created using the IM tool within the software, generating files that were sent via e-mail to the server (im@ridgeviewdiagnostics.com) where the IM calculations were performed (23). The result files where then evaluated for spots in the TraceDrawer 1.5 software, and the IM spots were quantified.

Accession numbers - Sequence data from this article can be found in the NCBI data libraries under accession numbers: At3g17970 (Toc64), At5g09420 (OM64), At5g21990 (AtTPR7), At5g02500 (HSP70.1), At5g52640 (HSP90.1), At5g56030 (HSP90.2), At56010 (HSP90.3), At5g56000 (HSP90.4).

RESULTS

Toc64, OM64 and AtTPR7 interact differentially with HSP70.1 and HSP90 isoforms - Several TPR domain containing docking proteins interact with HSP70 and HSP90, however it is unclear in how far they can discriminate between the cytosolic chaperones. For pea Toc64 interaction with the C-terminal peptides of HSP70 and HSP90 was shown, albeit with preference for HSP90 (14). Moreover, HSP90 was shown to be up-regulated in *toc64* mutants, suggesting a more differential function for HSP90 than HSP70 (5). Although OM64 is a close homologue of Toc64, and a parallel function to Tom70 in mitochondria has been suggested, chaperone association has not been investigated to date for this putative chaperone docking protein. We therefore tested binding of all three *Arabidopsis* TPR domain containing docking proteins (Toc64, OM64 and AtTPR7) to all cytosolic HSP90 isoforms in *Arabidopsis*, since HSP90 might act as a supportive factor in the cytosolic protein sorting process. In addition, we tested binding to HSP70.1, since this represents the isoform with the highest basal expression level in *Arabidopsis*. Only one isoform of HSP70 was chosen as HSP70 is known to interact with hydrophobic stretches of almost all preproteins in a rather unspecific manner, and previous analyses did not indicate that the strongly heat shock induced isoforms are involved in specification of targeting (26).

As a first step we generated recombinant proteins. For this, the coding sequence of *Toc64* and *OM64* lacking the N-terminal transmembrane domain and *AtTPR7* lacking the C-terminal transmembrane domain were fused to a His-tag replacing the transmembrane domain. The recombinant proteins were over-produced in *E. coli* and purified via Ni-NTA. HSP70.1 and HSP90 isoforms were fused to an N-terminal Strep-tag, which does not interfere with binding of the C-terminal EEVD motif to the TPR domain, and purified accordingly. Since TPR proteins are prone to aggregation in solution, we employed SEC to analyze the status of the purified TPR domain containing docking proteins (Fig. 1*A*-*C*). Toc64 and OM64 eluted as monomers whereas AtTPR7 seemed to form tetramers. Moreover, time dependent ultracentrifugation was performed (Fig. 1*D*). These analyses also verified that protein aggregation did not occur, even after 2 h incubation at RT.

Next, we employed an *in vitro* binding assay with the recombinant proteins. His-tagged TPR proteins were incubated either with Strep-HSP70.1, Strep-HSP90.1, Strep-HSP90.2, Strep-HSP90.3 or Strep-HSP90.4 and recovered by Ni-NTA. A sample without His-tagged TPR protein served as a control for each chaperone. The associated chaperones as well as the TPR proteins were separated by SDS-PAGE and detected by Coomassie staining (Fig. 2). Indeed, in accordance with earlier results, more HSP90 than HSP70 was recovered along with Toc64 (Fig. 2*A*). Interestingly, although the protein region of the TPR domain of mitochondrial OM64 displays 68 % identity to Toc64, it clearly showed only a weak binding to all HSP90 isoforms, while binding strongly to HSP70.1 (Fig. 2*B*). Similar to our earlier results AtTPR7 bound to both, HSP70.1 and HSP90 isoforms, although binding to HSP70.1 was more prominent (Fig. 2*C*). Note that in this assay no stoichiometric binding behavior can be visualized, since it is not to be expected that each TPR protein bound to Ni-beads interacts with a chaperone. Consequently, more TPR proteins than chaperones are visible in all cases. As a control, the recombinant chaperones showing the purity status are presented in Fig. 2*D*.

TPR docking proteins interact with oligomeric states of chaperones Since HSP70 and HSP90 are known to oligomerize (27-30), it was our aim to verify the oligomeric states of the HSP70 and HSP90 proteins used in this work and to analyze their binding to the TPR proteins. SEC was used to separate oligomeric chaperone states as well as receptor-chaperone complexes. Peak fractions were subjected to SDS-PAGE and immunoblot analysis. Two representative interactions were chosen: HSP70.1 with OM64 and HSP90.3 with Toc64. HSP70.1 (71 kDa) without binding partner was found to oligomerize (Fig. 3*A*), whereas unbound OM64 (62 kDa) elutes as a monomer (Fig. 3*B*). However, upon incubation of HSP70.1 and OM64 a new peak at the size of ~200 kDa appeared (Fig. 3*C*). This peak contained HSP70.1 as well as OM64 (Fig. 3*C*). HSP90.3 (80 kDa) is present as monomers, dimers, tetramers and oligomers (Fig. 3*D*), whereas Toc64 (59 kDa) also elutes as a monomer (Fig. 3*E*). Upon incubation of Toc64 with HSP90.3 the elution pattern changed and in

addition to HSP90.3 oligomers and Toc64 monomers a shoulder appeared at ~400 kDa, which contained HSP90.3 and Toc64 (Fig. 3*F*). The chromatograms indicate an interaction of the TPR proteins with chaperone oligomers, however, we cannot determine which exact oligomeric state of chaperones and TPR proteins interact with each other. As HSP70 and HSP90 formed large oligomers we performed time dependent ultracentrifugation to ensure that the chaperones are not aggregating. Indeed after SDS-PAGE and Coomassie staining almost all protein was found in the supernatant (Fig. 3*D*).

However, no reliable quantitative conclusion can be drawn from the data above. In the following we therefore applied further biophysical techniques to analyze the individual binding affinities in more detail.

Determination of receptor-chaperone binding kinetics by SPR and IM evaluation - To determine binding kinetics of Toc64, OM64 and AtTPR7 with HSP70.1 and HSP90 isoforms, we performed SPR analyses. For this, Toc64, OM64 and AtTPR7 were immobilized via amino-coupling onto a CM5 Sensor Chip, and increasing concentrations (0.1 µM-5 µM) of the chaperones were injected onto the chip surfaces (see Material and Methods for detail). In all cases, clear binding of the chaperones to the respective sensor surface could be observed (Fig. 4-6*A*). In each experiment, HSP70.1 seemed to bind more strongly to the respective ligand than the HSP90 isoforms. The HSP90.2, HSP90.3 and HSP90.4 isoforms seemed to interact with each receptor with similar affinity. HSP90.1 interaction with AtTPR7 and OM64 was slightly weaker than the other HSP90 isoforms (Fig. 4 and 5*A*). However, none of the sensorgrams followed a final and linear saturation, indicating that the curves did not reflect a single binding event and therefore no clear one-to-one interaction.

As HSP90 and HSP70 oligomerize, it can be assumed that the sensorgrams measured with SPR are a sum of different binding events. On the one hand we observed an interaction of the receptors with the chaperones, on the other hand an interaction of defined oligomeric chaperone states with each other. The even and steady slope of the binding curves indicates a homogeneous interaction of the oligomeric chaperone states. To calculate reliable binding constants and kinetic parameters a computational approach was chosen to analyse the sensorgramms. The measured curves can be approximated to the sum of primitive binding curves, each representing a monovalent interaction (31) with a unique combination of association rate k_a (on-rate) and dissociation rate k_d (off-rate) (and consequently an equilibrium dissociation constant $K_D = k_d/k_a$). We calculated IMs of each single sensorgram to determine and quantify the individual binding events represented by the curves. The algorithm splits the experimental SPR data set to several theoretical monovalent binding curves and spots the binding curves that, summed up, best fit the experimental data. By plotting the association rate k_a and the dissociation rate k_d within a two-dimensional distribution it is possible to display heterogeneous binding data as a map where each peak corresponds to one component that contributes to the cumulative binding curve (32). In case that these interaction events have almost similar on- and off-rates, no separate but fused peaks will appear. We interpreted a single peak that extents the size of one log magnitude to be composed of two peaks, as theoretically a single interaction event should not vary in binding kinetics by a factor of more than 10. In the IMs presented here, the large peaks that exceed a magnitude of > 1 in the log scale were evaluated as fused peaks that are overlapping in a wider area. These peaks were manually split up into two areas and regarded as two connected individual interactions. The shape of the SPR sensorgrams and the fact that HSP70 as well as HSP90 form oligomers, shows that the sensorgrams are composed of at least two interaction events. Such a fused peak was most dominant in the AtTPR7-HSP70.1 IM (Fig. 6*B*). Therefore, it was plausible, to split those peaks into two peaks with different affinities. As with any evaluation algorithm, there can be a "noise level" in IMs where a peak might be an artifact – either algorithm related or instrument/data related. The "fast-on/fast off peaks", with a high k_a and a low k_d, visible in nearly every IM were interpreted to represent bulk effects on the sensor surface. The determination of the peak weight parameter was helpful in this case. Peaks with a weight of less than 4 % do not represent real binding events and should therefore be disqualified from data interpretation, whereas those of more than 10 % cannot be neglected[2]. In most of the IMs presented in this study, small peaks with high on- and fast off-rates could be

observed. These peaks were interpreted as bulk effects and therefore neglected as they all showed peak weights between 0.1-2.0 %. In IMs of OM64-HSP70.1, OM64-HSP90.2, OM64-HSP90.3, OM64-HSP90.4, Toc64-HSP70.1, and Toc64-HSP90.4 peaks with a slow off component appeared (Fig. 4-6*B*). These could either result from instrument drift, or sticky impurities or represent real binding events. We used the peak weight as cut-off for interpreting these peaks, and also consulted the results of the pull-down and MST analyses for data interpretation. As the weights of these peaks within OM64-HSP90 isoforms as well as the Toc64-HSP70.1 and Toc64-HSP90.4 IMs were all in the range of 1 % and 4 % we neglected these peaks from interpretation. Only the slow off peak in the OM64-HSP70.1 IM was interpreted as a real binding event, as the peak weight was approximately 13 %.

The calculated interactions are displayed in a peak diagram related to the log of the respective association and dissociation constants, k_a and k_d. The IMs of the chaperones to the respective docking proteins Toc64, OM64 and AtTPR7 are shown in Fig. 4-6*B*. The calculated sensorgrams for each of the two interaction events that can be extracted from the respective IM analyses are presented in Fig. 4-6*C* and *D*. We found that in each IM one interaction had similar on and off-rates. We assumed that the oligomerization of the chaperones should be independent of the presence of the receptor and therefore interpreted the calculated curves in Fig. 4-6*D* (blue peaks and sensorgrams) to represent the chaperone oligomerization. The K_D values for chaperone-chaperone interaction were calculated to be approximately 4-13 µM for each of the chaperones in all tested interactions. The calculated sensorgrams with the higher variability in K_D values were therefore assumed to represent the binding events between the different chaperones and the Toc64, OM64 and AtTPR7 receptors, respectively. Toc64 showed binding with similar affinities to HSP70.1 (K_D=2.0 µM) as to all HSP90 isoforms (K_D=2.4-15.5 µM) (Fig. 4). In contrast, a very strong interaction could be observed between OM64 and HSP70.1, which showed a K_D=of 0.03 µM (Fig. 5). The HSP90 isoforms interacted with OM64 with much lower affinities compared to HSP70.1. HSP90.2, HSP90.3 and HSP90.4 had a similar affinity to OM64 (K_D=1.3-2.9 µM) and solely interaction with HSP90.1 was still weaker (K_D=20.2 µM). For AtTPR7 again HSP70.1 showed the highest affinity (K_D=1.0 µM) (Fig. 6). The HSP90 isoforms showed comparatively lower affinities (K_D=5.1-16.0 µM) to AtTPR7. Compared to HSP90.2-4, HSP90.1 binding to AtTPR7 was weaker (K_D=16.0 µM).

With respect to the binding kinetics, the differences in the receptor-HSP70.1 affinities to the receptor-HSP90s interactions are predominantly caused by differences in the off-rates (k_d) rather than on-rates (k_a) (Table 1). The lowest off-rates were observed for the AtTPR7-HSP70.1 and OM64-HSP70.1 interactions, calculated with k_d=5.25 x 10^{-4}/s and 3.49 x 10^{-4}/s, respectively. Only the OM64-HSP70.1 interaction was also characterized by a high on-rate (k_a=1.25 x 10^4/M x s) compared to the other interactions, whereas the AtTPR7-HSP70.1 and Toc64-HSP70.1 on-rates were in a similar range (k_a=5.41 x 10^2/M x s and 1.55 x 10^3/M x s). The high affinity of the OM64-HSP70.1 interaction is therefore caused by a high on-rate (k_a=1.25 x 10^4/M x s), which is almost 10-20-fold higher compared to the Toc64-HSP70.1 (1.55 x 10^3/M x s) and AtTPR7-HSP70.1 interactions (5.41 x 10^2/M x s), respectively. The lower affinity of the HSP90.1 isoform compared to the other HSP90 isoforms towards OM64 and AtTPR7 was also mainly caused by lower on-rates rather than high off-rates. In principle, the off-rates of all other HSP90-receptor interactions were in a more or less similar range and varied around 1-9 x 10^{-3}/s.

Determination of receptor-chaperone binding affinities using MST analysis - In contrast to SPR, MST is a novel method to directly monitor protein-protein interaction in solution and is therefore surface immobilization independent. Movement of proteins is monitored in a temperature gradient, and upon binding of the interaction partner the movement behavior is altered. A fluorescent tag is coupled to one of the binding partners, which allows detection of the thermophoretic movement in a small glass capillary. Upon addition of increasing concentrations of the binding partner, small changes of the hydration shell due to complex formation can be monitored. Binding curves result from changes in fluorescence response (33). To further evaluate AtTPR7-chaperone binding with an additional assay, we employed MST as a

second method (Fig. 7). AtTPR7 was coupled to the fluorescent tag, and increasing amounts of chaperones were used as analytes. Weakest binding was again observed for HSP90.1 (K_D=2.7 µM) to AtTPR7. In contrast, constitutively expressed HSP90 isoforms showed stronger binding to AtTPR7 with a more than two-fold lower K_D value (HSP90.2: K_D=1.2 µM, HSP90.3: K_D=1.2 µM, HSP90.4: K_D=1.0 µM). Nevertheless, strongest binding was monitored for HSP70.1 (K_D=0.3 µM) (Table 2). The same tendency of the K_D values can be observed using both methods. This data goes hand in hand with the obtained SPR data, and also verified the IM calculations from the SPR sensorgrams.

DISCUSSION

The aim of our study was to compare binding affinities of three TPR-domain containing docking proteins, Toc64 at the outer envelope of chloroplasts, OM64 at the outer membrane of mitochondria and AtTPR7 at the ER membrane, to the cytosolic chaperones HSP70.1 and the four isoforms of HSP90. Members of the HSP70 and HSP90 family have a suggested function in post-translational protein import into the respective compartments. In this context we aimed to investigate a potential role of HSP70 or HSP90 in the sorting process of preproteins to distinct organelles, since TPR domains of various proteins (e.g. HOP) have previously been shown to selectively discriminate between the two chaperones (23,34,35). As a first step, we performed *in vitro* pull-down experiments which showed the binding potential of the three TPR domain containing docking proteins to all tested chaperones, albeit with different intensities. However, since pull-down assays cannot supply quantitative data we chose SPR combined with IM evaluation as the central method to determine binding affinities; the obtained results are summarized in Fig. 8.

Previous data on Toc64, the chloroplast docking protein, has shown that the pea Toc64 isoform preferentially binds the C-terminal HSP90 peptide over the HSP70 peptide as determined by semi-quantitative pull-down experiments (14). We could show in our initial pull-down with the *Arabidopsis* Toc64 along with the constitutively expressed full length HSP70.1 and HSP90 isoforms that it has the potential to interact with all chaperones. SPR analyses revealed that binding affinities for all chaperones tested were in the micromolar range and showed no significant differences. However, by determining the on- and off-rates it became evident that association constants are higher towards HSP70.1 and HSP90.4 compared to the other HSP90 isoforms, although dissociation showed comparable values for all tested chaperones. Considering that the chaperones are suggested to play a role in preprotein recognition at organellar surfaces (14), we suggest that chloroplast preproteins can be delivered with the aid of both, HSP70 and HSP90, *in vivo.* HSP90 isoforms are not discriminated and therefore are possibly functionally redundant in this context.

OM64 is phylogenetically very closely related to Toc64, showing an overall sequence identity of 51 % (68 % within the TPR domain) (4). However, OM64 is located in the outer mitochondrial membrane and involved in the import of some mitochondrial preproteins (7). Therefore, it is likely that OM64 is functionally similar to the yeast and mammalian Tom70. The clamp-type TPR domain of Tom70 functions as docking site for HSP70 to receive mitochondrial preproteins, whereas mammalian Tom70 additionally binds to HSP90 (6,12). Surprisingly, our data revealed that OM64 binds to HSP70.1 with a much higher affinity in direct comparison to the HSP90 isoforms. This tendency is evident already from the pull-down experiments, and K_D values calculated for OM64-HSP70.1 were 100 times lower, in the nanomolar range, compared to the HSP90 isoforms. In an *in vivo* situation, with HSP70 and HSP90 present in the cytosol, preferential binding of HSP70 to OM64 can be expected. Although this data is surprising, especially considering the high sequence identity between OM64 and Toc64, it favors a model in which chloroplast preproteins are assisted by HSP90, whereas mitochondrial preproteins are preferentially bound to HSP70 in the cytosol. Moreover, initial results support this hypothesis, as we have so far been unable to demonstrate HSP90 binding to plant mitochondrial preproteins, not even to hydrophobic carrier proteins[3], mammalian counterparts of which bind to HSP90 (6).

Recently we identified AtTPR7 as an additional TPR domain containing docking protein associated to the ER Sec translocon in plants (19). We were interested in analyzing the binding potential to HSP90 in addition to HSP70,

especially since we could detect HSP90 binding in contrast to other studies by Abell and co-workers (36,37) (AtTPR7 is designated as OEP61 in this case). All binding affinities calculated for AtTPR7 and chaperones were found to be in the micromolar range. Although AtTPR7-HSP70.1 showed the strongest interaction, binding of AtTPR7 to HSP90 is also likely to occur *in vivo*. Interestingly, the binding affinity of HSP90.1 to AtTPR7 and OM64 was the weakest. This might indicate that the constitutively expressed chaperone isoforms (HSP70.1, HSP90.2-4) play a predominant role in preprotein targeting in contrast to the mainly heat shock induced isoform HSP90.1. Moreover, the HSP90.2, HSP90.3 and HSP90.4 isoforms are highly homologues (97-99 % identity), suggesting a redundant function, whereas HSP90.1 shows only 85-87 % identity to the other isoforms. The fact that we observed differences in the binding affinities of HSP90.1 to AtTPR7 and OM64 in comparison to the other HSP90 isoforms indicates that binding properties to the TPR domain are not only influenced by the presence of the C-terminal MEEVD motif, which is present in all HSP90 isoforms. Binding affinities seem also to be influenced by the entire protein, its amino acid composition as well as its higher order structure. In this respect the C-terminal amino acids adjacent to the MEEVD motif may play a role, since they could come into close proximity to the TPR clamp of the receptor. Sequence identity in the C-terminal 45 amino acids is reduced to 73-75 % when comparing HSP90.1 to the other isoforms (Fig. 9). Moreover, future structural analyses and site directed mutations of the individual TPR domains will reveal which residues interplay with the different chaperones and participate in conferring specificity.

In addition to the SPR data set for AtTPR7, we used MST as a novel approach, which is surface immobilization independent. The obtained binding affinities showed the same tendency as the corresponding SPR results. Slight differences in the determined K_D values between the two methods could result from the different principles of the two techniques. Whereas in MST measurements the two proteins are allowed to interact for several minutes until the interaction has reached a steady state equilibrium, only a transient interaction is monitored by determining on- and off-rates in SPR due to the quick change between buffer and binding partner. However, clearly the same tendencies are observed and both methods are ideally suited to act as complementary approaches.

In this study we have used a combinatory approach of biochemical, biophysical and computational methods to investigate protein-protein interactions and to quantify binding affinities of three TPR receptor proteins as well as five different full length chaperones. SPR in combination with IM and MST has proven to be a powerful approach to distinguish individual binding constants.

REFERENCES

1. Zimmermann, R., Eyrisch, S., Ahmad, M., and Helms, V. (2011) *Biochim Biophys Acta* **1808**, 912-924
2. Schleiff, E., and Becker, T. (2011) *Nat Rev Mol Cell Biol* **12**, 48-59
3. Ast, T., Cohen, G., and Schuldiner, M. (2013) *Cell* **152**, 1134-1145
4. Schlegel, T., Mirus, O., von Haeseler, A., and Schleiff, E. (2007) *Mol Biol Evol* **24**, 2763-2774
5. Sommer, M., Rudolf, M., Tillmann, B., Tripp, J., Sommer, M. S., and Schleiff, E. (2013) *Plant Cell Environ* **36**, 970-983
6. Young, J. C., Hoogenraad, N. J., and Hartl, F. U. (2003) *Cell* **112**, 41-50
7. Lister, R., Carrie, C., Duncan, O., Ho, L. H., Howell, K. A., Murcha, M. W., and Whelan, J. (2007) *Plant Cell* **19**, 3739-3759
8. Scheufler, C., Brinker, A., Bourenkov, G., Pegoraro, S., Moroder, L., Bartunik, H., Hartl, F. U., and Moarefi, I. (2000) *Cell* **101**, 199-210
9. Fan, A. C., Bhangoo, M. K., and Young, J. C. (2006) *J.Biol.Chem.* **281**, 33313-33324
10. Faou, P., and Hoogenraad, N. J. (2012) *Biochim Biophys Acta* **1823**, 348-357
11. Bhangoo, M. K., Tzankov, S., Fan, A. C., Dejgaard, K., Thomas, D. Y., and Young, J. C. (2007) *Mol.Biol.Cell* **18**, 3414-3428
12. Chan, N. C., Likic, V. A., Waller, R. F., Mulhern, T. D., and Lithgow, T. (2006) *J Mol Biol* **358**, 1010-1022
13. Feldheim, D., and Schekman, R. (1994) *J Cell Biol* **126**, 935-943
14. Qbadou, S., Becker, T., Mirus, O., Tews, I., Soll, J., and Schleiff, E. (2006) *EMBO J.* **25**, 1836-1847
15. Qbadou, S., Becker, T., Bionda, T., Reger, K., Ruprecht, M., Soll, J., and Schleiff, E. (2007) *J.Mol.Biol.* **367**, 1330-1346
16. Sohrt, K., and Soll, J. (2000) *J.Cell Biol.* **148**, 1213-1221
17. Carrie, C., Murcha, M. W., and Whelan, J. (2010) *BMC Plant Biol* **10**, 249
18. Chew, O., Lister, R., Qbadou, S., Heazlewood, J. L., Soll, J., Schleiff, E., Millar, A. H., and Whelan, J. (2004) *FEBS Lett.* **557**, 109-114
19. Schweiger, R., Muller, N. C., Schmitt, M. J., Soll, J., and Schwenkert, S. (2012) *J Cell Sci*
20. Schweiger, R., and S., S. (2013) *Plant Signal Behav* **8**
21. Sung, D. Y., Vierling, E., and Guy, C. L. (2001) *Plant Physiol* **126**, 789-800
22. Krishna, P., and Gloor, G. (2001) *Cell Stress.Chaperones.* **6**, 238-246
23. Schmid, A. B., Lagleder, S., Grawert, M. A., Rohl, A., Hagn, F., Wandinger, S. K., Cox, M. B., Demmer, O., Richter, K., Groll, M., Kessler, H., and Buchner, J. (2012) *EMBO J* **31**, 1506-1517
24. Lamberti, G., Gugel, I. L., Meurer, J., Soll, J., and Schwenkert, S. (2011) *Plant Physiol* **157**, 70-85
25. Fellerer, C., Schweiger, R., Schongruber, K., Soll, J., and Schwenkert, S. (2011) *Mol Plant* **4**, 1133-1145
26. Zhang, X. P., and Glaser, E. (2002) *Trends Plant Sci.* **7**, 14-21
27. Thompson, A. D., Bernard, S. M., Skiniotis, G., and Gestwicki, J. E. (2012) *Cell Stress Chaperones* **17**, 313-327
28. Kadota, Y., and Shirasu, K. (2012) *Biochim Biophys Acta* **1823**, 689-697
29. Nemoto, T., and Sato, N. (1998) *Biochem Journal* **330**, 989-995
30. Aprile, F. A., Dhulesia, A., Stengel, F., Roodveldt, C., Benesch, J. L., Tortora, P., Robinson, C. V., Salvatella, X. Dobson, C. M., and Cremades, N. (2013) *PLoS One* **8**
31. Barta, P., Bjorkelund, H., and Andersson, K. (2011) *Nucl Med Commun* **32**, 863-867
32. Altschuh, D., Bjorkelund, H., Strandgard, J., Choulier, L., Malmqvist, M., and Andersson, K. (2012) *Biochem Biophys Res Commun* **428**, 74-79
33. Seidel, S. A., Dijkman, P. M., Lea, W. A., van den Bogaart, G., Jerabek-Willemsen, M., Lazic, A., Joseph, J. S., Srinivasan, P., Baaske, P., Simeonov, A., Katritch, I., Melo, F. A., Ladbury, J. E., Schreiber, G., Watts, A., Braun, D., and Duhr, S. (2013) *Methods* **59**, 301-315

34. Carrigan, P. E., Nelson, G. M., Roberts, P. J., Stoffer, J., Riggs, D. L., and Smith, D. F. (2004) *J Biol Chem* **279**, 16185-16193
35. Brinker, A., Scheufler, C., Von Der Mulbe, F., Fleckenstein, B., Herrmann, C., Jung, G., Moarefi, I., and Hartl, F. U. (2002) *J Biol Chem* **277**, 19265-19275
36. Kriechbaumer, V., Tsargorodskaya, A., Mustafa, M. K., Vinogradova, T., Lacey, J., Smith, D. P., Abell, B. M., and Nabok, A. (2011) *Biophys J* **101**, 504-511
37. von Loeffelholz, O., Kriechbaumer, V., Ewan, R. A., Jonczyk, R., Lehmann, S., Young, J. C., and Abell, B. M. (2011) *Biochem J* **438**, 143-153

Acknowledgements - We thank Nano Temper (Munich, Germany) and Dr. Karl Andersson (Ridgeview Instruments, Uppsala, Sweden) for support and helpful discussions. Katharina Schöngruber and Stefanie Rapp are acknowledged for excellent technical assistance.

FOOTNOTES

*This work was supported by Deutsche Forschungsgemeinschaft (grants numbers SFB 1035, project A04 to J.S. and S.S.), Fonds der chemischen Industrie (grant number Do 187/22 to R.S.) and the Exc114/1.
[1]To whom correspondence should be addressed: Tel.: +49 89 2180 74760, Fax: +49 89 2180 74752, E-mail: serena.schwenkert@lmu.de and Tel.: +49 89 2180 74506; Fax: +49 89 2180 74520; E-mail: heermann@lmu.de
[2]Personal communication (K. Andersson, Ridgeview Instruments, Uppsala, Sweden)
[3]Unpublished data (S.S.)
[4]The abbreviations used are: TPR, tetratricopeptide repeat; HSP, heat shock protein; HOP, HSP70/90 organizing protein; SPR, Surface Plasmon Resonance; IM, Interaction Map®; MST, microscale thermophoresis; RU, resonance units; SEC, size exclusion chromatography

FIG. LEGENDS

FIG.1: SEC and ultracentrifugation of TPR receptor proteins. Toc64 (A), OM64 (B) and AtTPR7 (C) were analyzed on a Superdex 200 column. The void volume (V_0) and a calibration curve are indicated. (D) Toc64, OM64 and AtTPR7 were incubated at RT for the indicated time points and subsequently ultracentrifuged. Supernatant (S) and pellet (P) were analyzed by SDS-PAGE and Coomassie staining.

FIG.2: Interaction of chaperone isoforms with TPR receptor proteins. (A) Recombinant His-Toc64, (B) His-OM64 and (C) AtTPR7-His (30 µg) were incubated with Strep-tagged HSP70.1 and all four cytosolic HSP90 isoforms (500 µM). His-tagged TPR receptor proteins were affinity purified with Ni-NTA subsequently. All proteins were visualized by Coomassie staining. Samples without His-tagged TPR receptor proteins were used as controls. (D) Purified chaperones as used in the pull-down experiments are shown. Impurities are indicated with asterisks and correspond to the likewise indicated bands in A.

FIG. 3: Oligomerization of chaperones and complex formation analyzed by SEC. HSP70.1 (A) and OM64 (B) were analyzed individually and after incubation for 1 h at 4°C (C) by SEC. Peak fractions (1, 2, 3) were analyzed by SDS-PAGE and immunoblotting with the indicated antisera. HSP90.3 (D) and Toc64 (E) were analyzed individually and after incubation for 1 h at 4°C (F) by SEC. In the case of HSP90.3 (D) peaks corresponding to the sizes of monomers, dimers, tetramers and oligomeres are visible. Peak fractions (1, 2, 3) were analyzed by SDS-PAGE and immunoblotting with the indicated antisera. (G) HSP70.1 (left panel) and HSP90.3 (right panel) were incubated at RT for the indicated time points and subsequently ultracentrifuged. Supernatant (S) and pellet (P) were analyzed by SDS-PAGE and Coomassie staining.

FIG. 4: Chaperone binding to Toc64 and determination of binding affinities using SPR and IM analyses. (A) SPR analyses. Toc64 was immobilized via amine coupling onto a CM5 senor chip, and solutions of 0.1 µM (purple), 0.5 µM (dark blue), 0.75 µM (blue), 1 µM (green), 2 µM (yellow), 3 µM (orange), 4 µM (red) and 5 µM (dark purple), respectively, of each of the chaperones were passed over the chip. (B) IM analyses. The green spots represent the Toc64-chaperone interactions, the blue spots the chaperone-chaperone interactions (oligomerization). (C) Calculated sensorgrams for Toc64-chaperone interaction. (D) Calculated sensorgrams for chaperone-chaperone interaction. The calculated K_D values for each interaction are indicated below the respective sensorgrams.

FIG. 5: Chaperone binding to OM64 and determination of binding affinities using SPR and IM analyses. (A) SPR analyses. OM64 was immobilized via amine coupling onto a CM5 sensor chip, and solutions of 0.1 µM (purple), 0.5 µM (dark blue), 0.75 µM (blue), 1 µM (green), 2 µM (yellow), 3 µM (orange), 4 µM (red) and 5 µM (dark purple), respectively, of each of the chaperones were passed over the chip. (B) IM analyses. The green spots represent the OM64-chaperone interaction, the blue spots the chaperone-chaperone interactions (oligomerization). (C) Calculated sensorgrams for OM64-chaperone interaction. (D) Calculated sensorgrams for chaperone-chaperone interaction. The calculated K_D values for each interaction are indicated below the respective sensorgrams.

FIG. 6: Chaperone binding to AtTPR7 and determination of binding affinities using SPR and IM analyses. (A) SPR analyses. AtTPR7 was immobilized via amine coupling onto a CM5 sensor chip, and solutions of 0.1 µM (purple), 0.5 µM (dark blue), 0.75 µM (blue), 1 µM (green), 2 µM (yellow), 3 µM (orange), 4 µM (red) and 5 µM (dark purple), respectively, of each of the chaperones were passed over the chip. (B) IM analyses. The green spots represent the AtTPR7-chaperone interaction, the blue spots the chaperone-chaperone interactions (oligomerization). (C) Calculated sensorgrams for AtTPR7-chaperone interaction. (D) Calculated sensorgrams for chaperone-chaperone interaction. The calculated K_D values for each interaction are indicated below the respective sensorgrams.

FIG. 7: Chaperone binding to AtTPR7 determined by MST. Thermophoretic mobility was monitored upon chaperone titration to a constant fluorescence labeled AtTPR7 concentration of 30 nM. Strongest binding was observed for HSP70.1 (K_D 0.3 µM), weakest binding for HSP90.1 (K_D 2.7 µM).

FIG. 8: Overview of the TPR domain containing docking protein and chaperone binding affinities. OM64 preferentially binds HSP70.1, whereas Toc64 associates with HSP70.1 as well as with HSP90 isoforms. AtTPR7 can interact with both, HSP70.1 and HSP90 isoforms, although HSP90.1 binding is weaker. Grey scale and arrow thickness indicate binding strengths of chaperones to the respective docking proteins (light - dark grey corresponds to weak - strong binding).

FIG. 9: Sequence alignment of the 45 C-terminal amino acids of the four HSP90 isoforms. Grayscale indicates sequence identity.

TABLE 1: Association (k_a), dissociation constants (k_d) and K_D values of receptor-chaperone interactions calculated by IM analysis.

Chaperone	Receptor	k_a[1/M*s]	k_d[1/s]	K_D [µM]
HSP70.1		$1.55x10^{3}$	$3.03x10^{-3}$	2.0
HSP90.1		$3.57x10^{2}$	$3.45x10^{-3}$	9.7
HSP90.2	**Toc64**	$5.88x10^{2}$	$2.92x10^{-3}$	5.0
HSP90.3		$3.55x10^{2}$	$5.52x10^{-3}$	15.5
HSP90.4		$1.26x10^{3}$	$3.02x10^{-3}$	2.4
HSP70.1		$1.25x10^{4}$	$3.49x10^{-4}$	0.03
HSP90.1		$4.88x10^{2}$	$9.84x10^{-3}$	20.2
HSP90.2	**OM64**	$1.59x10^{3}$	$3.03x10^{-3}$	1.9
HSP90.3		$2.01x10^{3}$	$5.91x10^{-3}$	2.9
HSP90.4		$3.28x10^{3}$	$4.26x10^{-3}$	1.3
HSP70.1		$5.41x10^{2}$	$5.25x10^{-4}$	1.0
HSP90.1		$1.73x10^{2}$	$2.80x10^{-3}$	16.0
HSP90.2	**AtTPR7**	$1.72x10^{2}$	$1.73x10^{-3}$	10.0
HSP90.3		$3.65x10^{2}$	$1.86x10^{-3}$	5.1
HSP90.4		$1.97x10^{2}$	$1.10x10^{-3}$	5.6

TABLE 2: K_D values obtained from MST measurements with AtTPR7 and chaperones.

Chaperone	Receptor	K_D [µM]
HSP70.1		0.3
HSP90.1		2.7
HSP90.2	**AtTPR7**	1.2
HSP90.3		1.2
HSP90.4		1.0

SUPPLEMENTAL DATA S1:
Raw data of SPR analysis is shown along with the best fits.

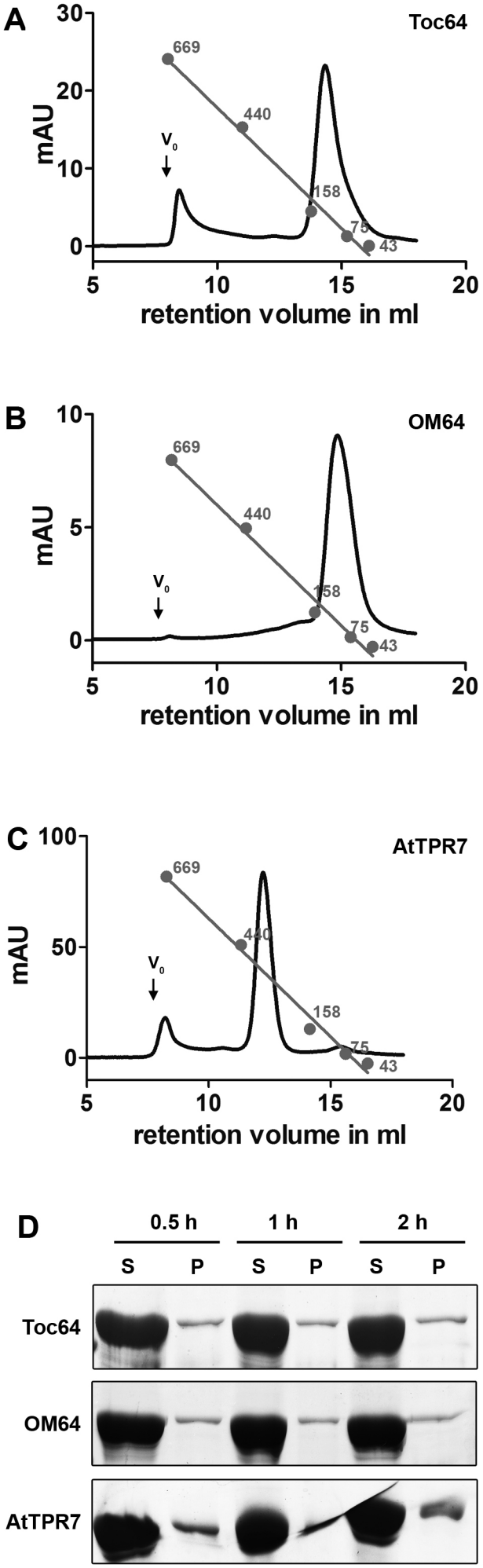

Figure 1

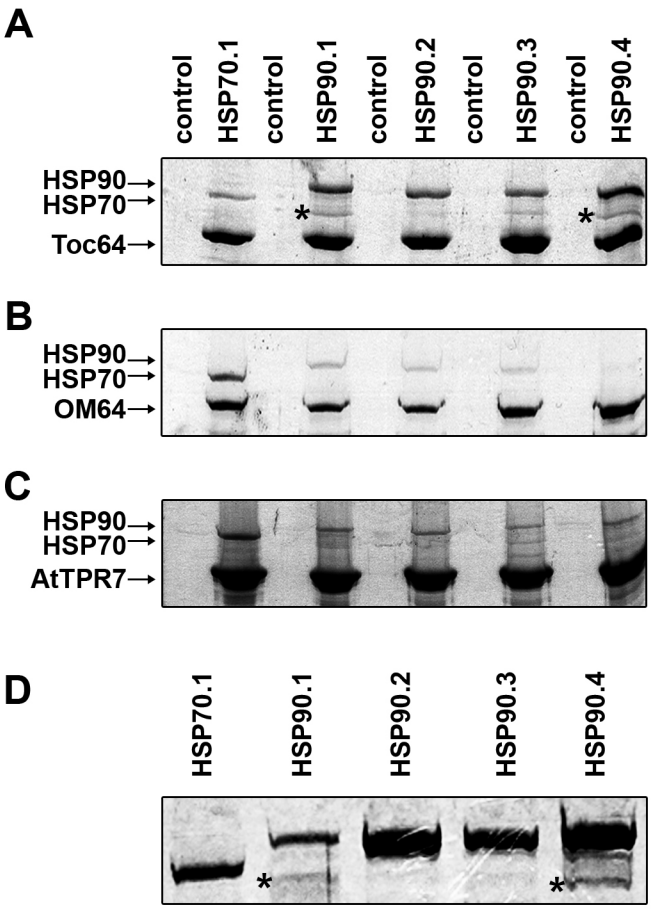

Figure 2

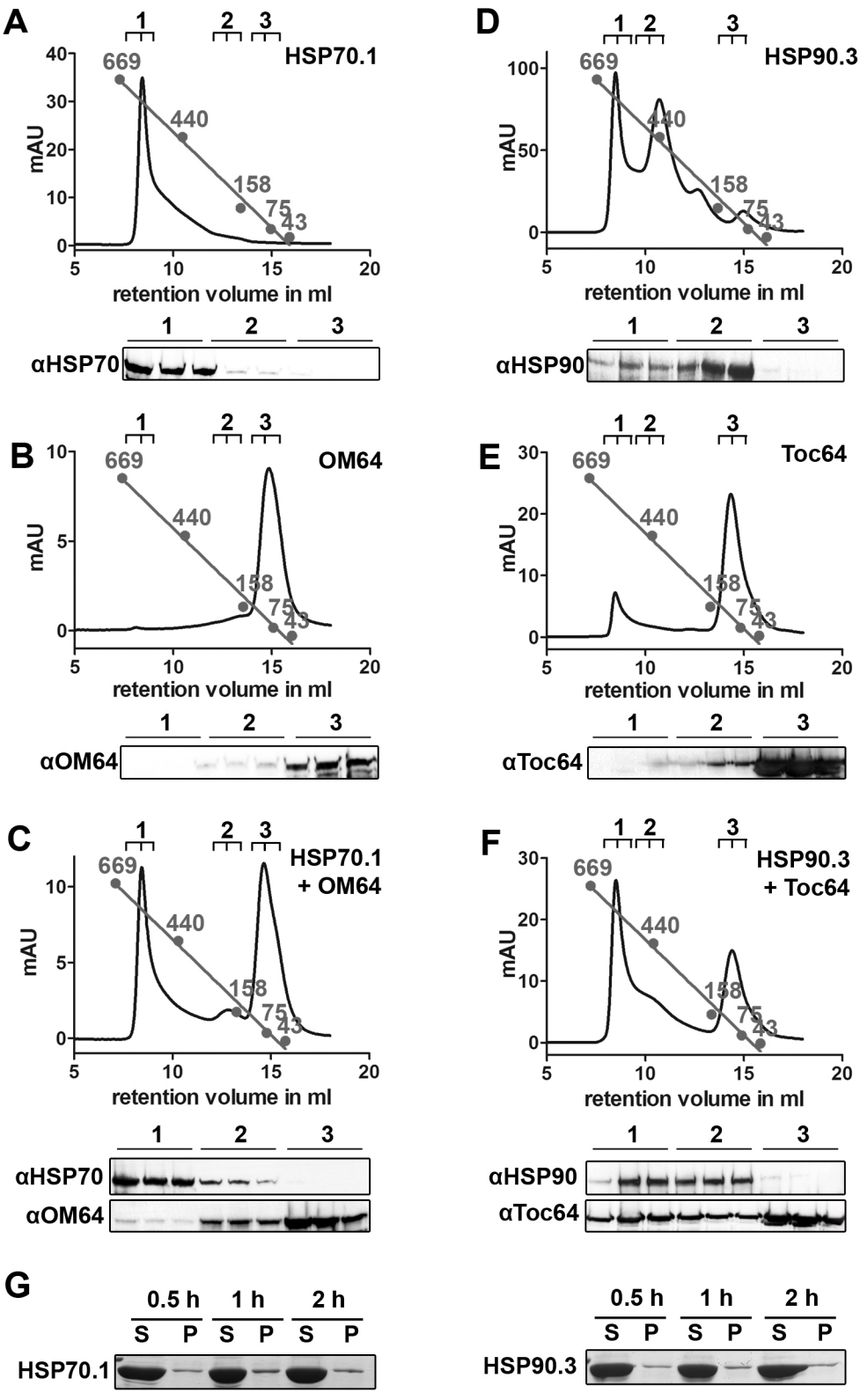

Figure 3

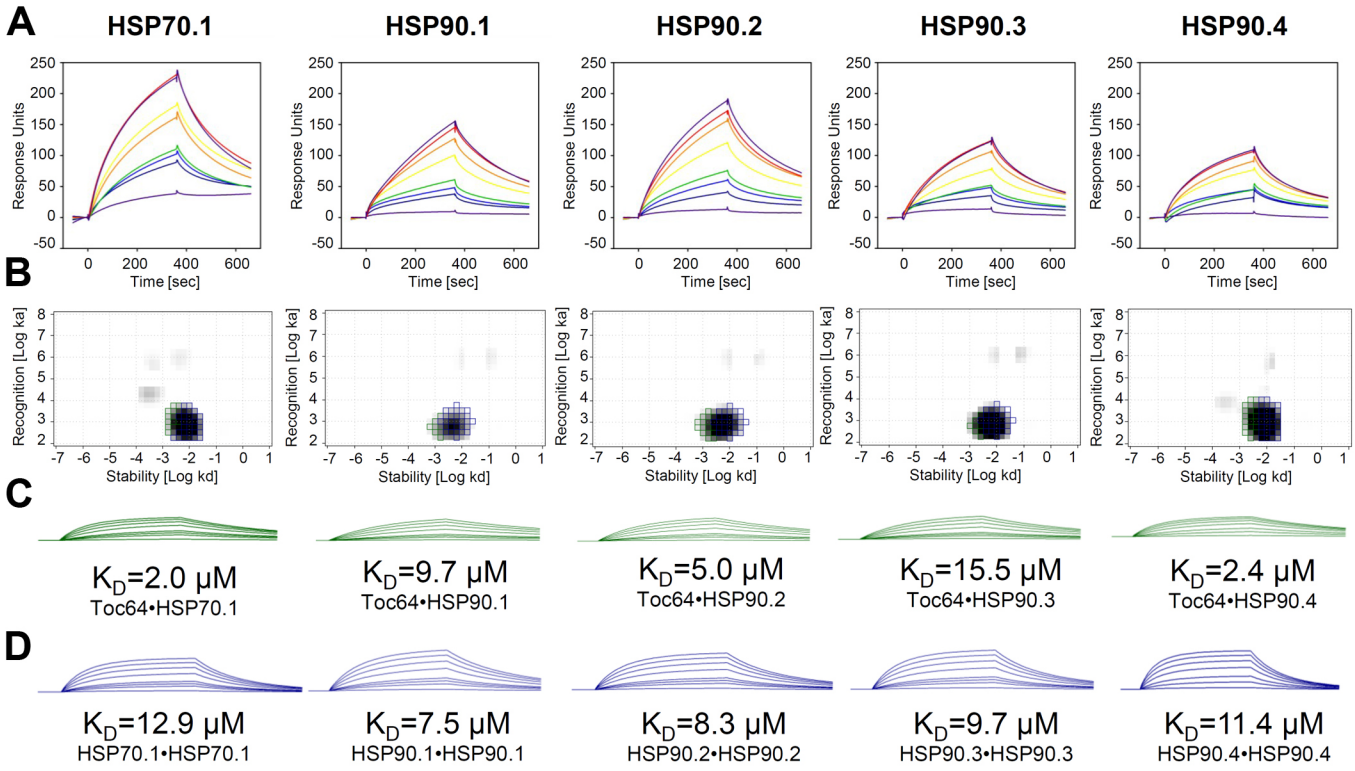

Figure 4

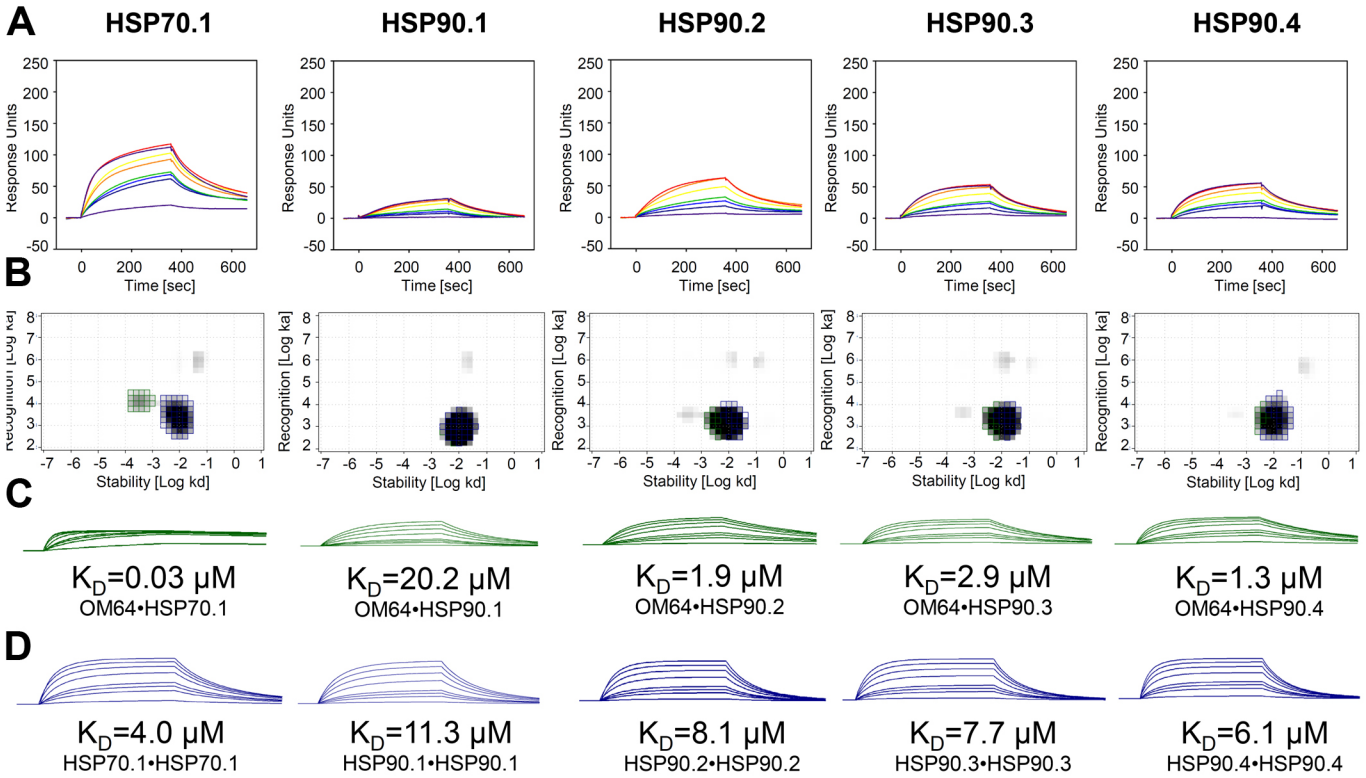

Figure 5

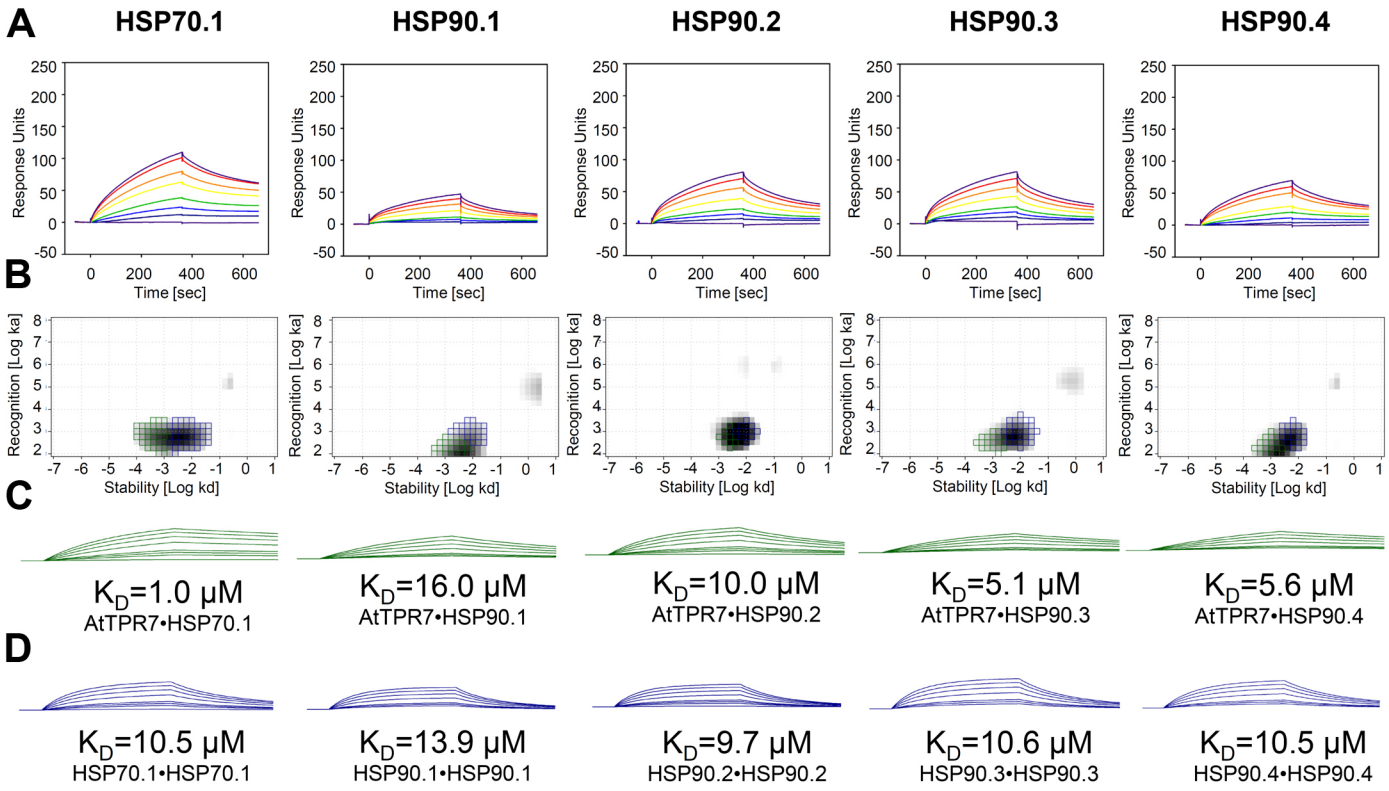

Figure 6

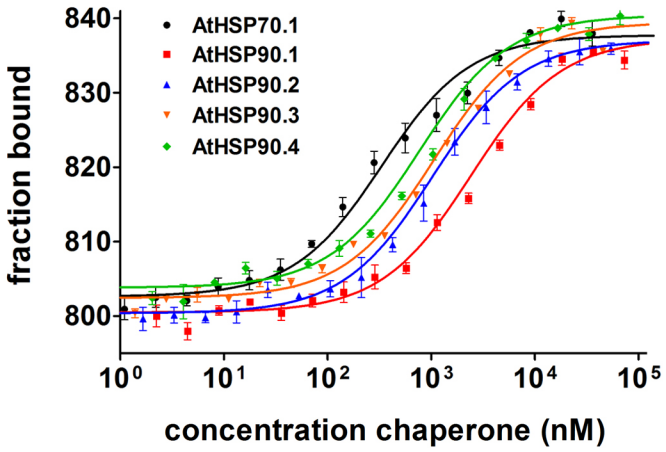

Figure 7

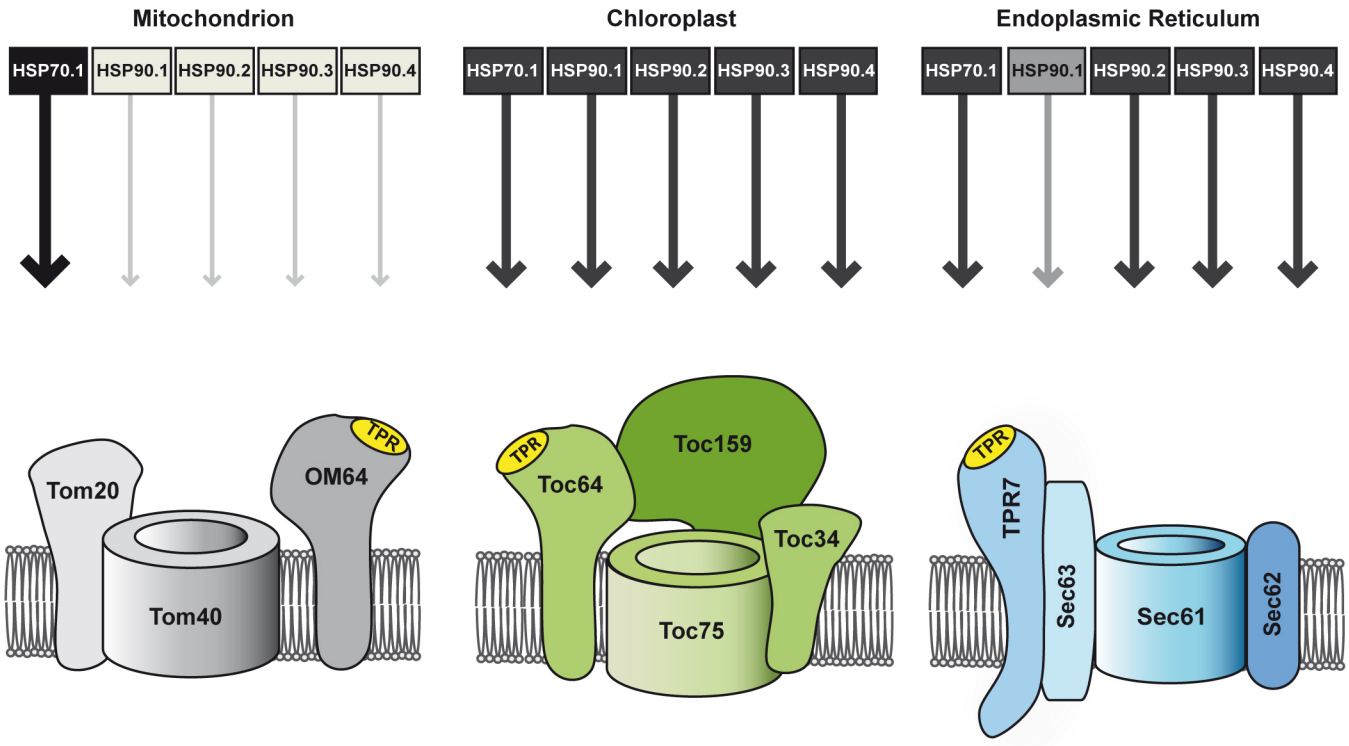

Figure 8

Figure 9

8 Discussion

In this study AtTPR7 was identified as a novel TPR domain containing docking protein localized at the ER membrane in *Arabidopsis*, in addition to Toc64 in the outer envelope of chloroplast and OM64 in the outer membrane of mitochondria. AtTPR7 interacts with the Sec translocon and has a potential function during post-translational translocation into the ER in *Arabidopsis*. Investigation of chaperone binding to the three TPR domain containing docking proteins revealed that mitochondrial preproteins might preferentially bind to HSP70 during targeting to the mitochondria whereas chloroplast preproteins might be delivered by HSP90 to the chloroplast. Furthermore, AtTPR7 as well as OM64 show weaker binding to the heat shock induced chaperone isoform indicating a predominant role of the constitutively expressed isoforms during preprotein targeting through the cytosol.

AtTPR7 contains a C-terminal transmembrane domain and three TPR motifs which reach from amino acid 102 to 212 forming a so called clamp-type TPR domain. Clamp-type TPR domains bind specifically to the conserved C-terminal EEVD motif of cytosolic HSP70 and HSP90 chaperones (Schlegel et al., 2007). The TPR domain is facing the cytosol thus allowing an interaction with cytosolic chaperones during preprotein transport. The localization of AtTPR7 at the ER membrane was proven by various experiments, since previous data suggested AtTPR7 to reside in the chloroplast membrane (von Loeffelholz et al., 2011). Additional experiments to those presented by von Loeffelholz et al. were performed to prove the localization at the ER membrane. On the one hand, the specificity of the antibody against full length AtTPR7 was shown with a T-DNA insertion mutant and immuno blot analysis of different cellular compartments revealed AtTPR7 to reside at the ER of *Arabidopsis* wild type leaves. On the other hand, AtTPR7 shifted in a magnesium shift assay widely used for indication of ER localization. Thereby, the chelating agent EDTA binds to magnesium ions which are necessary for the ribosomal subunits to associate with the ER membrane. Dissociation of the ribosomal subunits leads to a shift of ER membranes in a sucrose density gradient to lower density fractions detectable with antiserum against ER resident proteins. Toc64 concentrated in lower density fractions than AtTPR7 and showed differential behavior in the magnesium shift assay. Moreover, *in vitro* as well as *in vivo* studies revealed AtTPR7 as part of the Sec translocon. AtTPR7 co-purified with Sec63 as well as Sec62 in pull down experiments and AtTPR7 is co-migrating with Sec63 in blue native polyacrylamide gel electrophoresis. Moreover, AtTPR7 is in

close proximity to Sec63 as well as Sec62 *in vivo*, demonstrated by bimolecular fluorescence complementation (BiFC) experiments. Therefore, AtTPR7 can be considered to be part of the Sec post-translocon, comprising the major channel component Sec61, Sec63 (AtERdj2A) and Sec62, as it is found in yeast (**Figure 7**) (Harada et al., 2011). TPR7 is found in all plant species from the unicellular green algae to monocotyledonous and dicotyledonous plants but no homologs were identified in the mammalian or yeast genome.

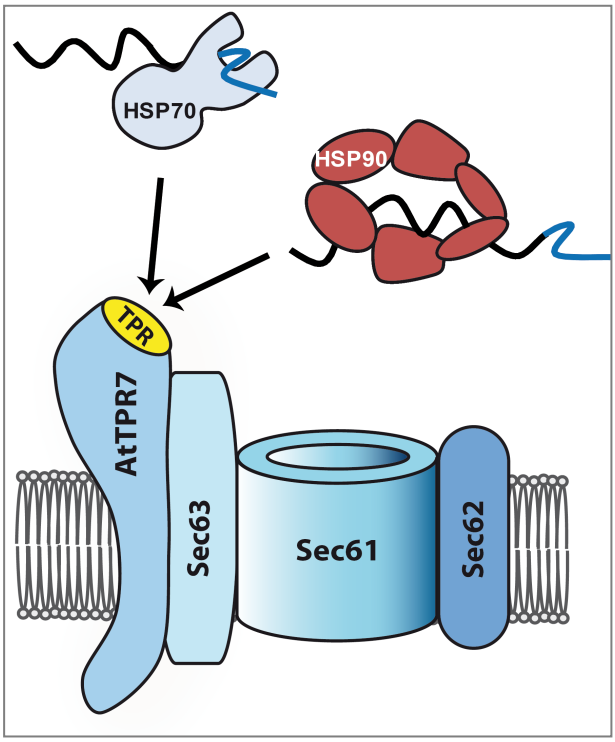

Figure 7: The Sec post-translocon at the plant ER membrane.

Sec61 is the major channel component of the Sec translocon at the ER membrane. AtTPR7 associates with the Sec translocon via Sec63 as well as Sec62 and has a cytosolic exposed TPR domain that interacts with HSP70 and HSP90 which may be involved in preprotein delivery during post-translational import into the ER.

The yeast post-translocon contains two additional components, Sec71p and Sec72p, whereas Sec71p serves as membrane anchor for the TPR domain containing docking protein Sec72p. These two components, as well as Sec62 are only associated to the Sec61 conducting channel during post-translational import into the yeast ER (Plath et al., 1998). Deletion of Sec71p leads to fast degradation of Sec72p (Feldheim and Schekman, 1994). Homologs for these proteins cannot be found in mammals or plants. Deletion of Sec71p and subsequent degradation of Sec72p leads to a translocation defect of specific preproteins, for example preprotoxin, which has to be processed in the cell during its way through the secretory system to become functional (Breinig et al., 2006). The yeast Sec71p mutant line is no longer able to transport preprotoxin into the ER and therefore no processed, secreted toxin can be detected in the medium. Full length AtTPR7 is able to complement this phenotype by inserting into the yeast ER membrane. The TPR domain of AtTPR7 seems to fulfill the function of Sec72p while the

transmembrane domain is compensating for Sec71p further indicating a function of AtTPR7 in post-translational import of preproteins into the ER in plants, thereby functionally replacing yeast Sec71p and Sec72p in plants.

TPR domain containing docking proteins are found in all organisms and cellular compartments as parts of translocon complexes at the organellar surfaces, playing a role during post-translational preprotein import (Kriechbaumer et al., 2012). In plants, Toc64 at the outer envelope of chloroplasts and OM64 at the outer membrane of mitochondria are highly homolog clamp-type TPR domain containing docking proteins. Previous data demonstrated Toc64 to bind to HSP70 as well as HSP90 during preprotein delivery to the chloroplast (Qbadou et al., 2006). OM64 seems to functionally replace Tom70 in plants, but chaperone interaction has not been investigated to date. AtTPR7 presents a third TPR domain containing docking protein next to Toc64 and OM64 in plants. AtTPR7 appears to functionally replace yeast Sec71p and Sec72p and is therefore believed to be involved in post-translational import into the plant ER. The AtTPR7 T-DNA insertion mutant shows no visible phenotype under all kinds of growth conditions. This goes along with previous data, demonstrating that the Toc64 as well as the OM64 mutant lines do not have an obvious phenotype, although, import of specific mitochondrial preproteins seem to be impaired in the OM64 mutant (Aronsson et al., 2007; Chew et al., 2004; Qbadou et al., 2007). Unfortunately, no preproteins for post-translational import into the plant ER were identified so far and no import competent microsomes could be established from *Arabidopsis* to date. Therefore, characterization of the AtTPR7 T-DNA insertion mutant with regards to the translocation efficiency of post-translationally imported preproteins remains to be resolved.

As mentioned above, previous data demonstrate the involvement of HSP70 and HSP90 in preprotein transport to the chloroplast receptor protein Toc64 (Qbadou et al., 2006). HSP90 mediates delivery of preproteins to the chloroplast although the recognition of HSP90 by Toc64 is not essential for cell survival. It seems that HSP90 guided preproteins can also be directly recognized by Toc34, since plants lacking Toc64 show no decreased import rates of selected preproteins (Aronsson et al., 2007). In this study a large number of chloroplast preproteins was tested for binding affinity to HSP90, HSP70 and 14-3-3. The 14-3-3 guidance complex, comprising a 14-3-3 dimer and a HSP70 with a total size of ~200 kDa, is binding to phosphorylated transit peptides of chloroplast preproteins and delivers those to the receptor

protein Toc34 which directly recognizes the preproteins (May and Soll, 2000). On the other hand a large set of preproteins was found to bind to HSP70 as well as HSP90 in the cytosol. In contrast to 14-3-3, the transit peptide as well as the mature part of the protein is necessary for HSP90 binding. Previous data assume that the HSP90 guidance complex has a size of ~350 kDa and consists of at least HSP70 and a HSP90 dimer (Qbadou et al., 2006). To investigate further subunits of the guidance complex, size exclusion chromatography was performed with *in vitro* translated HSP90 preproteins in wheat germ lysate. The radiolabeled preprotein could be detected in fractions of 200 to 500 kDa size. According to the HSP90 cycle in mammals (Rohl et al., 2013), it is likely that different assembly states of guidance complex components exist during preprotein delivery to the chloroplast. Mass spectrometry analyses of proteins co-immunoprecipitated with HSP90 antibodies identified two co-chaperones, HOP as well as the FK506 binding protein 73 (FKBP73). FKBP73 is a PPIase like the remodeling co-chaperones FKBP51 and FKBP52 in the mammalian HSP90 cycle (Rohl et al., 2013). Both co-chaperones bind to freshly synthesized preproteins in wheat germ lysate. HOP as well as FKBP73 contain TPR motifs forming a clamp-type domain responsible for HSP90 interaction (Kurek et al., 2002). Homologs of HOP can be identified in several plant species, although no client proteins have been identified *in vivo* in plants to date (Zhang et al., 2003). Furthermore, the function of wheat FKBP73 was only demonstrated *in vitro* using citrate synthase as substrate, however, *in vivo* no client protein has been found so far (Kurek et al., 2002). In summary, these data revealed a large number of preproteins associating with HSP90 and HSP70, next to the guidance complex containing 14-3-3 and HSP70. Furthermore, not only HOP but also the PPIase FKBP73 were identified as co-chaperones of HSP90, involved in delivery of preproteins to the chloroplast. Therefore, chloroplast preproteins make a new substrate class for HSP90 in plants.

In yeast and mammals mitochondrial carrier proteins form an already well known substrate class for HSP70 and HSP90 in the cytosol. Yeast Tom70 at the outer membrane of mitochondria recognizes HSP70 bound mitochondrial preproteins via its clamp-type TPR domain whereas in mammals additional HSP90 binding was shown (Young et al., 2003). OM64 seems to functionally replace Tom70 in plants, although chaperone binding to OM64 was not investigated to date (Chew et al., 2004). In this study AtTPR7 at the ER membrane was demonstrated to bind to HSP70 and HSP90 specifically via its TPR domain (**Figure 8**). Therefore preproteins might already be sorted within the cytosol maybe with the help of cytosolic

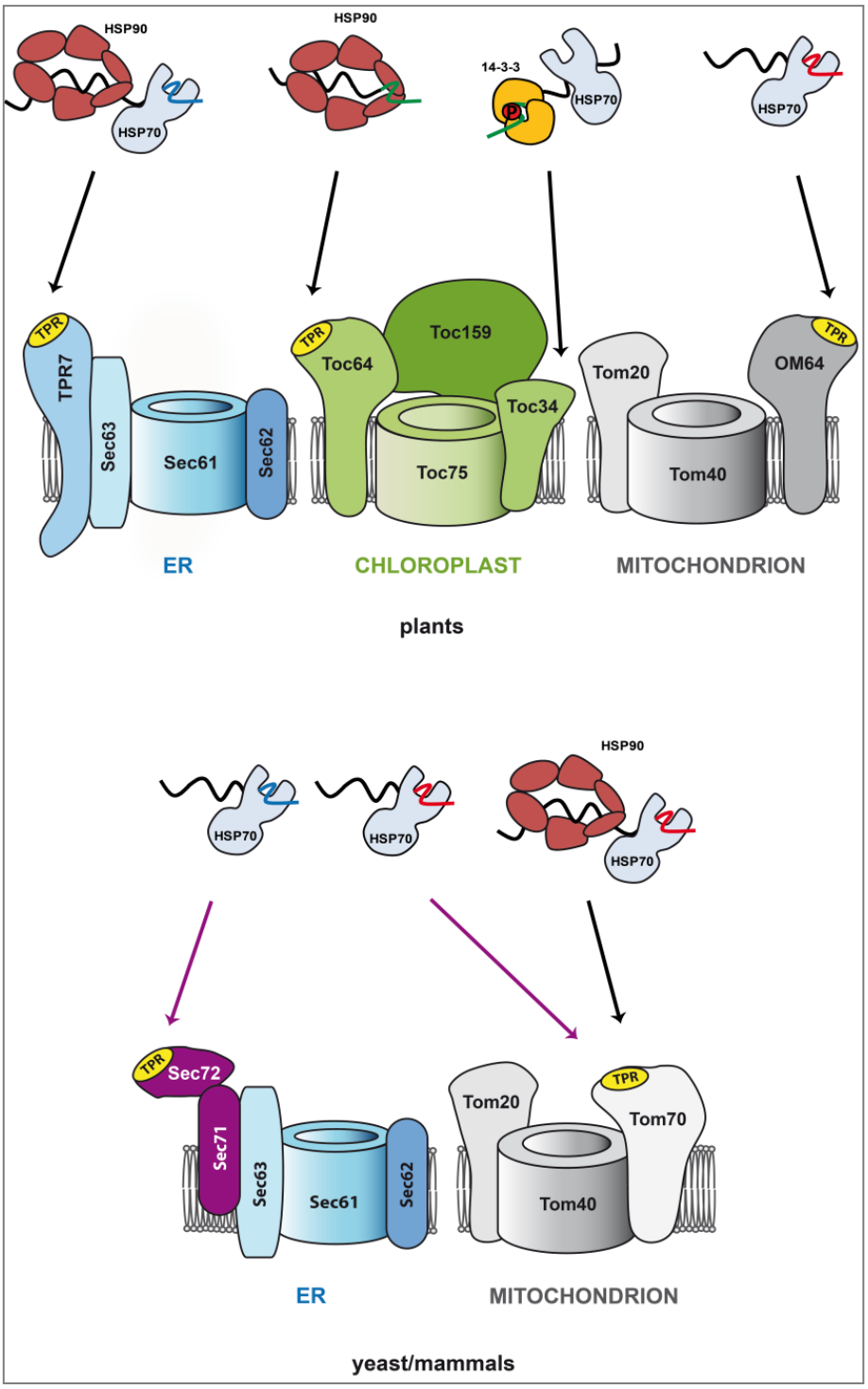

Figure 8: Chaperones involved in post-translational preprotein targeting to organelles.

Preproteins are fully synthesized on cytosolic ribosomes and are targeted to the respective organelles by cytosolic chaperones. In plants chloroplast preproteins can be transported to the TOC complex either by HSP90 or by HSP70 in concert with 14-3-3 proteins in case of phosphorylated presequences. HSP90 bound preproteins are indirectly recognized by Toc64 whereas HSP70/14-3-3 bound preproteins are directly bound by Toc34. Plant mitochondrial preproteins can be delivered to the TOM complex by HSP70 which binds to the receptor protein OM64 whereas ER preproteins seem to bind to both, HSP70 and HSP90, since both chaperones interact with the receptor protein AtTPR7 of the Sec translocon.
In yeast mitochondrial preproteins seem to be transported to the receptor protein Tom70 by HSP70, in mammals additionally by HSP90. Delivery of preproteins to the Sec translocon is only investigated in yeast, where HSP70 bound preproteins are recognized by the receptor protein Sec72. Sec72 and its membrane anchor Sec71 can only be found in yeast (purple color).

chaperones. Chaperones bind to preproteins in the cytosol to keep them in an import competent state and to prevent aggregation due to molecular crowding. Furthermore, the chaperones facilitate interaction with the TPR domain containing docking proteins at the translocon complexes, thereby enhancing the import efficiency of the bound preproteins into the organelle (Lister et al., 2007; Qbadou et al., 2006). Four isoforms of HSP90 as well as five HSP70 isoforms are present in the *Arabidopsis* cytosol (Krishna and Gloor, 2001; Lin et al., 2001). HSP70 is known to bind hydrophobic stretches of almost all proteins in a very unspecific manner (Zhang and Glaser, 2002), therefore the focus in this study was laid on the HSP90 isoforms as supporting factors during preprotein sorting in the cytosol. HSP90.1 is the most heat shock induced isoform and shows a sequence identity of 87 % to the other isoforms. HSP90.2, HSP90.3 and HSP90.4 are constitutively expressed and have a sequence identity of 96 % to each other (Cha et al., 2013; Krishna and Gloor, 2001). The potential of the three TPR domain containing docking proteins Toc64, OM64 and AtTPR7 to bind to HSP70 as well as to HSP90 was not only demonstrated by *in vitro* pull down experiments but also in case of AtTPR7 and Toc64 by *in vivo* BiFC interaction studies. However, no quantitative conclusions can be drawn from these data wherefore various biochemical, biophysical and computational methods were applied to calculate binding affinities for each interaction event. Surface plasmon resonance (SPR) spectroscopy revealed sensorgrams which did not follow a final saturation as expected for a typical monovalent interaction. The sensorgrams were a sum of two different interactions, on the one hand the interaction between the chaperones and the TPR domain containing docking proteins and on the other hand the chaperone oligomerization (Kadota and Shirasu, 2012; Thompson et al., 2012). Interaction Map analysis was applied as computational approach to separate the different binding events (Barta et al., 2011). The underlying algorithm splits the experimental SPR data into several theoretical monovalent binding events indicated as single spots in a graphical presentation. Chaperone oligomerization was assumed to be independent of the presence of receptor and thereby, we were able to assign each binding event a specific spot. Calculated K_D values by this computational approach were further verified by using microscale thermophoresis (MST). The K_D values show the same tendency with both methods, SPR and MST, whereas slight differences might have occurred due to the different underlying principles. While MST measures a steady state equilibrium of an interaction, SPR uses a fast exchange of analyte and buffer leading to a more precise detection of association

and dissociation rates. Both methods are highly comparable and the K_D values calculated by the interaction map analysis seem to be highly reliable.

OM64 at the outer membrane of mitochondria and Toc64 at the outer envelope of chloroplasts are highly homolog proteins of the same protein family. Both proteins show an overall sequence identity of 51 %, which is even higher within the TPR domain (68 %). The data revealed that Toc64 bound to HSP70 as well as to the HSP90 isoforms in a similar manner (**Figure 9**). The K_D values for all Toc64 chaperone interactions were in the micromolar range. On the other hand OM64 bound to HSP70 in a much higher extent than to the HSP90 isoforms. The K_D values calculated for the OM64 chaperone interactions revealed a 100 times higher affinity of HSP70 to OM64 in the nanomolar range. Furthermore, binding of the heat shock induced isoform HSP90.1 to OM64 was weaker than binding of the constitutively expressed HSP90 isoforms. In an *in vivo* situation with all HSP70 as well as HSP90 isoforms present in the cytosol it is likely that OM64 binds preferentially to HSP70 bound mitochondrial preproteins. Considering the high sequence identity between Toc64 and OM64 the different binding behavior is very surprising. However, this favors a model where mitochondrial preproteins are preferentially delivered by HSP70 to OM64 whereas, in contrast, Toc64 at the outer envelope of chloroplasts seems to bind preferentially to HSP90 bound preproteins. Since no HSP90 binding plant mitochondrial preproteins were identified to date HSP90 involvement in mitochondrial preprotein delivery was only shown in mammals so far (Young et al., 2003) (**Figure 8**). AtTPR7 at the ER membrane showed a binding potential to HSP70 as well as HSP90, although previous data could not detect HSP90 binding to AtTPR7 (Kriechbaumer et al., 2011; von Loeffelholz et al., 2011) (AtTPR7 is designated as OEP61 in that case). For that reason we investigated the K_D values not only by SPR but also by MST. Both methods revealed a binding potential of AtTPR7 to all tested chaperones in the micromolar range. Although HSP70 bound with a slightly higher affinity, binding to the HSP90 isoforms is also likely to occur *in vivo*. Interestingly, the binding affinity of the heat shock induced isoform HSP90.1 was 10 times lower compared to the constitutively expressed isoforms. The same was true for HSP90.1 binding to OM64. This leads to the assumption that the constitutively expressed isoforms play a predominant role during preprotein targeting rather than the heat shock induced isoform HSP90.1.

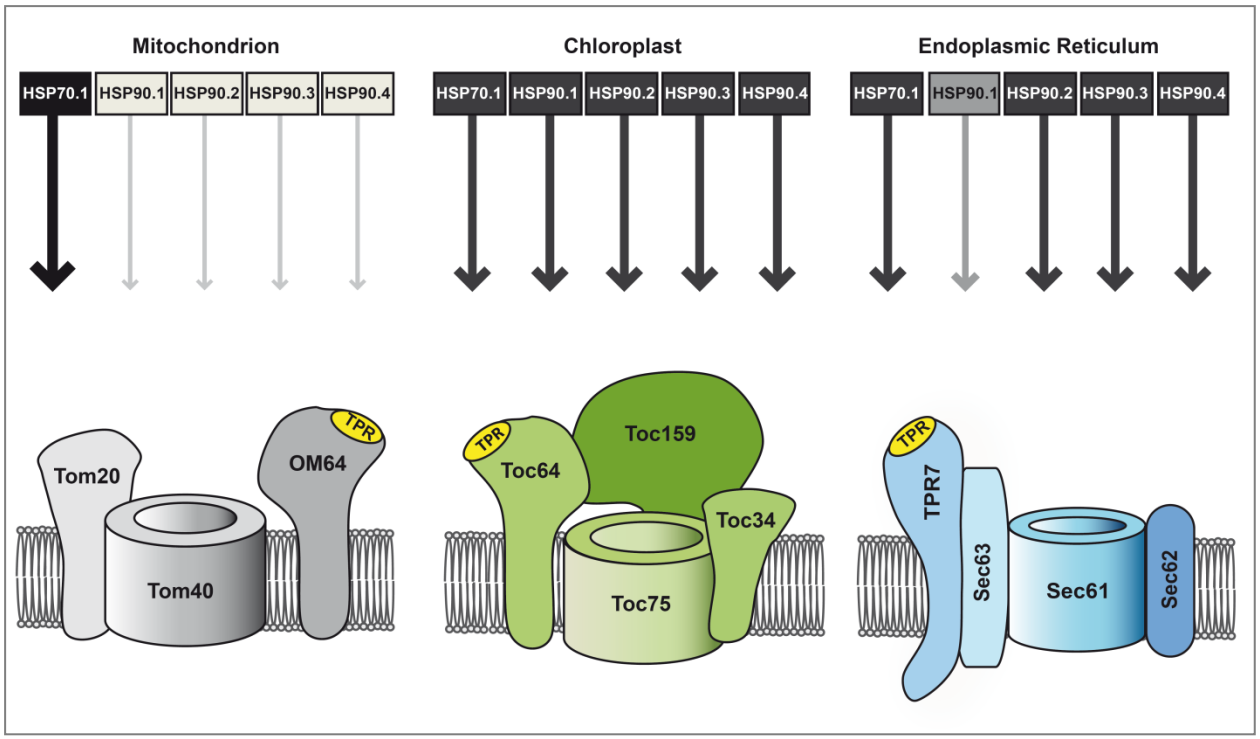

Figure 9: Overview of binding affinities between TPR domain containing docking proteins and cytosolic chaperones.

OM64 at the outer membrane of mitochondria might be associated with the TOM complex and preferentially binds to HSP70. Toc64 at the outer envelope of chloroplasts is dynamically associated to the TOC core complex. Toc64 associates with HSP70 as well as all HSP90 isoforms in the same manner. AtTPR7 at the ER membrane seems to be part of the Sec post-translocon and interacts with both, HSP70 as well as HSP90, although HSP90.1 binding is weaker. Grey scale and arrow thickness indicate binding strengths of chaperones to the respective docking proteins (light - dark grey corresponds to weak - strong binding).

In the Arabidopsis cytosol HSP70 and HSP90 are equally abundant. Unfortunately, *in vivo* it is not possible to distinguish the single chaperone isoforms from each other due to their high sequence identity. This makes it more difficult to connect the *in vitro* results to the actual *in vivo* situation. Nevertheless, the TPR domain containing docking proteins show different binding behavior to the respective full length chaperones and therefore not only the conserved EEVD motif at the C-terminus is influencing the binding properties but also the entire protein, its amino acid composition as well as its higher order structure. To what extent the binding of preproteins is influencing the TPR docking protein-chaperone interaction is still a challenge to investigate. Especially, since binding of the chaperones to the preproteins is another aspect which is not well understood. To date not much is known about the correlation between the signal sequences within preproteins and chaperone binding and to what extent this might influence the specificity of targeting. However, it is suggested that the chaperone-preprotein interaction occurs in a specific manner next to the TPR docking protein-chaperone interaction and therefore might have an additional regulatory function during the sorting process.

Although, the N-terminal targeting signals of chloroplast and mitochondrial preproteins have an overall positive charge and tend to form amphiphilic alpha helices (Bruce, 2000; Huang et al., 2009) the amino acid composition and the length are highly variable. Therefore recognition of a specific sequence motif by the molecular chaperones is very unlikely. Hence, the secondary structure of the targeting signal might influence the sorting process. Slight differences of the amino acid composition between chloroplast and mitochondrial targeting signals might be sufficient for proper targeting in some cases but also other factors like the receptors at the translocon complexes can influence the sorting process. The situation is getting even more complicated since an increasing number of proteins is found to be dual-targeted (Carrie et al., 2009). Dual targeting of preproteins is an aspect where little is known about the mechanism and the specificity of the targeting signal. In plants preproteins are known to be dual-targeted to chloroplasts and peroxisomes (Sapir-Mir et al., 2008), to chloroplasts and the nucleus (Schwacke et al., 2007) and to chloroplasts and the endoplasmic reticulum (Levitan et al., 2005) but most frequently dual targeting occurs to chloroplasts and mitochondria. One translation product can be dual-targeted in two ways, on the one hand by carrying two targeting signals on different ends of the protein and on the other hand by using an ambiguous targeting signal which targets the protein to two organelles. The ambiguous targeting signal is rather similar to a chloroplast and mitochondrial signal sequence with no significant differences classifying it as dual-targeted (Pujol et al., 2007). Furthermore, there is no direct evidence that dual-targeted preproteins are actively sorted, however, phosphorylation of a specific sequence motif might influence the targeting process (Martin et al., 2006). This might be similar to chloroplast preproteins where phosphorylation of the transit peptide leads to subsequent binding of the 14-3-3/HSP70 guidance complex within the transit peptide (Waegemann and Soll, 1996). Moreover, in mammals a 14-3-3 protein is involved in preproteins targeting to mitochondria. The mitochondrial import stimulation factor (MSF), a member of the 14-3-3 protein family, binds to basic amino acid residues in the mitochondrial presequence which might also be phosphorylated (Komiya et al., 1994). Since phosphorylation of mitochondrial preproteins is not described in plants so far phosphorylation might be one prerequisite for transport of dual-targeted preproteins to chloroplasts.

In addition, many chloroplast preproteins are known to interact with the HSP70/HSP90 guidance complex. Thereby, HSP90 needs the full length protein for binding rather than the transit peptide alone. Furthermore, mitochondrial carrier proteins are a protein class known to

bind to HSP70 and HSP90 in the cytosol (de Marcos-Lousa et al., 2006; Young et al., 2003). On the one hand some carrier proteins carry their targeting signal as N-terminal presequence, whereas on the other hand many other carrier proteins do not contain an N-terminal presequence but already have specific signals within their native structure of six transmembrane helices (Zara et al., 2009). The targeting signals can be highly variable in length and amino acid composition and therefore might influence import efficiency in different ways. For some carrier proteins the N-terminal presequence provides the binding site for HSP70 whereas HSP90 binds mainly in the mature part of the protein. Thereby HSP70 is necessary for efficient targeting while HSP90 binding is important to prevent aggregation of the protein (Zara et al., 2009). On the other hand some carrier preproteins do not provide a chaperone binding site within their presequence. In this case HSP70 and HSP90 bind within the mature part at a similar level to mediate targeting. Many other carrier proteins which do not contain an N-terminal presequence carry internal binding sites for HSP70 and HSP90 to support the import into the inner membrane of mitochondria (Bhangoo et al., 2007). Since in plants OM64 at the outer membrane of mitochondria seems to bind mainly to HSP70 whereas Toc64 at the outer envelope of chloroplasts might preferentially bind to HSP90, selective chaperone binding might be another aspect influencing the targeting process of dual-targeted preproteins.

Like the mitochondrial and chloroplast targeting signals the N-terminal signal peptides of ER luminal proteins have only little restrictions referring to the amino acid sequence and length of the sequence (Nielsen et al., 1997). Overall the signal peptide forms an alpha helical conformation which is necessary to fulfill its function as an ER targeting signal (McKnight et al., 1989). Most ER proteins are co-translationally transported into the ER, however, small secretory proteins were described to enter the ER post-translationally assisted by the protein calmodulin which binds selectively to the N-terminal signal peptide (Shao and Hegde, 2011). Although HSP70 binding to the receptor protein Sec72p was demonstrated in yeast (Feldheim and Schekman, 1994) nothing is known about how, why and where HSP70 binds to ER preproteins and which role HSP90 plays within the post-translational translocation pathway.

Taken together, only little is known about the role of molecular chaperones, especially HSP70 and HSP90, during the targeting process of preproteins to various organelles. Since post-translational preprotein targeting and sorting in the cytosol can be regulated at several distinct steps it is a fundamental question how the targeting mechanisms were established during

evolution and how organellar biogenesis and therefore cellular activity is maintained. Since it is known that the sequence conservation between the respective targeting signals is not very high and therefore cannot be the only prerequisite for proper targeting it is highly intriguing to further investigate the involvement of HSP70 and HSP90 as well as the TPR domain containing docking proteins at the organellar membranes in more detail. Future analyses, especially solving the crystal structure of the TPR domains of the receptor proteins, will give us more details about how the discrimination mechanism is achieved and which role the TPR domain containing docking proteins as well as the chaperones play in the process of protein sorting in the plant cell.

9 References

Abe, Y., T. Shodai, T. Muto, K. Mihara, H. Torii, S. Nishikawa, T. Endo, and D. Kohda. 2000. Structural basis of presequence recognition by the mitochondrial protein import receptor Tom20. *Cell*. 100:551-560.

Aronsson, H., P. Boij, R. Patel, A. Wardle, M. Topel, and P. Jarvis. 2007. Toc64/OEP64 is not essential for the efficient import of proteins into chloroplasts in Arabidopsis thaliana. *Plant J*. 52:53-68.

Ast, T., G. Cohen, and M. Schuldiner. 2013. A network of cytosolic factors targets SRP-independent proteins to the endoplasmic reticulum. *Cell*. 152:1134-1145.

Barta, P., H. Bjorkelund, and K. Andersson. 2011. Circumventing the requirement of binding saturation for receptor quantification using interaction kinetic extrapolation. *Nucl Med Commun*. 32:863-867.

Becker, T., M. Jelic, A. Vojta, A. Radunz, J. Soll, and E. Schleiff. 2004. Preprotein recognition by the Toc complex. *EMBO J*. 23:520-530.

Bhangoo, M.K., S. Tzankov, A.C. Fan, K. Dejgaard, D.Y. Thomas, and J.C. Young. 2007. Multiple 40-kDa heat-shock protein chaperones function in Tom70-dependent mitochondrial import. *Mol Biol Cell*. 18:3414-3428.

Bose, S., T. Weikl, H. Bugl, and J. Buchner. 1996. Chaperone function of Hsp90-associated proteins. *Science*. 274:1715-1717.

Bracher, A., and F.U. Hartl. 2006. Hsp90 structure: when two ends meet. *Nat Struct Mol Biol*. 13:478-480.

Breinig, F., T. Sendzik, K. Eisfeld, and M.J. Schmitt. 2006. Dissecting toxin immunity in virus-infected killer yeast uncovers an intrinsic strategy of self-protection. *Proc Natl Acad Sci U S A*. 103:3810-3815.

Brix, J., K. Dietmeier, and N. Pfanner. 1997. Differential recognition of preproteins by the purified cytosolic domains of the mitochondrial import receptors Tom20, Tom22, and Tom70. *J Biol Chem*. 272:20730-20735.

Bruce, B.D. 2000. Chloroplast transit peptides: structure, function and evolution. *Trends Cell Biol*. 10:440-447.

Carrie, C., E. Giraud, and J. Whelan. 2009. Protein transport in organelles: Dual targeting of proteins to mitochondria and chloroplasts. *FEBS J*. 276:1187-1195.

Cha, J.Y., G. Ahn, J.Y. Kim, S.B. Kang, M.R. Kim, M. Su'udi, W.Y. Kim, and D. Son. 2013. Structural and functional differences of cytosolic 90-kDa heat-shock proteins (Hsp90s) in Arabidopsis thaliana. *Plant Physiol Biochem*. 70C:368-373.

Chacinska, A., C.M. Koehler, D. Milenkovic, T. Lithgow, and N. Pfanner. 2009. Importing mitochondrial proteins: machineries and mechanisms. *Cell*. 138:628-644.

Chan, N.C., V.A. Likic, R.F. Waller, T.D. Mulhern, and T. Lithgow. 2006. The C-terminal TPR domain of Tom70 defines a family of mitochondrial protein import receptors found only in animals and fungi. *J Mol Biol*. 358:1010-1022.

Chew, O., R. Lister, S. Qbadou, J.L. Heazlewood, J. Soll, E. Schleiff, A.H. Millar, and J. Whelan. 2004. A plant outer mitochondrial membrane protein with high amino acid sequence identity to a chloroplast protein import receptor. *FEBS Lett*. 557:109-114.

Constan, D., R. Patel, K. Keegstra, and P. Jarvis. 2004. An outer envelope membrane component of the plastid protein import apparatus plays an essential role in Arabidopsis. *Plant J*. 38:93-106.

Dalbey, R.E., and G. Von Heijne. 1992. Signal peptidases in prokaryotes and eukaryotes--a new protease family. *Trends Biochem Sci*. 17:474-478.

de Marcos-Lousa, C., D.P. Sideris, and K. Tokatlidis. 2006. Translocation of mitochondrial inner-membrane proteins: conformation matters. *Trends Biochem Sci*. 31:259-267.

Deshaies, R.J., and R. Schekman. 1989. SEC62 encodes a putative membrane protein required for protein translocation into the yeast endoplasmic reticulum. *J Cell Biol*. 109:2653-2664.

Dittmar, K.D., D.R. Demady, L.F. Stancato, P. Krishna, and W.B. Pratt. 1997. Folding of the glucocorticoid receptor by the heat shock protein (hsp) 90-based chaperone machinery. The role of p23 is to stabilize receptor.hsp90 heterocomplexes formed by hsp90.p60.hsp70. *J Biol Chem*. 272:21213-21220.

Dunnwald, M., A. Varshavsky, and N. Johnsson. 1999. Detection of transient in vivo interactions between substrate and transporter during protein translocation into the endoplasmic reticulum. *Mol Biol Cell*. 10:329-344.

Fang, H., and N. Green. 1994. Nonlethal sec71-1 and sec72-1 mutations eliminate proteins associated with the Sec63p-BiP complex from S. cerevisiae. *Mol Biol Cell*. 5:933-942.

Faou, P., and N.J. Hoogenraad. 2012. Tom34: a cytosolic cochaperone of the Hsp90/Hsp70 protein complex involved in mitochondrial protein import. *Biochim Biophys Acta*. 1823:348-357.

Feldheim, D., and R. Schekman. 1994. Sec72p contributes to the selective recognition of signal peptides by the secretory polypeptide translocation complex. *J Cell Biol*. 126:935-943.

Fellerer, C., R. Schweiger, K. Schongruber, J. Soll, and S. Schwenkert. 2011. Cytosolic HSP90 cochaperones HOP and FKBP interact with freshly synthesized chloroplast preproteins of Arabidopsis. *Mol Plant*. 4:1133-1145.

Harada, Y., H. Li, J.S. Wall, and W.J. Lennarz. 2011. Structural studies and the assembly of the heptameric post-translational translocon complex. *J Biol Chem*. 286:2956-2965.

Hirsch, S., E. Muckel, F. Heemeyer, G. von Heijne, and J. Soll. 1994. A receptor component of the chloroplast protein translocation machinery. *Science*. 266:1989-1992.

Huai, Q., H. Wang, Y. Liu, H.Y. Kim, D. Toft, and H. Ke. 2005. Structures of the N-terminal and middle domains of E. coli Hsp90 and conformation changes upon ADP binding. *Structure*. 13:579-590.

Huang, S., N.L. Taylor, J. Whelan, and A.H. Millar. 2009. Refining the definition of plant mitochondrial presequences through analysis of sorting signals, N-terminal modifications, and cleavage motifs. *Plant Physiol*. 150:1272-1285.

Kadota, Y., and K. Shirasu. 2012. The HSP90 complex of plants. *Biochim Biophys Acta*. 1823:689-697.

Kessler, F., G. Blobel, H.A. Patel, and D.J. Schnell. 1994. Identification of two GTP-binding proteins in the chloroplast protein import machinery. *Science*. 266:1035-1039.

Komiya, T., N. Hachiya, M. Sakaguchi, T. Omura, and K. Mihara. 1994. Recognition of mitochondria-targeting signals by a cytosolic import stimulation factor, MSF. *J Biol Chem*. 269:30893-30897.

Kriechbaumer, V., A. Tsargorodskaya, M.K. Mustafa, T. Vinogradova, J. Lacey, D.P. Smith, B.M. Abell, and A. Nabok. 2011. Study of receptor-chaperone interactions using the optical technique of spectroscopic ellipsometry. *Biophys J*. 101:504-511.

Kriechbaumer, V., O. von Loffelholz, and B.M. Abell. 2012. Chaperone receptors: guiding proteins to intracellular compartments. *Protoplasma*. 249:21-30.

Krishna, P., and G. Gloor. 2001. The Hsp90 family of proteins in Arabidopsis thaliana. *Cell Stress Chaperones*. 6:238-246.

Kurek, I., F. Pirkl, E. Fischer, J. Buchner, and A. Breiman. 2002. Wheat FKBP73 functions in vitro as a molecular chaperone independently of its peptidyl prolyl cis-trans isomerase activity. *Planta*. 215:119-126.

Lakkaraju, A.K., R. Thankappan, C. Mary, J.L. Garrison, J. Taunton, and K. Strub. 2012. Efficient secretion of small proteins in mammalian cells relies on Sec62-dependent posttranslational translocation. *Mol Biol Cell*. 23:2712-2722.

Lee, C.T., C. Graf, F.J. Mayer, S.M. Richter, and M.P. Mayer. 2012. Dynamics of the regulation of Hsp90 by the co-chaperone Sti1. *EMBO J*. 31:1518-1528.

Levitan, A., T. Trebitsh, V. Kiss, Y. Pereg, I. Dangoor, and A. Danon. 2005. Dual targeting of the protein disulfide isomerase RB60 to the chloroplast and the endoplasmic reticulum. *Proc Natl Acad Sci U S A*. 102:6225-6230.

Li, J., J. Soroka, and J. Buchner. 2012. The Hsp90 chaperone machinery: conformational dynamics and regulation by co-chaperones. *Biochim Biophys Acta*. 1823:624-635.

Lin, B.L., J.S. Wang, H.C. Liu, R.W. Chen, Y. Meyer, A. Barakat, and M. Delseny. 2001. Genomic analysis of the Hsp70 superfamily in Arabidopsis thaliana. *Cell Stress Chaperones*. 6:201-208.

Lister, R., C. Carrie, O. Duncan, L.H. Ho, K.A. Howell, M.W. Murcha, and J. Whelan. 2007. Functional definition of outer membrane proteins involved in preprotein import into mitochondria. *Plant Cell*. 19:3739-3759.

Macasev, D., E. Newbigin, J. Whelan, and T. Lithgow. 2000. How do plant mitochondria avoid importing chloroplast proteins? Components of the import apparatus Tom20 and Tom22 from Arabidopsis differ from their fungal counterparts. *Plant Physiol*. 123:811-816.

Martin, T., R. Sharma, C. Sippel, K. Waegemann, J. Soll, and U.C. Vothknecht. 2006. A protein kinase family in Arabidopsis phosphorylates chloroplast precursor proteins. *J Biol Chem*. 281:40216-40223.

Martin, W., and R.G. Herrmann. 1998. Gene transfer from organelles to the nucleus: how much, what happens, and Why? *Plant Physiol*. 118:9-17.

May, T., and J. Soll. 2000. 14-3-3 proteins form a guidance complex with chloroplast precursor proteins in plants. *Plant Cell*. 12:53-64.

McKnight, C.J., M.S. Briggs, and L.M. Gierasch. 1989. Functional and nonfunctional LamB signal sequences can be distinguished by their biophysical properties. *J Biol Chem*. 264:17293-17297.

McLaughlin, S.H., F. Sobott, Z.P. Yao, W. Zhang, P.R. Nielsen, J.G. Grossmann, E.D. Laue, C.V. Robinson, and S.E. Jackson. 2006. The co-chaperone p23 arrests the Hsp90 ATPase cycle to trap client proteins. *J Mol Biol*. 356:746-758.

Meyer, H.A., H. Grau, R. Kraft, S. Kostka, S. Prehn, K.U. Kalies, and E. Hartmann. 2000. Mammalian Sec61 is associated with Sec62 and Sec63. *J Biol Chem*. 275:14550-14557.

Meyer, P., C. Prodromou, C. Liao, B. Hu, S.M. Roe, C.K. Vaughan, I. Vlasic, B. Panaretou, P.W. Piper, and L.H. Pearl. 2004. Structural basis for recruitment of the ATPase activator Aha1 to the Hsp90 chaperone machinery. *EMBO J*. 23:1402-1410.

Moczko, M., B. Ehmann, F. Gartner, A. Honlinger, E. Schafer, and N. Pfanner. 1994. Deletion of the receptor MOM19 strongly impairs import of cleavable preproteins into Saccharomyces cerevisiae mitochondria. *J Biol Chem*. 269:9045-9051.

Muller, L., M.D. de Escauriaza, P. Lajoie, M. Theis, M. Jung, A. Muller, C. Burgard, M. Greiner, E.L. Snapp, J. Dudek, and R. Zimmermann. 2010. Evolutionary gain of function for the ER membrane protein Sec62 from yeast to humans. *Mol Biol Cell*. 21:691-703.

Ng, D.T., J.D. Brown, and P. Walter. 1996. Signal sequences specify the targeting route to the endoplasmic reticulum membrane. *J Cell Biol*. 134:269-278.

Ngosuwan, J., N.M. Wang, K.L. Fung, and W.J. Chirico. 2003. Roles of cytosolic Hsp70 and Hsp40 molecular chaperones in post-translational translocation of presecretory proteins into the endoplasmic reticulum. *J Biol Chem*. 278:7034-7042.

Nielsen, H., J. Engelbrecht, S. Brunak, and G. von Heijne. 1997. Identification of prokaryotic and eukaryotic signal peptides and prediction of their cleavage sites. *Protein Eng*. 10:1-6.

Plath, K., W. Mothes, B.M. Wilkinson, C.J. Stirling, and T.A. Rapoport. 1998. Signal sequence recognition in posttranslational protein transport across the yeast ER membrane. *Cell*. 94:795-807.

Pujol, C., L. Marechal-Drouard, and A.M. Duchene. 2007. How can organellar protein N-terminal sequences be dual targeting signals? In silico analysis and mutagenesis approach. *J Mol Biol*. 369:356-367.

Qbadou, S., T. Becker, T. Bionda, K. Reger, M. Ruprecht, J. Soll, and E. Schleiff. 2007. Toc64--a preprotein-receptor at the outer membrane with bipartide function. *J Mol Biol*. 367:1330-1346.

Qbadou, S., T. Becker, O. Mirus, I. Tews, J. Soll, and E. Schleiff. 2006. The molecular chaperone Hsp90 delivers precursor proteins to the chloroplast import receptor Toc64. *EMBO J*. 25:1836-1847.

Retzlaff, M., F. Hagn, L. Mitschke, M. Hessling, F. Gugel, H. Kessler, K. Richter, and J. Buchner. 2010. Asymmetric activation of the hsp90 dimer by its cochaperone aha1. *Mol Cell*. 37:344-354.

Rohl, A., J. Rohrberg, and J. Buchner. 2013. The chaperone Hsp90: changing partners for demanding clients. *Trends Biochem Sci*. 38:253-262.

Sapir-Mir, M., A. Mett, E. Belausov, S. Tal-Meshulam, A. Frydman, D. Gidoni, and Y. Eyal. 2008. Peroxisomal localization of Arabidopsis isopentenyl diphosphate isomerases suggests that part of the plant isoprenoid mevalonic acid pathway is compartmentalized to peroxisomes. *Plant Physiol*. 148:1219-1228.

Saraogi, I., and S.O. Shan. 2011. Molecular mechanism of co-translational protein targeting by the signal recognition particle. *Traffic*. 12:535-542.

Scheufler, C., A. Brinker, G. Bourenkov, S. Pegoraro, L. Moroder, H. Bartunik, F.U. Hartl, and I. Moarefi. 2000. Structure of TPR domain-peptide complexes: critical elements in the assembly of the Hsp70-Hsp90 multichaperone machine. *Cell*. 101:199-210.

Schlegel, T., O. Mirus, A. von Haeseler, and E. Schleiff. 2007. The tetratricopeptide repeats of receptors involved in protein translocation across membranes. *Mol Biol Evol*. 24:2763-2774.

Schleiff, E., and T. Becker. 2011. Common ground for protein translocation: access control for mitochondria and chloroplasts. *Nat Rev Mol Cell Biol*. 12:48-59.

Schleiff, E., M. Jelic, and J. Soll. 2003. A GTP-driven motor moves proteins across the outer envelope of chloroplasts. *Proc Natl Acad Sci U S A*. 100:4604-4609.

Schwacke, R., K. Fischer, B. Ketelsen, K. Krupinska, and K. Krause. 2007. Comparative survey of plastid and mitochondrial targeting properties of transcription factors in Arabidopsis and rice. *Mol Genet Genomics*. 277:631-646.

Seedorf, M., K. Waegemann, and J. Soll. 1995. A constituent of the chloroplast import complex represents a new type of GTP-binding protein. *Plant J*. 7:401-411.

Shao, S., and R.S. Hegde. 2011. A calmodulin-dependent translocation pathway for small secretory proteins. *Cell*. 147:1576-1588.

Shiau, A.K., S.F. Harris, D.R. Southworth, and D.A. Agard. 2006. Structural Analysis of E. coli hsp90 reveals dramatic nucleotide-dependent conformational rearrangements. *Cell*. 127:329-340.

Sohrt, K., and J. Soll. 2000. Toc64, a new component of the protein translocon of chloroplasts. *J Cell Biol*. 148:1213-1221.

Thompson, A.D., S.M. Bernard, G. Skiniotis, and J.E. Gestwicki. 2012. Visualization and functional analysis of the oligomeric states of Escherichia coli heat shock protein 70 (Hsp70/DnaK). *Cell Stress Chaperones*. 17:313-327.

Tyedmers, J., M. Lerner, C. Bies, J. Dudek, M.H. Skowronek, I.G. Haas, N. Heim, W. Nastainczyk, J. Volkmer, and R. Zimmermann. 2000. Homologs of the yeast Sec complex subunits Sec62p and Sec63p are abundant proteins in dog pancreas microsomes. *Proc Natl Acad Sci U S A*. 97:7214-7219.

van Wilpe, S., M.T. Ryan, K. Hill, A.C. Maarse, C. Meisinger, J. Brix, P.J. Dekker, M. Moczko, R. Wagner, M. Meijer, B. Guiard, A. Honlinger, and N. Pfanner. 1999. Tom22 is a multifunctional organizer of the mitochondrial preprotein translocase. *Nature*. 401:485-489.

von Heijne, G. 1985. Signal sequences. The limits of variation. *J Mol Biol*. 184:99-105.

von Heijne, G., and K. Nishikawa. 1991. Chloroplast transit peptides. The perfect random coil? *FEBS Lett*. 278:1-3.

von Loeffelholz, O., V. Kriechbaumer, R.A. Ewan, R. Jonczyk, S. Lehmann, J.C. Young, and B.M. Abell. 2011. OEP61 is a chaperone receptor at the plastid outer envelope. *Biochem J*. 438:143-153.

Waegemann, K., and J. Soll. 1996. Phosphorylation of the transit sequence of chloroplast precursor proteins. *J Biol Chem*. 271:6545-6554.

Wickner, W., and R. Schekman. 2005. Protein translocation across biological membranes. *Science*. 310:1452-1456.

Yamamoto, M., D. Maruyama, T. Endo, and S. Nishikawa. 2008. Arabidopsis thaliana has a set of J proteins in the endoplasmic reticulum that are conserved from yeast to animals and plants. *Plant Cell Physiol*. 49:1547-1562.

Young, J.C., N.J. Hoogenraad, and F.U. Hartl. 2003. Molecular chaperones Hsp90 and Hsp70 deliver preproteins to the mitochondrial import receptor Tom70. *Cell*. 112:41-50.

Zara, V., A. Ferramosca, P. Robitaille-Foucher, F. Palmieri, and J.C. Young. 2009. Mitochondrial carrier protein biogenesis: role of the chaperones Hsc70 and Hsp90. *Biochem J*. 419:369-375.

Zeytuni, N., and R. Zarivach. 2012. Structural and functional discussion of the tetra-trico-peptide repeat, a protein interaction module. *Structure*. 20:397-405.

Zhang, X.P., and E. Glaser. 2002. Interaction of plant mitochondrial and chloroplast signal peptides with the Hsp70 molecular chaperone. *Trends Plant Sci*. 7:14-21.

Zhang, Z., M.K. Quick, K.C. Kanelakis, M. Gijzen, and P. Krishna. 2003. Characterization of a plant homolog of hop, a cochaperone of hsp90. *Plant Physiol*. 131:525-535.

Zimmermann, R., S. Eyrisch, M. Ahmad, and V. Helms. 2011. Protein translocation across the ER membrane. *Biochim Biophys Acta*. 1808:912-924.

10 Danksagung

Zu guter Letzt möchte ich mich noch bei den Menschen bedanken die mich die letzten 3 Jahre nicht nur im Labor sondern auch Privat unterstützt haben.

In erster Linie möchte ich mich bei Professor Dr. Jürgen Soll bedanken, nicht nur für die Möglichkeit in seiner Arbeitsgruppe zu arbeiten sondern auch für zahlreiche Tipps und Tricks die ich von ihm lernen durfte und dafür, dass er jederzeit ein offenes Ohr für wissenschaftliche Fragestellungen hatte.

Weiterhin gilt ganz besonderer Dank Dr. Serena Schwenkert für ihre unschlagbar gute Betreuung, ihre guten Ideen, ihre immerwährende Unterstützung, für ihr Vertrauen und für zahlreiche nette Gespräche.

Dem gesamten Soll Lab und insbesondere der AG Schwenkert danke ich für das angenehme Arbeitsklima, die Kollegialität und Unterstützung sowie für die schöne gemeinsam verbrachte Zeit.

Dabei hervorzuheben sind meine Laborkolleginnen Dr. Christine Fellerer und Sabine Nick von Braun, die stets für eine heitere, entspannte und freundschaftliche Atmosphäre im Labor gesorgt haben. Weiterhin möchte ich Manuela Urbischek danken, ohne die das letzte Jahr im Labor sehr viel langweiliger verlaufen wäre.

Ganz besonderer Dank gilt meinen Freunden Annika, Stefan und Abbad.

Außerdem möchte ich mich herzlich bei meinen Eltern bedanken, die mich während meines gesamten Lebensweges stets unterstützt und ermutigt haben und die mir ein fester und wichtiger Rückhalt sind!

Zu guter Letzt möchte ich meinem Freund Tony danken! …Einfach für Alles…